

This is to certify that the

thesis entitled

Hysteresis and transitions between
multiple steady states of the Schlögl
model

presented by

J. Kottalam

has been accepted towards fulfillment
of the requirements for

Ph. D degree in Physical Chemistry

Katha C. Aust

Major professor

Date 3/9/84



RETURNING MATERIALS:
Place in book drop to
remove this checkout from
your record. FINES will
be charged if book is
returned after the date
stamped below.

--	--	--

HYSTERESIS AND TRANSITIONS BETWEEN MULTIPLE STEADY STATES
OF THE SCHLÖGL MODEL

By

J Kottalam

A DISSERTATION

Submitted to

Michigan State University

in partial fulfillment of the requirements
for the degree of

DOCTOR OF PHILOSOPHY

Department of Chemistry

1984

ABSTRACT

HYSTERESIS AND TRANSITIONS BETWEEN MULTIPLE STEADY STATES OF THE SCHLÖGL MODEL

By

J Kottalam

Several interesting phenomena are associated with multiple steady states in reacting systems far from equilibrium. To study these phenomena in simplest form, Schlögl introduced a cubic reaction model for autocatalytic isomerization. In the parameter space for this model there is a region in which two stable steady states and an unstable steady state are found. In this dissertation spontaneous transitions between the stable nonequilibrium steady states of the Schlögl model and hysteresis in induced transitions are analyzed.

The stochastic dynamics are described by a birth-and-death master equation. The time-dependent solutions of the master equation can be constructed using the eigenvalues and the eigenvectors of the transition matrix in the master equation. If the system parameters lie in the interior of the multiple steady-state region, then the system undergoes Kramers relaxation. The Kramers rule is valid for the Schlögl model only if both the ratio of the two eigenvalues closest to zero is substantially different from unity and the shapes of the two peaks in the slowest decaying mode match the corresponding peaks of the stationary mode. The region where the

Kramers rule breaks down is determined. The eigenvectors and the time-dependent solutions are displayed for points close to the boundary separating the single and multiple steady-state regions and for points well in the interior.

If the system is prepared at a single steady state and an externally controllable concentration parameter is increased at a fixed rate and then decreased at the same rate, the response of the system generates a hysteresis loop. This effect has been simulated both deterministically and stochastically. The deterministic results indicate a static contribution to hysteresis in the multiple steady-state region, while this contribution disappears when fluctuations are taken into account. In the single steady-state region both deterministic and stochastic results indicate that hysteresis is purely dynamic.

Noyes has proposed a criterion for relative stability of stable steady states in multistable systems. This criterion is based on coupling two reacting systems by material exchange and determining the final state of the coupled system. It is shown in this dissertation that such a coupled system exhibits more steady states than do the individual systems, and that the mixing experiments are not suitable for a study of relative stability. It is also shown that variation in the rate of material exchange shifts the steady states of the coupled system; these shifts are analyzed for cubic and quartic models.

TO MY MOTHER

who showed me the pleasure of learning

AND FATHER

who showed me the value of education

ACKNOWLEDGMENTS

I am grateful to all who assisted me during this endeavour. The contributions of only a few are mentioned here.

Needless to say that this work and much of what I have learnt would be impossible without the excellent guidance of Dr. Katharine Hunt. She is a perfect example for the definition of a guide: "Let not the wise disturb the minds of the ignorant; let him, working with devotion, show them the joy of good work." (Gita 3:26).

Sunil taught me computer programming. He was always there to pick me up whenever the computer and other facets of life trampled me down. The few friends I did have during my stay at MSU served the purpose of having millions of friends.

Of all contributions from my wife, the only thing I find words to express is that she typed the manuscript.

My interest in mathematics was created by my mother in my childhood. My education is a manifestation of my parents' intelligence and wisdom. Therefore, my achievements, if any, are really theirs.

TABLE OF CONTENTS

LIST OF FIGURES	vii
CHAPTER I INTRODUCTION	1
CHAPTER II MODERN METHODS FOR MACROSCOPIC CHEMICAL KINETICS	7
2.1 The Schlögl model and the deterministic analysis	7
2.2 The stochastic formulation	11
2.3 Methods of solution	20
CHAPTER III A REVIEW OF STUDIES ON THE SCHLÖGL MODEL	32
3.1 Further properties of the steady states	32
3.2 Coexistence of two phases	36
3.3 Approximate solution of master equation	44
3.4 Relative stability	47
3.5 Mean field theory and multivariate master equation approaches to include local fluctuations	59
3.6 Critical phenomena	73
CHAPTER IV A STUDY OF ASYMPTOTIC RELAXATION IN THE SCHLÖGL MODEL USING EIGENVECTORS OF THE TRANSITION MATRIX	83
4.1 The Schlögl model and its stochastic formulation	84

4.2 Transition between the two stable steady states	87
4.3 The validity of Kramers relaxation	98
CHAPTER V HYSTERESIS IN TRANSITIONS BETWEEN MULTIPLE NONEQUILIBRIUM STEADY STATES OF THE SCHLÖGL MODEL	127
5.1 Schlögl model and its steady states	127
5.2 Deterministic simulation of hysteresis	129
5.3 Stochastic simulation	134
CHAPTER VI DETERMINISTIC STUDY OF MULTIPLE STEADY STATES IN COUPLED FLOW TANK REACTORS	141
6.1 Multiple steady states in a single continuously stirred flow-tank reactor	142
6.2 Coupled flow-tank reactors	146
6.3 Comparison with the Noyes analysis	168
CHAPTER VII FUTURE WORK AND DEVELOPMENT	173
APPENDIX A Proof that the transitions generating hysteresis cannot occur before a marginal stability point is reached according to the deterministic rate equation	175
APPENDIX B Method and program to find the eigenvalues of the transition matrix	178
APPENDIX C Programs to construct the eigenvectors of the transition matrix	183
APPENDIX D Deterministic simulation of hysteresis	204
APPENDIX E Stochastic simulation of hysteresis	208

APPENDIX F	Special features of the cubic mechanism	
	in a flow tank reactor	213
REFERENCES		217

LIST OF FIGURES

Figure 2.1 The steady states of the Schlögl model	9
Figure 4.1 Eigenvectors of the transition matrix \underline{A} for the Schlögl model, when the parameters correspond to a point in the interior of the multiple steady-state region	88
Figure 4.2 Time evolution of probability distribution when the parameters correspond to a point in the interior of the multiple steady-state region. Initial distribution is $\delta(x-500)$.	94
Figure 4.3 Time evolution of probability distribution. Initial distribution is $\delta(x-50)$.	95
Figure 4.4 Time evolution of probability distribution. Initial distribution is $\delta(x-253)$, peaked at the unstable steady-state X-value	96
Figure 4.5 Time evolution of probability distribution. Initial distribution is $\delta(x-230)$	97
Figure 4.6 The first three nonzero eigenvalues of the transition matrix \underline{A} . $c_4 = 3.33333$.	104
Figure 4.7 The first three nonzero eigenvalues of the transition matrix \underline{A} . $c_4 = 1.7$	105
Figure 4.8 The first three nonzero eigenvalues of the transition matrix \underline{A} . $c_4 = 1.3$ (no multiple steady states)	106

Figure 4.9	Regions of the parameter space where the conditions on the eigenvalues (equation (4.31)) is satisfied.	108
Figure 4.10	Eigenvectors of the transition matrix \underline{A} near a marginal stability point	110
Figure 4.11	Time evolution of the probability distribution near a marginal stability point	115
Figure 4.12	Eigenvectors of the transition matrix near the critical point	116
Figure 4.13	Time evolution of probability distribution near the critical point. Initial distributions are a) $\delta(x-120)$, b) $\delta(x-300)$, and c) $\delta(x-182)$	120
Figure 4.14	Time evolution of probability distribution near the critical point and near a marginal stability point. Initial distributions are a) $\delta(x-300)$, b) $\delta(x-100)$, and c) $\delta(x-190)$.	123
Figure 5.1	Results from deterministic (curves with arrows) and stochastic (noisy curves) simulations of hysteresis in the multistable region ($c_4 = 1.7$). The S-shaped curve is the set of steady states	131
Figure 5.2	Results from deterministic (curves with arrows) and stochastic (noisy curves) simulation of hysteresis in the single steady-state region. ($c_4 = 1.3$).	132

Figure 5.3	Area inside the hysteresis loop versus the rate of change of B. (Deterministic results)	133
Figure 5.4	Comparison of deterministic (upper line) and stochastic simulation (lower line) results. $c_4 = 1.7$.	139
Figure 5.5	Comparison of deterministic (upper line) and stochastic simulation (lower line) results. $\beta = 50$.	140
Figure 6.1	Steady states for the cubic model in a single flow tank reactor.	147
Figure 6.2	Steady states of coupled reactors system for Noyes cubic model. $k_0 = 1.5 \times 10^{-5} \text{ s}^{-1}$	150
Figure 6.3	Steady states of coupled reactor system for the cubic model. $k_0 = 2.7 \times 10^{-5} \text{ s}^{-1}$	152
Figure 6.4	Steady states of coupled reactor system for the cubic model. $k_0 = 2.516963 \times 10^{-5} \text{ s}^{-1}$	153
Figure 6.5	The potential function ϕ for the cubic model with $k_0 = 2.517 \times 10^{-5} \text{ s}^{-1}$ and $k_x = 0$.	156
Figure 6.6	The potential function ϕ for the cubic model with $k_0 = 2.517 \times 10^{-5} \text{ s}^{-1}$ and $k_x = 4.0 \times 10^{-5} \text{ s}^{-1}$	157
Figure 6.7	The potential function ϕ for the cubic model. $k_0 = 2.517 \times 10^{-5} \text{ s}^{-1}$ and $k_x = 9.061 \times 10^{-5} \text{ s}^{-1}$.	158
Figure 6.8	The potential ϕ for the cubic model. $k_0 = 1.5 \times 10^{-5} \text{ s}^{-1}$ and $k_x = 3.9 \times 10^{-5} \text{ s}^{-1}$	159

Figure 6.9 The potential ϕ for the quartic model.

$$k_0 = 3.374 \times 10^{-5} \text{ s}^{-1} \text{ and } k_x = 1.28 \times 10^{-5} \text{ s}^{-1}. \quad 160$$

Figure 6.10 The potential ϕ for the cubic model.

$$k_0 = 3.5 \times 10^{-5} \text{ s}^{-1} \text{ and } k_x = 1.1 \times 10^{-4} \text{ s}^{-1}. \quad 161$$

Figure 6.11 Comparison of steady state patterns of
the single and coupled flow reactors. 172

CHAPTER I
INTRODUCTION

All efforts to understand natural phenomena involve observation, deduction, induction, and investigation, which are characteristic of human intellect. One of the methods is mathematical modeling, in which a physical system is first observed, mathematical relations are deduced, these relations are applied inductively (or generalized) to other similar systems, and these systems are investigated to verify the relations. Since models are deduced from limited observations, they need not be complete, and we should incorporate modifications as the scope of the models widens to include new fields of investigation.

A chemist's ambition is to completely understand all aspects of chemical reactions. One such aspect is the variation in the concentrations of different species during a reaction. These variations can be investigated at several levels of precision. One extreme is to view matter as continuous bulk material with the amounts of each substance varying smoothly in time, governed by the law of mass action. In this case the equations of motion for chemical concentrations are ordinary differential equations. On the other hand, the exact (classical) treatment would involve the study of encounters between various molecules using the equations of motion for the position and velocity vectors of each atom in

each molecule. Although such "molecular dynamics" calculations are being carried out, a typical laboratory situation involves $O(10^{23})$ molecules each having $O(10^1)$ atoms or more. Moreover, the number of observations actually made on a system in the laboratory is very small compared to the number of independent data elements that would be available from an exact theoretical treatment. Hence in statistical mechanics the encounters between molecules are viewed as frequently occurring random events and the attempt is made to derive the expected values of the few observable quantities and the expected deviations from those values. Thus we are often satisfied with the macroscopic description. When the deviations are large the system may exhibit phenomena which cannot be treated by deterministic methods. Then we need to incorporate stochastic character into the theory.

Let us consider a spatially homogeneous mixture of n reacting chemical species whose particle numbers $x^{(1)}$, $x^{(2)}$, ..., $x^{(n)}$ are components of \underline{x} . In macroscopic chemical kinetics the time evolution of \underline{x} is given by a first-order ordinary differential equation:

$$\frac{d\underline{x}}{dt} = \underline{F}(\underline{x}). \quad (1.1)$$

This equation is nonlinear except in special cases and is usually autonomous (i.e., $\underline{F}(\underline{x})$ is usually independent of t).

The steady states of the system are those points \underline{X}_s in state-space at which the numbers of all chemical species are stationary with respect to time.

$$\left. \frac{d\underline{X}}{dt} \right|_{\underline{X}=\underline{X}_s} = \underline{F}(\underline{X}_s) = 0. \quad (1.2)$$

If the system is closed, we call the steady state an equilibrium state. For systems operating at or near equilibrium conditions, the steady state is unique, and it is globally and asymptotically stable. Asymptotic and global stability mean that the system will eventually arrive at the steady state starting from an arbitrary initial condition. This is a consequence of the minimum entropy production principle¹.

However, an open system forced away from the linear regime near equilibrium by a matter flux across its boundaries can exhibit exotic phenomena such as the presence of several steady states and periodic oscillation. If one of these structures (steady-states or oscillatory solutions of equation (1.1)) is unstable, then the solutions of the deterministic differential equations do not describe the system adequately. If a one-variable system has more than one steady states, not all can be stable. Suppose there are two stable steady states X_1 and X_3 for the single-variable system; then in the neighborhood of X_1 the system moves towards X_1 and therefore away from X_3 (and similarly for X_3). This implies the

existence of another point between X_1 and X_3 from whose neighborhood the system can only move away; this is an unstable steady state. By the same argument,² two stable steady states in a two-variable system must be accompanied by an unstable steady state, a saddle point, or an unstable limit cycle.[†] In these situations we need to study the system in more detail.

In the stochastic description, sometimes called the mesoscopic description, the system can occupy any possible state with a finite probability at a given time. Thus we use a probability distribution over the species-number space in place of the species number to specify the state of the system at a given time. We again use the law of mass action, but we use it to calculate the probability of transition from one state to another and not to calculate the rate of the reaction directly. Using the transition probability we arrive at a partial differential equation - called the master equation - governing the evolution of the probability distribution in time.

For example, when the parameters take certain values, the Schlögl model³ has three steady states, one of which is

[†] Near a saddle point the motion is towards the point in one direction and away from it in a perpendicular direction. A limit cycle is a periodic solution of a set of differential equations in two dependent variables.

unstable.⁴ According to the deterministic rate equations only one of the stable steady states can be reached from a particular initial point, but according to the master equation⁵ both stable steady states and their neighborhoods can be reached with significant probability independent of the initial distribution. Moreover, when an external parameter is varied beyond a threshold value, the system undergoes a transition from one stable steady state to another. When we reverse this variation, the threshold for the reverse transition is different. The extent of this hysteresis effect is markedly different in the deterministic and stochastic descriptions.

In the next chapter the stability analysis of deterministic steady states and the stochastic formulation are illustrated using the Schlögl model as an example. Methods for solving the stochastic equations are also explained. Chapter III provides a review of the literature on topics related to multiple steady-state systems; coexistence of two phases, relative stability of steady states, critical phenomena, and alternate formulations of stochastic kinetics are discussed. In chapter IV results for the time evolution of the probability distribution as described by the master equation are presented. In chapter V deterministic and stochastic simulations of hysteresis in the Schlögl model are presented. These studies are based on a master equation which takes into account uniform fluctuations in the particle number, but excludes spatial fluctuations. For a more realistic description,

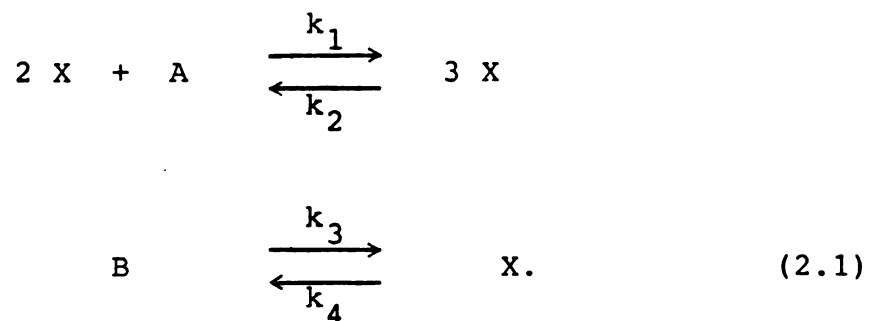
particularly in the vicinity of the critical point, both kinds of fluctuations should be considered. In chapter VI the effects of coupling two open reacting systems are studied. Chapter VII contains suggestions for future work on these problems.

CHAPTER II

MODERN METHODS FOR MACROSCOPIC CHEMICAL KINETICS

2.1 THE SCHLÖGL MODEL AND THE DETERMINISTIC ANALYSIS

A system is said to be within the linear regime around an equilibrium state if the thermodynamic fluxes (e.g., rate of reaction) are linear combinations of the forces (e.g., chemical affinity). In this region, it is well known that there can be only one stable steady state.¹ Several models have been proposed to study chemical kinetics far away from equilibrium. One model exhibiting multiple steady states is Schlögl's termolecular model.³ It consists of the reactions



Here the numbers of molecules of A and B are kept at predetermined constant values by contact with external reservoirs or by appropriate feeding into or removal from the reactor. We assume the reactor to be efficiently stirred so that the system is always homogeneous and diffusion effects need not be considered. The constants k_1 , k_2 , k_3 , and k_4 are specific rate constants independent of the size of the

system. While the rate constants are characteristic of a reaction mechanism, the concentrations of A and B can be controlled externally. For convenience we will also set the numbers of A and B molecules equal and denote the number by B. Then the deterministic rate equation is

$$\frac{d\chi}{dt} = k_1 b \chi^2 - k_2 \chi^3 + k_3 b - k_4 \chi, \quad (2.2)$$

where $\chi = X/V$ and $b = B/V$ are the concentrations of X and B (and A) respectively, and V is the volume of the system.

The steady states of the system are the real solutions of the algebraic equation

$$\frac{k_1}{V^2} B X^2 - \frac{k_2}{V^2} X^3 + k_3 B - k_4 X = 0. \quad (2.3)$$

The steady states are displayed in Figure 2.1 for various values of the parameters. It can be shown⁵ that for

$\eta = \frac{k_1 k_4}{k_2 k_3} < 9$, there is only one steady state for all values

of B, while for $\eta > 9$ there is a range of B values in which there are three steady states (see Figure 2.1).

Let X_1 , X_2 , and X_3 be the roots of this cubic equation. The stability of each steady state can be deduced by a linear stability analysis. The rate equation can be written as

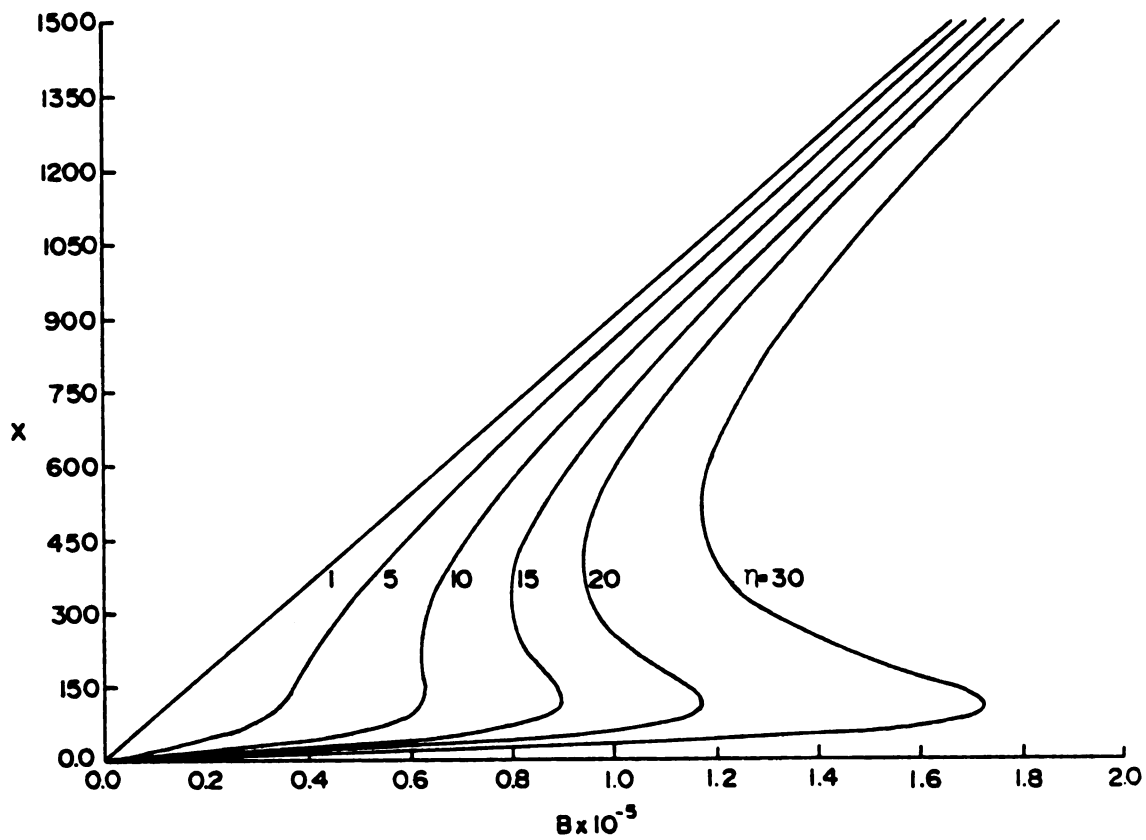


Figure 2.1 The steady states of the Schlögl model. The number of X molecules at steady state as a function of the number of B molecules for various values of the rate constants.

$$\frac{dX}{dt} = -\frac{k_2}{v^2}(X-X_1)(X-X_2)(X-X_3). \quad (2.4)$$

Let us consider an arbitrarily small deviation δX_i from X_i ($i=1,2,3$). Substituting $\delta X_i = X - X_i$ in equation (2.4) gives

$$\begin{aligned} \frac{d\delta X_i}{dt} &= -\frac{k_2}{v^2}(\delta X_i + X_i - X_1)(\delta X_i + X_i - X_2)(\delta X_i + X_i - X_3) \\ &= \kappa_i \delta X_i \end{aligned} \quad (2.5)$$

to first order in δX_i , where

$$\kappa_1 = -\frac{k_2}{v^2}(X_1 - X_2)(X_1 - X_3)$$

$$\kappa_2 = -\frac{k_2}{v^2}(X_2 - X_1)(X_2 - X_3)$$

$$\text{and } \kappa_3 = -\frac{k_2}{v^2}(X_3 - X_1)(X_3 - X_2). \quad (2.6)$$

These linear differential equations have the solutions

$$\delta X_i = \delta X_i^0 e^{\kappa_i t}. \quad (2.7)$$

The steady state X_i is stable, marginally stable, or

unstable according to whether an arbitrarily small deviation δX_i decays, remains stationary, or grows, and this in turn depends upon the sign of $\text{Re}(\kappa_i)$. From the definition of κ_i one concludes the following: If all roots are real, with $X_1 < X_2 < X_3$, then X_1 and X_3 are stable and X_2 is unstable. Whenever X_2 coincides with either X_1 or X_3 (or both) it is marginally stable. If there is a complex pair of roots, then the real root is always stable.

2.2 THE STOCHASTIC FORMULATION

In order to study transitions between two stable steady states where the average value of X reaches and passes through the unstable steady state value, the deterministic analysis is not adequate. For a better description, we consider the number of molecules of X in a fixed volume at a given time as a discrete random variable. Accordingly we focus on the probability $P(x,t)$ that the random variable X has value x at time t . The evolution of this distribution is determined by the occurrence of chemical reactions at random as explained below.

A stochastic process is completely determined by specifying an initial distribution and a hierarchy of conditional distributions; i.e.,

$P(x_{n+1}, t_{n+1} | x_0, t_0; x_1, t_1; \dots; x_n, t_n)$ denotes the conditional probability that the system has x_{n+1} molecules of X at time t_{n+1} given that it had x_0 at time t_0 , x_1 at time t_1 , and so on,

where x_0, x_1, \dots, x_n are d -dimensional vectors for a process with d variables. If it happens that

$$P(x_{n+1}, t_{n+1} | x_0, t_0; x_1, t_1; \dots; x_n, t_n) = P(x_{n+1}, t_{n+1} | x_n, t_n) \quad (2.8)$$

for all n , then the process described by this conditional probability is called a Markov process. In other words, of all conditions specified in the past, only the most recent is relevant in determining the future evolution of a Markov process. This does not imply that the future is independent of the past, but this dependence is entirely contained in the present. If the Markov process satisfies the additional condition

$$P(x_{n+1}, t_{n+1} | x_n, t_n) = P(x_{n+1}, t_{n+1} + \tau | x_n, t_n + \tau), \quad (2.9)$$

then the process is said to be a stationary (or time-homogeneous) Markov process. The Markovian character of stochastic processes corresponds to the first order nature of differential equations whereas the stationary property corresponds to the autonomous behavior of deterministic differential equations. Just as an n -th order deterministic differential equation can be transformed to a set of n coupled first order equations,⁶ a non-Markov stochastic process requiring the specification of n conditions for its complete description can be transformed to a Markov process in nd variables.⁷

A Markov process is completely determined by specifying an initial distribution and a transition probability $P(x,t|y,s)$. Using elementary theorems of probability theory it can be shown that

$$P(x,t+s) = \sum_y P(x,t+s|y,t) P(y,t). \quad (2.10)$$

This equation is called Kolmogorov's equation. Using first principles of differentiation, we obtain the master equation⁸

$$\frac{\partial}{\partial t} P(x,t) = \sum_y A_{xy} P(y,t), \quad (2.11)$$

where

$$A_{xy} = \lim_{s \rightarrow 0^+} \frac{P(x,t+s|y,t) - \delta_{xy}}{s} \quad (2.12)$$

is the probability of transition per unit time from state y to state x . A_{xy} is called the transition probability rate or infinitesimal transition probability when $x \neq y$. Using the normalization condition on $P(y,t+s|x,t)$ namely,

$$P(x,t+s|x,t) = 1 - \sum_{y \neq x} P(y,t+s|x,t), \quad (2.13)$$

we get

$$A_{xx} = - \sum_{y \neq x} A_{yx}. \quad (2.14)$$

The postulates of stochastic chemical kinetics are

- 1) Chemical reactions are Markov random processes.
- 2) Given that the system has x molecules at time t , the probability that a reaction step will occur in the interval $(t, t+\delta t)$ is

$$a_m(x, t) \delta t + o(\delta t), \quad (2.15)^\dagger$$

where $a_m(x, t)$ is proportional to the number of reactant combinations leading to the m -th step at time t . For example, if the second step in a list of all elementary reactions is $3X \rightarrow 2X + A$, then $a_2(x, t) = c_2 x(x-1)(x-2)/3!$

The second postulate gives the transition probability as

$$A_{xy}(t) = \sum_m a_m(y, t), \quad (2.16)$$

where m ranges over all reaction steps which result in a net change of $y \rightarrow x$ in the species number. The Markov property is implied in the deterministic formulation also. The second postulate is the analog of the law of mass action. Thus the random variation of X is the only addition to the theory.

[†] The meaning of $o(\delta t)$: If $\delta a = o(\delta t)$, then by definition

$$\lim_{\delta t \rightarrow 0} \frac{\delta a}{\delta t} = 0, \text{ or equivalently, } o(\delta t) = O(\delta t^\epsilon), \quad \epsilon > 1.$$

For example, the (infinitesimal) transition probability for the Schlögl model is given by^{5,9}

$$A_{xy} = \begin{cases} a_+(y) & \text{for } y = x-1 \\ a_-(y) & \text{for } y = x+1 \\ -a_+(y) - a_-(y) & \text{for } y = x \\ 0 & \text{for } |x-y| > 1, \end{cases} \quad (2.17)$$

where

$$a_+(x) = c_1 B x(x-1)/2! + c_3 B, \quad (2.18)$$

$$a_-(x) = c_2 x(x-1)(x-2)/3! + c_4 x, \quad (2.19)$$

x and y range over nonnegative integers, and the c_i are the proportionality constants which are related to the rate constants k_i . The relation is made by taking the deterministic limit in the master equation.¹⁰ We find

$$k_i = V^{m_i-1} c_i / n_i! \quad (2.20)$$

where n_i is the molecularity of the i -th step in X and m_i is the total molecularity of the i -th step (e.g., $n_1 = 2$, $m_1 = 3$). The master equation for the Schlögl model is

$$\begin{aligned} \frac{\partial}{\partial t} P(x,t) &= a_+(x-1)P(x-1,t) + a_-(x+1)P(x+1,t) \\ &\quad - [a_+(x) + a_-(x)]P(x,t). \end{aligned} \quad (2.21)$$

The stationary distribution $P_s(x)$ is the solution of

$$\frac{\partial}{\partial t} P(x,t) = 0,$$

$$\begin{aligned} \text{i.e., } a_+(x-1)P_s(x-1) + a_-(x+1)P_s(x+1) \\ = [a_+(x) + a_-(x)]P_s(x). \end{aligned} \quad (2.22)$$

From this the detailed balance relation

$$a_+(x-1)P_s(x-1) = a_-(x)P_s(x) \quad (2.23)$$

follows by induction. The detailed balance relation gives the expression for the normalized $P_s(x)$ as

$$P_s(x) = \frac{\prod_{y=1}^x a_+(y-1)/a_-(y)}{\sum_z \prod_{y=1}^z a_+(y-1)/a_-(y)}. \quad (2.24)$$

This can be written as⁵

$$P_s(x) = P_s(0)e^{-\phi(x)} \quad (2.25)$$

in standard form, where the "stochastic potential" $\phi(x)$ is given by

$$\phi(x) = \sum_{y=1}^x \ln \frac{a_-(y)}{a_+(y-1)}. \quad (2.26)$$

Although the master equation should be regarded as the fundamental equation in this treatment, it is often convenient to work with other approximate equations such as the Fokker-Planck equation and the Langevin equation which may be solved by standard mathematical techniques. The master equation can also be written as

$$\frac{\partial}{\partial t} P(x, t) = \sum_y A_{xy} P(y, t) = \sum_z A(x-z, z) P(x-z, t), \quad (2.27)$$

where $A(x-z, z)$ is the infinitesimal transition probability for a change $z \neq 0$ in the number of molecules in a system containing $x-z$ molecules, and $A(x, 0)$ is fixed by

$$\sum_z A(x-z, z) = 0. \text{ Expanding each term on the right hand side}$$

as a Taylor series about $z = 0$ in the first argument of $A(x-z, z)$ and in $P(x-z)$ yields

$$\frac{\partial}{\partial t} P(x, t) = \sum_z \sum_m \frac{1}{m!} \frac{\partial^m}{\partial x^m} [A(x, z) P(x, t)] (-z)^m. \quad (2.28)$$

This is the Kramers-Moyal expansion.¹¹ The Fokker-Planck equation¹² is obtained by neglecting terms corresponding to $m > 2$. Thus it reads

$$\begin{aligned} \frac{\partial}{\partial t} P(x, t) = & - \sum_z z \frac{\partial}{\partial x} [A(x, z) P(x, t)] \\ & + \frac{1}{2} \sum_z z^2 \frac{\partial^2}{\partial x^2} [A(x, z) P(x, t)]. \end{aligned} \quad (2.29)$$

For the Schlögl model, from equation (2.17)

$$A(x, z) = \begin{cases} a_+(x) & \text{for } z = 1 \\ -a_+(x) - a_-(x) & \text{for } z = 0 \\ a_-(x) & \text{for } z = -1 \\ 0 & \text{for } |z| > 1. \end{cases} \quad (2.30)$$

Hence the Fokker-Planck equation becomes

$$\frac{\partial}{\partial t} P(x, t) = -\frac{\partial}{\partial x} [r(x)P(x, t)] + \frac{1}{2} \frac{\partial^2}{\partial x^2} [a(x)P(x, t)], \quad (2.31)$$

where

$$r(x) = a_+(x) - a_-(x), \quad (2.32)$$

$$\text{and } a(x) = a_+(x) + a_-(x). \quad (2.33)$$

In general neglecting terms with $m > 2$ cannot be justified. Van Kampen¹³ and Kubo et al¹⁴ have developed systematic expansion procedures in power series of a small parameter (usually the inverse system size). Gillespie¹⁵ has shown that if $A(x, z) = 0$ for $z > 1$, then the Fokker-Planck equation when discretized with unit step size[†]

[†]Discretizing with unit step size means approximating $\partial P/\partial x$ by $\Delta P/\Delta x$ with $\Delta x = 1$; then $\Delta P = P(x, t) - P(x-1, t)$.

reproduces the master equation exactly, whereas the conditions $A(x, \pm 2) \neq 0$ and $A(x, z) = 0$ for $|z| > 2$ require four terms to be kept in the Kramers-Moyal expansion. Matsuo et al¹⁶ have discussed methods of constructing Fokker-Planck equations from the deterministic equations describing physical processes. Obtaining the coefficients $r(x)$ and $a(x)$ in the Fokker-Planck equation from the Kramers-Moyal expansion is one of the methods. Another method is to adjust the coefficients in such a way that the resulting stationary distribution coincides with the stationary distribution given by the master equation (2.24). The two term Fokker-Planck equation is useful because it describes the process specified by the stochastic differential equation¹⁷

$$(I) \quad dX_t = r(X_t)dt + \sqrt{a(X_t)}dW_t \quad (2.34)$$

or, equivalently,

$$(S) \quad dX_t = [r(X_t) - \frac{1}{2} a_x(X_t)]dt + \sqrt{a(X_t)}dW_t, \quad (2.35)$$

where (I) and (S) indicate Itô and Stratonovich calculi respectively, W_t is the normal Wiener process and a_x is the derivative of a . Such processes are relatively well understood mathematically. When $a(x)$ is a constant independent of x , the resulting stochastic equation

$$dX_t = r(X_t)dt + \sqrt{a}dW_t, \quad (2.36)$$

is the Langevin equation, which has played an important role in the theory of Brownian motion.¹⁸

2.3 METHODS OF SOLUTION

Since the master equation is a linear differential equation in $P(x,t)$, its solution can be written formally in terms of the eigenvalues and eigenvectors of the transition matrix \underline{A} , when \underline{A} is independent of time.

Relation (2.14), namely

$$\sum_y A_{yx} = 0 \quad \text{for all } x, \quad (2.37)$$

means that the rows of \underline{A} are linearly dependent and this implies $\det \underline{A} = 0$. Thus the equation

$$\sum_y A_{xy} P_s(y) = 0 \quad (2.38)$$

has a nontrivial solution under the constraint

$$\sum_x P_s(x) = 1.$$

This guarantees the existence of a normalized stationary distribution. This distribution is unique if and only if all states of the process communicate with each other; i.e., if and only if any arbitrary state can be reached from any other state in finite time. If this condition is not satisfied the

process degenerates into several disjoint processes.¹⁹ For the Schlögl model the requirement for uniqueness is satisfied, since $a_+(x) > 0$ for all x and $a_-(x) > 0$ for all $x > 0$.

Since the stationary distribution is an eigenvector corresponding to zero eigenvalue (see equation (2.38)), zero is always an eigenvalue of \underline{A} . Though detailed balance implies the existence of a stationary distribution, the converse is not true. However, detailed balance implies additional properties of the eigenvalues.

In addition to (2.37) and $A_{xy} > 0$ for all $y \neq x$, if detailed balance also holds

$$(\text{i.e., if } A_{xy} P_s(y) = A_{yx} P_s(x)), \quad (2.39)$$

then the nonzero eigenvalues of \underline{A} are real and negative.⁸

Proof:

Consider the matrices

$$W_{xy} = \delta_{xy} P_s(x)^{\frac{1}{2}}, \quad (2.40)$$

$$\underline{S} = \underline{W}^{-1} \underline{A} \underline{W}. \quad (2.41)$$

\underline{S} is obviously real and it has the same eigenvalues as \underline{A} . Further

$$\begin{aligned} S_{xy} &= P_s(x)^{-\frac{1}{2}} A_{xy} P_s(y)^{\frac{1}{2}} \\ &= P_s(x)^{-\frac{1}{2}} A_{yx} P_s(x) P_s(y)^{-\frac{1}{2}} \end{aligned}$$

$$\begin{aligned}
&= P_S(y)^{-\frac{1}{2}} A_{yx} P_S(x)^{\frac{1}{2}} \\
&= S_{yx}; \qquad (2.42)
\end{aligned}$$

i.e., \underline{S} is also symmetric. Hence the eigenvalues are real. Let \underline{Q}_j be an eigenvector of \underline{S} corresponding to an eigenvalue $\lambda_j \neq 0$.

$$\begin{aligned}
\underline{Q}_j \underline{S} \underline{Q}_j &= \sum_{x,y} Q_{xj} S_{xy} Q_{yj} \\
&= \sum_x S_{xx} Q_{xj}^2 + \sum_{x,y \neq x} Q_{xj} S_{xy} Q_{yj} \\
&= - \sum_{x,y \neq x} A_{yx} Q_{xj}^2 + \sum_{x,y \neq x} S_{xy} Q_{xj} Q_{yj} \\
&= - \sum_{x,y > x} A_{yx} Q_{xj}^2 - \sum_{x,y < x} A_{yx} Q_{xj}^2 \\
&\quad + \sum_{x,y > x} S_{xy} Q_{xj} Q_{yj} + \sum_{x,y < x} S_{xy} Q_{xj} Q_{yj} \\
&= - \sum_{x,y > x} A_{yx} Q_{xj}^2 - \sum_{x,y > x} A_{xy} Q_{yj}^2 \\
&\quad + \sum_{x,y > x} S_{xy} Q_{xj} Q_{yj} + \sum_{x,y > x} S_{yx} Q_{xj} Q_{yj} \\
&= - \sum_{x,y > x} A_{xy} \left\{ \frac{P_S(y)}{P_S(x)} Q_{xj}^2 + Q_{yj}^2 \right. \\
&\quad \left. - 2 \left(\frac{P_S(y)}{P_S(x)} \right)^{\frac{1}{2}} Q_{xj} Q_{yj} \right\}
\end{aligned}$$

$$\begin{aligned}
&= - \sum_{x, y > x}^{23} A_{xy} \left\{ Q_{yj} - \left(\frac{P_S(y)}{P_S(x)} \right)^{\frac{1}{2}} Q_{xj} \right\}^2 \\
&\leq 0 \quad \text{since } A_{xy} > 0 \text{ for } y \neq x. \quad (2.43)
\end{aligned}$$

By choice of $\underline{Q}_{.j}$,

$$\lambda_j = \frac{\underline{Q}_{.j} \underline{S} \underline{Q}_{.j}}{\underline{Q}_{.j}^2} ;$$

so (2.43) implies

$$\lambda_j \leq 0, \quad (2.44)$$

which was to be proved.

Since \underline{A} is not symmetric the eigenvectors of \underline{A} and \underline{A}^T are not the same, but a relation between them can be deduced by use of \underline{S} . Let the columns of \underline{Q} be the normalized eigenvectors of \underline{S} in a particular order and $\underline{\Lambda}$ be the diagonal matrix containing the eigenvalues. Then

$$\underline{Q}^T \underline{S} \underline{Q} = \underline{\Lambda} \quad \text{and} \quad \underline{Q}^T \underline{Q} = \underline{1} ; \quad (2.45)$$

$$\text{i.e., } \underline{Q}^T \underline{W}^{-1} \underline{A} \underline{W} \underline{Q} = \underline{\Lambda} ,$$

$$\text{or } \underline{L}^T \underline{A} \underline{R} = \underline{\Lambda} , \quad (2.46)$$

where

$$\underline{\underline{L}} = \underline{\underline{W}}^{-1} \underline{\underline{Q}} \quad (2.47)$$

$$\text{and } \underline{\underline{R}} = \underline{\underline{W}} \underline{\underline{Q}} \quad (2.48)$$

Thus $\underline{\underline{L}}_{\cdot j}$ and $\underline{\underline{R}}_{\cdot j}$ are the j -th eigenvectors of $\underline{\underline{A}}$ and $\underline{\underline{A}}^T$ respectively. Moreover,

$$\underline{\underline{L}}^T \underline{\underline{R}} = \underline{\underline{Q}}^T \underline{\underline{W}}^{-1} \underline{\underline{W}} \underline{\underline{Q}} = \underline{\underline{1}} .$$

Eliminating $\underline{\underline{Q}}$ between (2.47) and (2.48), we have

$$\underline{\underline{L}} = \underline{\underline{W}}^{-2} \underline{\underline{R}} . \quad (2.49)$$

The solution of $\frac{\partial}{\partial t} \underline{\underline{P}} = \underline{\underline{A}} \underline{\underline{P}}$ can now be written (when $\underline{\underline{A}}$ is time-independent) as

$$P(x, t) = \sum_j \alpha_j R_{xj} e^{\lambda_j t}, \quad (2.50)$$

where

$$\alpha_j = \sum_i \frac{R_{ij} P(i, 0)}{P_s(i)}, \quad (2.51)$$

and $P(i, 0)$ is the initial distribution. The eigenvalue equation for the k -th eigenvector $\underline{\underline{R}}_{\cdot k}$ is

$$\sum A_{ij} R_{jk} = \lambda_k R_{ik} \quad i = 0, 1, \dots$$

Summing over i , it becomes

$$\sum_i \sum_j A_{ij} R_{jk} = \lambda_k \sum_i R_{ik}.$$

Since $\sum_i A_{ij} = 0$, it follows[†] that

$$\sum_i R_{ik} = 0 \quad \text{if } \lambda_k \neq 0. \quad (2.52)$$

This means that $\sum_i P(i,t) = 1$ provided $\sum_i P_s(i) = 1$.

Thus we need to diagonalize the matrix \underline{A} in order to solve this problem completely. \underline{A} is infinite dimensional, but for a nonexplosive chemical reaction we can always find a large region of the state space outside which there is no significant probability to find the system. Since reaction steps of high molecularity are not common, \underline{A} is always a narrow band matrix. For the Schlögl model it is tridiagonal.

The matrix diagonalization method is valid only if the transition probabilities are time-independent, i.e., if the system is autonomous. Gillespie has devised a numerical algorithm for stochastically simulating any chemically reacting system¹⁰ and he has extended it to include

[†] assuming that $\sum_j A_{ij} R_{jk}$ converges uniformly in i so that we can interchange the order of the two infinite summations.

nonautonomous systems²⁰. This simulation should exactly reproduce the solution of the master equation, since it is also based on the same postulates from which the latter has been derived.

To derive the master equation we used the postulates to arrive at the transition probability $A_{xy}(t)\delta t + o(\delta t)$ that an event occurs in $(t, t+\delta t)$ resulting in a transition from y to x . Instead we now focus on the probability $P(\tau, m; x, t)d\tau$ that the next event occurs in $(t+\tau, t+\tau+d\tau)$ and that it is the m -th reaction step, given that the system has x molecules of X at time t ;

$$P(\tau, m; x, t)d\tau = P_0(\tau; x, t) a_m(x, t+\tau)d\tau, \quad (2.53)$$

where $P_0(\tau; x, t)$ is the probability that no reaction occurred in $(t, t+\tau)$ given that the system is at x at time t .

Decomposing the interval $(t, t+s+\delta s)$ into $(t, t+s)$ and $(t+s, t+s+\delta s)$ we find that the probability that the m -th step does not occur in $(t, t+s+\delta s)$ is given by

$$P_{0m}(s+\delta s; x, t) = [1 - a_m(x, t+s)\delta s - o(\delta s)] P_{0m}(s; x, t), \quad (2.54)$$

Therefore,

$$\frac{\partial}{\partial s} P_{0m}(s; x, t) = - a_m(x, t+s) P_{0m}(s; x, t). \quad (2.55)$$

Solving this first order differential equation with the initial condition $P_{0m}(0;x,t) = 1$, we obtain

$$P_{0m}(\tau;x,t) = \exp \left\{ - \int_t^{t+\tau} a_m(x,s) ds \right\}. \quad (2.56)$$

Thus the probability $P_0(\tau;x,t)$ that none of the steps occurs in $(t,t+\tau)$ is

$$P_0(\tau;x,t) = \prod_m P_{0m}(\tau;x,t) = \exp \left\{ - \int_t^{t+\tau} a(x,s) ds \right\}, \quad (2.57)$$

where

$$a(x,t) = \sum_m a_m(x,t), \quad (2.58)$$

and finally from (2.53)

$$P(\tau,m;x,t) = a_m(x,t+\tau) \exp \left\{ - \int_t^{t+\tau} a(x,s) ds \right\}. \quad (2.59)$$

For a given x and t , this is the density function of a joint distribution in τ and m . In order to simulate the process determined by this density, we first obtain the probability $P_1(\tau;x,t)d\tau$ that the next reaction occurs in $(t+\tau,t+\tau+d\tau)$

irrespective of which step it is.

$$\begin{aligned}
 P_1(\tau; x, t) &= \sum_m P(\tau, m; x, t) \\
 &= a(x, t+\tau) \exp \left\{ - \int_t^{t+\tau} a(x, s) ds \right\}. \quad (2.60)
 \end{aligned}$$

Then the probability $P_2(m|\tau; x, t)$ that the next reaction is the m -th step given that the next reaction occurs in $(t+\tau, t+\tau+d\tau)$ is

$$P_2(m|\tau; x, t) = \frac{P(\tau, m; x, t)}{P_1(\tau; x, t)} = \frac{a_m(x, t+\tau)}{a(x, t+\tau)}. \quad (2.61)$$

The simulation algorithm consists of selecting a random number τ distributed according to $P_1(\tau; x, t)$ and another random number m distributed according to $P_2(m|\tau; x, t)$ when the system is at x at t . The distribution functions corresponding to $P_1(\tau; x, t)$ and $P_2(m|\tau; x, t)$ are respectively

$$F_1(\tau; x, t) = \int_0^\tau P_1(s; x, t) ds \quad (2.62)$$

$$\text{and } F_2(m|\tau; x, t) = \sum_{v=1}^m P_2(v|\tau; x, t) \quad (2.63)$$

The range of the function F_1 is $[0, 1]$ and the range of F_2 is a subset of the above interval. The probability that τ lies between τ_1 and τ_2 is given by

$$\int_{\tau_1}^{\tau_2} P_1(s; x, t) ds = F_1(\tau_2; x, t) - F_1(\tau_1; x, t).$$

Thus the distribution of τ in $[0, \infty]$ according to $P_1(\tau; x, t)$ corresponds to the uniform distribution of F_1 in $[0, 1]$. Hence to implement the selection of τ , we choose a uniform random number r_1 in $[0, 1]$ and set

$$\tau = F^{-1}(r_1; x, t); \quad (2.64)$$

similarly we select another random number r_2 and choose m such that

$$F_2(m-1 | \tau; x, t) < r_2 \leq F_2(m | \tau; x, t). \quad (2.65)$$

Having selected τ and m , we advance time by τ and carry out the m -th step in the reaction scheme. The whole procedure is then repeated for the new state. This iteration produces a random path in time of the system. To get the mean path we take a large number of these trajectories and average.

The state of a system close to equilibrium is given by a Gaussian distribution for which the mean is the most probable value;²¹ in systems far from equilibrium the mean trajectory need not be the most probable one. The above algorithm is suitable for finding mean quantities. An approach that focuses attention on the most probable quantities and deviations from them is the path integral approach.²² Let us

consider the stochastic differential equation

$$(I) \quad dx_t = -r(x_t)dt + dw_t \quad (2.66)$$

or, equivalently,

$$(S) \quad dx_t = -r(x_t)dt + dw_t. \quad (2.67)$$

The Green's function $P(x_f, t_f | x_0, t_0)$ (i.e., the probability that the system reaches x_f at t_f given that it is x_0 at t_0) is given by the integral of a functional over the class of continuous functions $x(t)$ subject to the end point conditions $x(t_f) = x_f$ and $x(t_0) = x_0$, namely

$$P(x_f, t_f | x_0, t_0) = \int \exp \left\{ - \int_{t_0}^{t_f} L(\dot{x}, x, \tau) d\tau \right\} \mathcal{D}[x(t)], \quad (2.68)$$

where

$$L(\dot{x}, x, t) = \frac{1}{2} [\dot{x}(t) + r(x(t))]^2 - \frac{1}{2} \frac{d}{dx}(r(x)). \quad (2.69)$$

In other words, each path connecting (x_0, t_0) and (x_f, t_f) is

assigned a probability density $\exp \left\{ - \int_{t_0}^{t_f} L(\dot{x}, x, \tau) d\tau \right\}$ and the

total probability is obtained by summing the contributions of individual paths. The most heavily weighted path is obtained

by minimizing the functional $\int_{t_0}^{t_f} L(\dot{x}, x, \tau) d\tau$ subject to the end conditions. Thus the path with maximum probability density is given by the solution of

$$\frac{d^2x}{dt^2} = r(x) \frac{dr}{dx} - \frac{1}{2} \frac{d^2r}{dx^2}. \quad (2.70)$$

Similar path integral expressions have been developed²³ in special cases for the most probable path of a process satisfying

$$(I) \quad dX_t = r(X_t)dt + \sqrt{a(X_t)}dW_t. \quad (2.71)$$

CHAPTER III

A REVIEW OF STUDIES ON THE SCHLÖGL MODEL

Chemical reactions as a rule are nonlinear processes from the thermodynamic point of view; i.e., the rate of reaction is nonlinear in chemical affinity. Hence chemical reaction models are convenient for studying phenomena that are impossible in the linear regime. With this aim, Schlögl introduced in 1971 two reaction models and showed the presence of multiple steady states.^{3,4} He also showed the possibility of phase transitions and critical phenomena. Since then these phenomena have been extensively studied by various authors using both models, especially the termolecular model. A summary of the important studies on the termolecular model is given in this chapter.

3.1 FURTHER PROPERTIES OF THE STEADY STATES

The rate equation for the Schlögl model is

$$\frac{dx}{dt} = -k_2x^3 + k_1[A]x^2 - k_4x + k_3[B]. \quad (3.1)$$

In terms of the scaled variables

$$n = \frac{3k_2}{k_1[A]}x, \quad (3.2)$$

$$\text{and } t_s = \frac{k_1^2[A]^2}{9k_2}t, \quad (3.3)$$

it becomes

$$\begin{aligned}\frac{dn}{dt_s} &= -n^3 + 3n^2 - \beta_1 n + \beta_2 \\ &= F'(n),\end{aligned}\tag{3.4}$$

where

$$\beta_1 = \frac{9k_2 k_4}{k_1^2 [A]^2}\tag{3.5}$$

$$\beta_2 = \frac{27k_2^2 k_3 [B]}{k_1^3 [A]^3}.\tag{3.6}$$

The critical point is given by

$$\beta_1^c = 3, \quad \beta_2^c = 1, \quad n^c = 1.\tag{3.7}$$

Consider an arbitrary $\beta_2 > 0$. For this β_2 there is a set of concentration values n_s and corresponding β_1 values $\beta_1(n_s)$ such that a system described by $n = n_s$, $\beta_1 = \beta_1(n_s)$ and β_2 is at steady state; i.e., $F'(n_s, \beta_1) = 0$. By solving this we get a relation between β_1 and n_s . Then the steady state equation can be written as

$$F'(n_s, \beta_1(n_s)) = 0.\tag{3.8}$$

Differentiating this, we obtain

$$\frac{dF'}{dn_s} = \frac{\partial F'}{\partial n_s} + \frac{\partial F'}{\partial \beta_1} \frac{d\beta_1}{dn_s} = 0.$$

From the results following equation (2.7) we have

$$\frac{\partial F'}{\partial n_s} = 0$$

at any marginal stability point, while

$$\frac{\partial F'}{\partial \beta_1} = -n \neq 0$$

in general. Therefore,

$$\frac{d\beta_1}{dn_s} = 0 \tag{3.9}$$

at any marginal stability point. Since the two marginal stability points merge at the critical point, it is an inflection point; i.e.,

$$\frac{d^2\beta_1}{dn_s^2} = 0 \tag{3.10}$$

at the critical point. From (3.8) we also obtain

$$\frac{d^2 F'}{dn_s^2} = \frac{\partial^2 F'}{\partial n_s^2} + \frac{\partial^2 F'}{\partial n_s \partial \beta_1} \frac{d\beta_1}{dn_s} + \frac{\partial F'}{\partial \beta_1} \frac{d^2 \beta_1}{dn_s^2} + \frac{d\beta_1}{dn_s} \frac{\beta}{\partial \beta_1} \left(\frac{dF'}{dn_s} \right) = 0 \quad (3.11)$$

The second, third, and fourth terms contain factors of

$\frac{d\beta_1}{dn_s}$ and $\frac{d^2 \beta_1}{dn_s^2}$ which vanish at the critical point. Thus equation

(3.11) leads to

$$\frac{\partial^2 F'}{\partial n_s^2} = 0 \quad (3.12)$$

at the critical point. These relations can be generalized to multicomponent systems.²⁴

The above properties are possessed by the Schlögl model when the concentrations of A and B are kept constant. Escher and Ross²⁵ have recently considered the Schlögl model with constant flux of A, B, and X, and have studied the number and stability of steady states. Let the input be a mixture of these chemicals (of fixed composition) entering the reactor at rate J and let the output have the same rate J. The reactor is assumed to be well stirred so that the output stream has the same composition as the material in the reactor. If the input stream contains no A, then the system does not exhibit instability. If the input stream contains only A, then interesting steady state structures are obtained. For example, there exists a particular concentration of A

in the input stream such that the following situation is observed: For small values of J the system has two stable steady states and one unstable steady state. As J increases two of them disappear leaving a single stable steady state. At a still higher value of J two more steady states appear, but both are unstable. With further increase in J one of the unstable states becomes stable, and eventually a single stable steady state remains. Escher and Ross also studied a general case where all species are in the input mixture. In this case there are two disjoint regions of J where there are unstable steady states. The instability in the higher J value range is accompanied by two stable steady states, whereas the lower range has a limit cycle oscillation in the concentration space.

3.2 COEXISTENCE OF TWO PHASES

Let the Schlögl reactions occur in a reactor which is not being stirred and let the concentrations of A and B be kept constant. If A and B diffuse very rapidly but X diffuses slowly, then the rate equation becomes

$$\frac{\partial}{\partial t} \chi(\underline{r}, t) = D \nabla_{\underline{r}}^2 \chi(\underline{r}, t) + F[\chi(\underline{r}, t)], \quad (3.13)$$

where

$$F(\chi) = -k_2 \chi^3 + k_1 [A] \chi^2 - k_4 \chi + k_3 [B] \quad (3.14)$$

and D is the diffusion coefficient for X . First we seek steady states⁴ which are uniform along two spatial dimensions and vary only along one coordinate r_3 . These steady states are solutions of

$$\frac{\partial^2 n}{\partial x_3^2} = n^3 - 3n^2 + \beta_1 n - \beta_2 = -\frac{dU}{dn}, \quad (3.15)$$

where

$$x_i = \frac{k_1 [A]}{3\sqrt{Dk_2}} r_i \quad i = 1, 2, 3. \quad (3.16)$$

For the analysis below, it is useful to note that this is the equation of motion of a classical unit mass moving in the potential

$$U(n) = -\frac{n^4}{4} + n^2 - \beta_1 \frac{n}{2} + \beta_2 n, \quad (3.17)$$

if x_3 is identified with the time coordinate and n with position. To determine the steady-state coexistence criterion for this case we further impose the boundary conditions

$$n(x_3 = -\infty) = n_1$$

$$\text{and } n(x_3 = +\infty) = n_3, \quad (3.18)$$

so that the concentration of X takes on two different

homogeneous steady state values (n_1 and n_3) at the extremes of the r_3 coordinate. Equation (3.15) and boundary conditions (3.18) together describe the motion of a classical body from one maximum of the potential $U(n_1)$ where it was at rest at $t = -\infty$ to the second maximum $U(n_3)$ where it comes to rest at $t = +\infty$. This motion is possible only if the potential maxima are equal; i.e.,

$$U(n_1) = U(n_3). \quad (3.19)$$

This condition is satisfied when the three steady states are related by

$$n_2 = (n_1 + n_3) / 2. \quad (3.20)$$

Equation (3.20) is Schlögl's coexistence condition. The homogeneous steady states become

$$\begin{aligned} n_1 &= 1 - \sqrt{3-\beta_1} \\ n_2 &= 1 \\ n_3 &= 1 + \sqrt{3-\beta_1} \end{aligned} \quad (3.21)$$

and $\beta_1 = \beta_2 + 2$ at the coexistence point.

Next we seek steady states with spherical symmetry varying along the radial coordinate $r = |\underline{r}|$ and satisfying

the boundary conditions

$$n(r=0) = n_3$$

$$\text{and } n(r=\infty) = n_1. \quad (3.22)$$

Such states can be considered as droplets of the condensed phase with composition n_3 in a medium of composition n_1 .

The steady state equation becomes

$$D' \frac{\partial^2 n}{\partial r^2} = - \frac{2D'}{r} \frac{\partial n}{\partial r} - \frac{dU}{dn}, \quad (3.23)$$

where $D' = \frac{9k_2 D}{k_1^2 A^2}$. This corresponds to the motion of a

mass in the potential U with dissipation of energy due to friction. A solution exists if the energy lost is equal to the potential difference; i.e., if

$$U(n_2) - U(n_1) = 2D' \int_0^\infty \frac{1}{r} \left(\frac{\partial n}{\partial r} \right)^2 dr. \quad (3.24)$$

If we assume that the radius r_0 of the droplet is substantially larger than the thickness of the boundary layer over which the concentration change is significant, then equation (3.24) leads to the condition for the existence of droplets:

$$\beta_2 = \beta_1 - 2 + \frac{2}{r_0} \sqrt{2D'} \left\{ 1 - \frac{\beta_1}{3} \right\}. \quad (3.25)$$

Similarly, the boundary conditions

$$n(r=0) = n_1$$

$$\text{and } n(r=\infty) = n_3 \quad (3.26)$$

correspond to a steady bubble of composition n_1 in a medium of composition n_3 . The condition for a bubble of radius r_0 is

$$\beta_2 = \beta_1 - 2 - \frac{2}{r_0} \sqrt{2D'} \left\{ 1 - \frac{\beta_1}{3} \right\}. \quad (3.27)$$

Using a linear analysis, Schlögl et al²⁶ have recently studied the effects of small fluctuations in systems with coexisting steady states varying only along the r_3 coordinate. When Schlögl's coexistence condition is satisfied, we have by the transformation $y = n - 1$

$$\frac{dy}{dt_s} = \nabla_x^2 y - y(y^2 - y_0^2), \quad (3.28)$$

where $y_0 = \sqrt{3-\beta_1}$ and t_s and x_i are defined by equations (3.3) and (3.16) respectively. The coexistence solution of this equation is

$$y^* = y_0 \tanh (y_0 x_3 / \sqrt{2}) . \quad (3.29)$$

After the change of variable

$$\zeta = \tanh (y_0 x_3 / \sqrt{2}) , \quad (3.30)$$

the linearized equation in terms of the deviation

$$\psi = (y - y^*) / y_0 \quad (3.31)$$

becomes

$$\frac{d}{dt_s} \psi = \frac{y_0^2}{2} (1 - \zeta^2) \mathcal{D}_2^2 \psi + \Delta \psi , \quad (3.32)$$

where

$$\Delta = \frac{\partial^2}{\partial x_1^2} + \frac{\partial^2}{\partial x_2^2} \quad (3.33)$$

and

$$\mathcal{D}_\ell^\mu = \frac{\partial}{\partial \zeta} (1 - \zeta^2) \frac{\partial}{\partial \zeta} + \ell(\ell+1) - \frac{\mu^2}{1 - \zeta^2} . \quad (3.34)$$

Introducing the separation of variables

$$\psi(x_1, x_2, \zeta, t_s) = \Omega(x_1, x_2) u(\zeta) \Gamma(t_s) ,$$

we get

$$\mathcal{D}_2^\mu u = 0 , \quad (3.35)$$

$$(\Delta + k^2) \Omega = 0 , \quad (3.36)$$

$$\text{and } \Gamma(t_s) = e^{-\nu t_s}, \quad (3.37)$$

with

$$\nu = k^2 + (4-\mu^2) \frac{y_0^2}{2}. \quad (3.38)$$

The mode with smallest ν is given by the associated Legendre function,

$$P_2^2(\zeta) = 3(1-\zeta^2) = \frac{3\sqrt{2}}{y_0} \frac{\partial \zeta}{\partial x_3} \quad (3.39)$$

with $\nu = k = 0$, and therefore the solution including the small deviation is

$$\begin{aligned} y &= y^*(x_3) + y_0 \psi(x_3) \\ &= y^*(x_3) + \frac{3\sqrt{2}\Omega_0}{y_0} \frac{d}{dx_3} y^*(x_3) \\ &= \left\{ 1 + \delta x_3 \frac{\partial}{\partial x_3} \right\} y^*(x_3) \\ &= y^*(x_3 + \delta x_3), \end{aligned} \quad (3.40)$$

where $\delta x_3 = 3\sqrt{2}\Omega_0 / y_0$. Thus this lowest mode called a "Goldstone mode"²⁷ results in a slight shift along x_3 . The shifted solution is also stationary.

All time-dependent modes that vanish at infinity include

the factor

$$\begin{aligned}
 u_L &= P_2^1(\zeta) = -3\zeta(1-\zeta^2)^{\frac{1}{2}} \\
 &= -\frac{3 \sinh (y_0 x_3 / \sqrt{2})}{[\cosh (y_0 x_3 / \sqrt{2})]^2}.
 \end{aligned} \tag{3.41}$$

This determines the long-time decay of perturbations along the x_3 coordinate. There is also a continuous spectrum of solutions $P_2(\zeta)$ that oscillate at infinity.

When the coexistence condition is not satisfied, there is no stationary solution to equation (3.13). However, there are solutions which move along the x_3 coordinate with constant velocity, c . The solutions are given by

$$y(t) = y_0 \tanh [(x_3 - ct_s)y_0/2], \tag{3.42}$$

where

$$c = \sqrt{2} [n_2 - (n_1 + n_3)/2]. \tag{3.43}$$

Here again there is a nondecaying Goldstone mode moving with the same velocity, c . For

$$\left| n_2 - \frac{n_1 + n_3}{2} \right| < \frac{1}{3} y_0, \tag{3.44}$$

the long-time regression is controlled by another discrete mode. When the inequality (3.44) is not satisfied, the long-time regression is controlled by the lowest of the continuous spectrum of modes.

3.3. APPROXIMATE SOLUTION OF MASTER EQUATION

Matsuo²⁸ has developed WKB-type solution to the master equation in the limit of large system size. As already seen (equation (2.41)), the master equation can be transformed to a form with symmetric matrix:

$$\frac{\partial}{\partial t} Q(x,t) = \sum_y S_{xy} Q(y,t). \quad (3.45)$$

Its solution is

$$Q(x,t) = Q_0(x) + \sum_{j=1}^{\infty} p_j e^{\lambda_j t} Q_j(x) \quad (3.46)$$

where $\underline{S} \underline{Q}_j = \lambda_j \underline{Q}_j$. Let us denote the diagonal elements of \underline{S} by $S_0(x)$ and the off-diagonal elements by $-S_+(x)$. Then the eigenvalue equation is

$$[S_0(x) - \lambda_j] Q_j(x) = S_+(x-1)Q_j(x-1) + S_+(x)Q_j(x+1). \quad (3.47)$$

We look for solutions of the WKB type, namely

$$Q(x) = \operatorname{Re} \left\{ C(x) \exp \int^x w(y) dy \right\}, \quad (3.48)$$

where C and w are assumed to be slowly varying functions of x . Substituting this in the equation and its derivative and neglecting small quantities such as $C(x+1) - C(x)$, we get expressions for $C(x)$ and $w(x)$. The functional form of the solution depends on which of the following three situations obtains:

$$\begin{aligned} \text{a)} \quad & -2S_+(x) < S_0(x) - \lambda < 2S_+(x) \\ \text{b)} \quad & S_0(x) - \lambda > 2S_+(x) \\ \text{c)} \quad & S_0(x) - \lambda < -2S_+(x). \end{aligned} \quad (3.49)$$

We obtain quantum conditions on the eigenvalues by matching the solutions in adjacent regions. For the Schlögl model the state space can be divided into five regions separated by x_1, x_2, x_3 and x_4 , in which conditions a, b, a, b, a are satisfied in order. If the middle region is macroscopic in size, then the two a-regions can be considered independent and the connection conditions are simplified. In this approximation the eigenvalue λ must satisfy one of the following conditions:

$$\frac{1}{\pi} \int_{x_1}^{x_2} q(x) dx = \ell_1 + \frac{1}{2},$$

$$\frac{1}{\pi} \int_{x_3}^{x_4} q(x) dx = \ell_2 + \frac{1}{2}, \quad (3.50)$$

where ℓ_1 and ℓ_2 are nonnegative integers and

$$q(x) = \cos^{-1} \left\{ \frac{S_0(x) - \lambda}{2S_+(x)} \right\}. \quad (3.51)$$

From this condition we can obtain the density of eigenstates

$$\rho(\lambda) = \frac{d\ell_1}{d\lambda} + \frac{d\ell_2}{d\lambda}. \quad (3.52)$$

It is found that in the limit $\varepsilon_1 = V^{-1} \rightarrow 0$, the density of eigenstates near $\lambda = 0$ diverges at the marginal stability points and the critical point. This divergence is given by

$$\begin{aligned} \lim_{\varepsilon_1, \lambda \rightarrow 0} \rho(\lambda) &\sim \lambda^{-1/4} && \text{(marginal stability points)} \\ &\sim \lambda^{-1/3} && \text{(critical point)}. \end{aligned} \quad (3.53)$$

Since the eigenvalues accumulate near $\lambda = 0$, the decay to the stationary distribution becomes infinitely slow. This is called "critical slowing down".

When there are three distinct steady states, it can be shown that the first decay mode has one node and the second has the largest of its three peaks in the vicinity of the unstable steady state. Thus we can find the relaxation times

from the unstable steady states to be

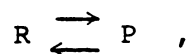
$$\lambda_1^{-1} = [k_2 (X_2 - X_1) (X_3 - X_2)]^{-1} \quad (3.54)$$

where k_2 is the rate constant of the second step; similarly, an expression can be obtained for the relaxation time from the metastable state to the stable one.

3.4 RELATIVE STABILITY

We have already seen Schlögl's coexistence condition. When this condition is not satisfied, it is clear from equation (3.42) that the system will eventually become homogeneous. If n_2 is closer to n_1 than to n_3 , then the final state will be n_1 ; otherwise, it will be n_3 . This can be regarded as a criterion for relative stability of the two stable steady states. Other proposed criteria are discussed below.

Noyes²⁹ has considered a general reaction scheme with a single reactant R producing a single product P,



occurring in a continuous flow reactor. The Schlögl scheme with constant flow boundary conditions is included in this class of models. The rate equation is

$$\frac{dR}{dt} = k_0 (R_0 - R) - v(R), \quad (3.55)$$

where $v(R)$ is the net rate of reaction, k_0 is the rate of flow of matter through the reactor and R_0 is the concentration of R in the input stream. It is assumed that the reactor is efficiently stirred at all times; then the composition of the output stream is the same as the composition in the reactor itself. Functions for $v(R)$ can be selected so that there are two stable steady states R_α and R_β for a range of k_0 values. Let us prepare two adjacent flow reactors with identical external conditions including the flux rate $k_0 R_0$, but at different stable steady states. In order to determine the relative stability of the two states, Noyes has proposed making small holes in the wall between these reactors thereby allowing hydrodynamic mixing with a rate constant k_x . For small k_x the concentration of R in the two tanks will be perturbed to the new values R_α' and R_β' .

Noyes has given a criterion, namely

$$k_0 + \left(\frac{\partial v}{\partial R} \right)_{R_\alpha} = 0, \quad (3.56)$$

at which a slight increase of k_x is claimed to cause the R_α' state to disappear and the combined system to settle with both reactors in the R_β state indicating that R_β is more stable. If

$$k_0 + \left(\frac{\partial v}{\partial R} \right)_{R_\beta} = 0 \quad (3.57)$$

happens first as a consequence of mixing with steadily increasing k_x , then the higher stability is assigned to R_α . As will be seen in chapter VI, this criterion and the proposed mixing experiment are unsuitable for determining relative stability.

Another criterion for relative stability is obtained by taking the thermodynamic limit in the stationary distribution of the master equation.³⁰⁻³² To do this, we should first extract the system size dependence from all parameters and take the limit as $V \rightarrow \infty$, $X \rightarrow \infty$ while X/V remains fixed. The rate constants have the volume dependence

$$c_i = k_i n_i! V^{1-m_i}, \quad (2.20)$$

where n_i is the molecularity of the i -th step in X and m_i is the total molecularity of the i -th step. The master equation for the concentration $\chi = X/V$ becomes

$$\begin{aligned} \frac{\partial}{\partial t} P(\chi, t) &= a_+(\chi - \epsilon_1) P(\chi - \epsilon_1, t) + a_-(\chi + \epsilon_1) P(\chi + \epsilon_1, t) \\ &\quad - [a_+(\chi) + a_-(\chi)] P(\chi, t). \end{aligned} \quad (3.58)$$

Its stationary solution is given recursively by

$$P_s(\chi) = \frac{a_+(\chi - \epsilon_1)}{a_-(\chi)} P_s(\chi - \epsilon_1), \quad (3.59)$$

where

$$\varepsilon_1 = 1/V,$$

$$b = B/V,$$

$$a_+(\chi) = \frac{k_1}{2}vb(\chi - \varepsilon_1) + k_3bV,$$

$$\text{and } a_-(\chi) = \frac{k_2}{6}V\chi(\chi - \varepsilon_1)(\chi - 2\varepsilon_1) + k_4V. \quad (3.60)$$

$P_s(\chi)$ has local maxima at χ_1 and χ_3 and a local minimum at χ_2 , where $\chi_1 < \chi_2 < \chi_3$ are the steady state concentrations. First we evaluate

$$\lim_{V \rightarrow \infty} \frac{P_s(\chi)}{P_s(\chi_1)} \quad \text{for } 0 < \chi < \chi_1 ;$$

in terms of the function

$$G(z) = \frac{a_-(z + \varepsilon_1)}{a_+(z)}, \quad (3.61)$$

$$\ln \frac{P_s(\chi)}{P_s(\chi_1)} = \ln G_\chi + \ln G_{\chi + \varepsilon_1} + \dots + \ln G_{\chi_1 - \varepsilon_1}$$

$$= V \int_{\chi}^{\chi_1} \ln G(z) dz \quad (3.62)$$

for large V . The integral representation is verified by writing

the integral as a Riemann sum with $\Delta z = \varepsilon_1$. Since $P_S(z)$ is increasing in $0 < z < \chi_1$, $G(z) < 1$ in this range and the integral is negative. The required ratio thus goes to zero in the thermodynamic limit. Following the same procedure it can also be shown that

$$\lim_{V \rightarrow \infty} \frac{P_S(\chi)}{P_S(\chi_1)} = 0 \quad \text{for } \chi_1 < \chi < \chi_2$$

$$\text{and } \lim_{V \rightarrow \infty} \frac{P_S(\chi)}{P_S(\chi_3)} = \delta_{\chi\chi_3} \quad \text{for } \chi_2 < \chi < \infty. \quad (3.63)$$

Thus the stationary distribution becomes sharply peaked at either or both of the stable steady states as the volume of the system increases without bound. Finally the relative stability is determined by

$$\lim_{V \rightarrow \infty} \frac{P_S(\chi_1)}{P_S(\chi_3)} = \lim_{V \rightarrow \infty} \exp \left\{ V \int_{\chi_1}^{\chi_3} \ln G(z) dz \right\} \quad (3.64)$$

which is zero, one or infinity depending on whether the integral is negative, zero or positive. Thus the equistability condition is given by

$$\int_{\chi_1}^{\chi_3} \ln G(z) dz = 0. \quad (3.65)$$

Procaccia and Ross³³ have studied relative stability

based on the nonequilibrium thermodynamics developed by Levine.^{34,35} Let us consider an open system whose microscopic states \underline{x} are numerous compared to the macroscopic information available in terms of \underline{X} . Then the distribution over the microscopic states must satisfy

$$\sum_{\underline{x}} x_i P(\underline{x}, t) = X_i(t) \quad \text{for } i = 0, 1, \dots, M \quad (3.66)$$

where $x_0 = 1$ imposes normalization. These equations are insufficient to determine $P(\underline{x}, t)$. Of all the distributions satisfying (3.66) the one with minimum information content is postulated to describe the system, in the absence of any other information. This distribution also maximizes the entropy function

$$S[P] = - \sum_{\underline{x}} P(\underline{x}, t) \ln [P(\underline{x}, t)/g(\underline{x})], \quad (3.67)$$

where $g(\underline{x})$ is the degeneracy of state \underline{x} . When \underline{x} specifies the number of molecules of each type, the degeneracy is

$$g(\underline{x}) = \left(\sum_{i=1}^M x_i \right)! / \prod_{j=1}^M x_j! \quad (3.68)$$

The distribution thus obtained is

$$P(\underline{x}, t) = g(\underline{x}) \exp \left\{ - \sum_{j=0}^M \mu_r(t) x_r \right\}, \quad (3.69)$$

where $\mu_r(t)$ is the Lagrangian multiplier corresponding to the r -th constraint (3.66). The function

$$e^{\mu_0} = \sum_{\underline{x}} g(\underline{x}) \exp \left\{ - \sum_{i=1}^M \mu_i(t) x_i \right\} \quad (3.70)$$

is called the partition function. From the conservation of total probability,

$$\frac{\partial \mu_0}{\partial t} = - \sum_{i=1}^M x_i(t) \frac{\partial \mu_i}{\partial t}. \quad (3.71)$$

In the following analysis the equilibrium state is used as a reference state. (This state is attained in the Schlögl model only when the flux constraints are removed.) Denoting equilibrium quantities with a superscript e , the entropy deficiency is defined as

$$K[P(t), P^e] = \sum_{\underline{x}} P(\underline{x}, t) \ln \frac{P(\underline{x}, t)}{P^e(\underline{x})}. \quad (3.72)$$

Substituting (3.69) into (3.72) we find

$$K(t) = - \Delta \mu_0(t) - \sum_{i=1}^M \Delta \mu_i(t) x_i(t) \quad (3.73)$$

where $\Delta \mu_i(t) = \mu_i(t) - \mu_i^e$. In analogy with classical mechanical

equations, we look for a function $L(\{X_i\}, \{\dot{X}_i\})$ such that

$$\frac{d}{dt} \Delta\mu_i = \left(\frac{\partial L}{\partial X_i} \right)_{X_{j \neq i}, \dot{X}_k} \quad (3.74)$$

This equation is satisfied if L is defined as

$$L = \sum_{i=1}^M \Delta\mu_i \frac{dX_i}{dt} \quad (3.75)$$

To prove this, we first note that

$$\begin{aligned} \frac{dK}{dt} &= - \frac{d\Delta\mu_0}{dt} - \sum_{i=1}^M X_i \frac{d\Delta\mu_i}{dt} - \sum_{i=1}^M \Delta\mu_i \frac{dX_i}{dt} \\ &= - \sum_{i=1}^M \Delta\mu_i \frac{dX_i}{dt} = -L \end{aligned} \quad (3.76)$$

using (3.71). Now

$$\left(\frac{\partial L}{\partial X_i} \right)_{X_{j \neq i}, \dot{X}_k} = - \frac{d}{dt} \left(\frac{\partial K}{\partial X_i} \right)_{X_{j \neq i}, \dot{X}_k} = \frac{d}{dt} \Delta\mu_i \quad (3.77)$$

from (3.73).

The assumption of maximum entropy at all times has led to the equation of evolution (3.77). This evolution equation is now used to study the relative stability in the Schlögl

model. First since $g(\underline{x})$ is a multinomial coefficient, we may write the partition function as

$$e^{\mu_0} = \left(\sum_{i=1}^M e^{-\mu_i} \right)^N, \quad (3.78)$$

where $N = \sum_{i=1}^M x_i$ is assumed to remain constant in time. By

differentiating (3.70) we find

$$\frac{\partial \mu_0}{\partial \mu_i} = -x_i. \quad (3.79)$$

Differentiating (3.78) and comparing with (3.71),

$$\frac{d\mu_i}{dt} = -\frac{1}{x_i} \frac{dx_i}{dt}. \quad (3.80)$$

The evolution equation for the Schlögl model becomes

$$\begin{aligned} \frac{1}{x} \frac{dx}{dt} &= \frac{\partial L}{\partial x} \\ &= \frac{\partial \Delta \mu_A}{\partial x} \frac{dA}{dt} + \frac{\partial \Delta \mu_X}{\partial x} \frac{dX}{dt} + \frac{\partial \Delta \mu_B}{\partial x} \frac{dB}{dt}, \end{aligned} \quad (3.81)$$

where $\frac{dA}{dt}$ and $\frac{dB}{dt}$ are changes due to the reactions alone.

Suppose we start the system at the stable state x_1 at $t = -\infty$. If the other steady state is more stable, it is expected that

the system will evolve to X_3 given enough time. This transition will occur only if the evolution equation is satisfied.

Multiplying by $\frac{dX}{dt}$ and integrating from $t = -\infty$ to $t = \infty$ gives

$$-\int_{-\infty}^{\infty} \frac{1}{X} \left(\frac{dX}{dt} \right)^2 dt = \int_{-\infty}^{\infty} \frac{\partial L}{\partial X} \frac{dX}{dt} dt = \int_{X_1}^{X_3} \frac{\partial L}{\partial X} dX \quad (3.82)$$

under the hypothesis that a transition occurs, i.e., $X(t=\infty)=X_3$. Since the left hand side is negative semidefinite, X_3 is more stable than X_1 only if the integral on the right hand side is negative. If it is positive, then the reverse transition can occur. Thus the equistability condition is

$$\int_{X_1}^{X_3} \frac{\partial L}{\partial X} dX = 0. \quad (3.83)$$

Relative stability can also be studied using first passage times based on the master equation.³⁶ We consider the mean time τ_u of first arrival at X_3 if the system starts from X_1 at time zero and we restrict attention to single variable systems such as the Schlögl model. Let $v_{\pm}(x)$ be the average number of $x \rightarrow x \pm 1$ transitions executed and $t_u(x)$ be the average time spent in state x during the passage from X_1 to X_3 . Then from equation (2.60), we have

$$\frac{t_u(x)}{v_+(x) + v_-(x)} = \frac{1}{a(x)}. \quad (3.84)$$

for the mean residence time at state x and from (2.61)

$$\frac{v_{\pm}(x)}{v_{+}(x) + v_{-}(x)} = \frac{a_{\pm}(x)}{a(x)} \quad (3.85)$$

Solving these equations for $t_u(x)$, we get

$$t_u(x) = \frac{v_{\pm}(x)}{a_{\pm}(x)}. \quad (3.86)$$

Since every trajectory under consideration has exactly one $X_3-1 \rightarrow X_3$ transition,

$$v_{+}(X_3-1) = 1. \quad (3.87)$$

Every trajectory starting from X_1 must also satisfy certain conditions in order to reach X_3 . At a state $x < X_1$ it must execute an equal number of $x \rightarrow x+1$ and $x+1 \rightarrow x$ transitions and at any state between X_1 and X_3 it must execute one more $x \rightarrow x+1$ transition than the reverse. Since all trajectories satisfy these conditions, so does the average.

$$v_{+}(x-1) = v_{-}(x) + h(x-X_1) \quad \text{for } x < X_3 \quad (3.88)$$

where $h(x)$ is the Heaviside step function. Thus we have a recursion relation for $t_u(x)$:

$$t_u(x-1) = \frac{a_{-}(x)}{a_{+}(x-1)} t_u(x) + \frac{h(x-X_1)}{a_{+}(x-1)}, \quad x < X_2-1 \quad (3.89)$$

with

$$t_u(X_3-1) = \frac{1}{a_{+}(X_3-1)}.$$

The mean first passage time is given by summing the mean times spent in all accessible intermediate states.

$$\tau_u = \sum_{x=0}^{X_3-1} t_u(x), \quad (3.90)$$

Similarly we can derive for the downward transition

$$\tau_d = \sum_{x=X_1+1}^{\infty} t_d(x), \quad (3.91)$$

where

$$t_d(X_1+1) = \frac{1}{a_-(X_1+1)},$$

and in general

$$t_d(x+1) = \frac{a_+(x)}{a_-(x+1)} t_d(x) + \frac{h(X_3-x)}{a_-(x+1)}. \quad (3.92)$$

Then we can define relative stability based on the difference $\tau_u - \tau_d$. If this is negative, the upper steady state X_3 is more stable and conversely. Thus the equistability criterion is

$$\tau_u = \tau_d. \quad (3.93)$$

A more rigorous and direct derivation of the same expression

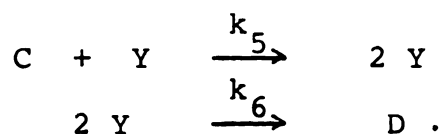
for the first passage time from the master equation is available in reference 37.

We have several coexistence conditions based on different criteria for relative stability. Schlögl's criterion includes the effects of diffusion but neglects fluctuations, whereas the two thermodynamic criteria (equations (3.65) and (3.83)) and the kinetic criterion (3.93) are based on descriptions neglecting spatial fluctuations. These two kinds of criteria need not agree. In an intermediate situation it is possible³⁸ that a local fluctuation large enough for a phase transition arises due to the chemical reactions in the system but it diffuses away rather than causing a transition. On the other hand, when a slowly moving boundary is predicted by Schlögl's criterion, one may expect several dynamic patches of the two phases due to local fluctuations. Thus the actual coexistence point should lie between the points predicted by Schlögl's criterion and the thermodynamic criteria. Local fluctuations in nonequilibrium system can be investigated using the multivariate master equation described in the next section.

3.5 MEAN FIELD THEORY AND MULTIVARIATE MASTER EQUATION APPROACHES TO INCLUDE LOCAL FLUCTUATIONS.

The master equation based on uniform concentrations of the species in the reacting mixture is called the birth and death equation. Malek-Mansour and Nicolis³⁹ have advanced

several criticisms of this method. They have stated that the prescription for calculating transition probabilities treats the reactive encounters of molecules as equally likely irrespective of the position of these molecules in the reaction vessel. This statement is simply not true. What appears in the master equation is the probability that a reactive collision will occur somewhere in the reactor, which is different from the probability that a given set of molecules will undergo a reactive collision. This point has been amply clarified by Gillespie.⁴⁰ Another criticism is based on a study of the apparently pathological reaction scheme



The deterministic analysis gives an unstable steady state $Y = 0$ and a stable steady state,

$$Y = k_5 C / k_6, \quad (3.94)$$

but the stationary distribution of the birth and death master equation is

$$P_s(Y=y) = \delta_{y0}. \quad (3.95)$$

According to equation (3.95) the system settles into the

state predicted to be unstable by the deterministic analysis. From this result Malek-Mansour and Nicolis concluded that the transition probability calculated using the birth-and-death model is wrong; this conclusion is based on the expectation that the deterministic analysis always gives the correct stability. A careful consideration of the reaction scheme reveals that the result obtained from the master equation represents a genuine phenomenon consistent with the assumed mechanism.⁴¹ In the vicinity of the null state, the first reaction is much more likely to occur than the second due to the presence of C. Nonetheless it is possible that the few remaining Y molecules will react, eliminating Y from the system. Once the system has reached the null state, Y molecules can no longer be produced. This means that the null state will be eventually reached due to fluctuations and it is the only asymptotically stable state. Thus the model system is expected to behave as predicted by the birth-and-death master equation. It is the deterministic equation that gives wrong results due to the neglect of fluctuations.

However the master equation does have limitations, as correctly pointed out by the authors mentioned above.³⁹ They have developed a mean field theory to remove the limitations arising from neglect of spatially inhomogeneous fluctuations. Although the birth-and-death master equation includes fluctuations in particle number, it assumes the concentration of the chemical species to be uniform throughout

the reactor. This need not be the case when stirring and diffusion are not efficient. Hence a realistic system can have properties such as a finite correlation length which is a measure of the effective wavelength of local fluctuations.

The mean field approach starts by considering a subvolume ΔV which is comparable in size to the cube of the correlation length. The birth-and-death description is assumed to be valid within this subvolume. Then the probability distribution for the entire system $P(x_i, x_o, t)$ evolves according to

$$\frac{\partial}{\partial t} P(x_i, x_o, t) = R_{ch}(\Delta V) + R_{ch}(V-\Delta V) + T(\Delta V, V-\Delta V), \quad (3.96)$$

where x_i is the number of molecules in ΔV and x_o is the number of molecules outside ΔV . $R_{ch}(\Delta V)$ is the reaction probability term arising from birth and death processes in ΔV and T arises from the transport of matter across the boundary of ΔV .

Assuming that the transport of heat is very fast (so that the system remains isothermal), T may be calculated using the position and velocity distributions from the kinetic theory of gases. Next the mean field assumption is introduced and the evolution equation is summed over the external variables, x_o and $V-\Delta V$. The system is required to be homogeneous on the average, i.e.,

$$\langle x_o / (V-\Delta V) \rangle = \langle x_i / \Delta V \rangle . \quad (3.97)$$

Moreover, the particle distributions in ΔV and in $V-\Delta V$ are assumed to be uncorrelated, so that

$$P(x_i, x_0, t) = P_{\Delta V}(x_i, t) P_{V-\Delta V}(x_0, t). \quad (3.98)$$

Using these relations, a closed equation is derived for the evolution of the probability distribution in V :

$$\begin{aligned} \frac{\partial}{\partial t} P_{\Delta V}(x_i, t) = & R_{ch}(\Delta V) + \mathcal{D}\langle x \rangle [P_{\Delta V}(x_i+1, t) - P_{\Delta V}(x_i, t)] \\ & + \mathcal{D}[(x_i+1)P_{\Delta V}(x_i+1, t) - x_i P_{\Delta V}(x_i, t)]. \end{aligned} \quad (3.99)$$

In equation (3.99) \mathcal{D} is the effective frequency of diffusion passage of particles across the boundary of ΔV and is related to the diffusion coefficient D and mean free path by

$$\mathcal{D} = \frac{D}{\text{mean free path } \times \text{coherence length of fluctuations}}. \quad (3.100)$$

If the characteristic time scale of macroscopic changes due to chemical reaction is much longer than that of diffusion, then there is an expansion parameter.⁴² For example, in the Schlögl model if

$$\epsilon_2 = \frac{c_2}{6\mathcal{D}} = \frac{k_2}{(\Delta V)^2 \mathcal{D}} \quad (3.101)$$

is small, then the "nonlinear" master equation becomes

$$\frac{\partial}{\partial t'} P(x, t') = R_{ch} + \varepsilon_2^{-1} \left\{ \langle x \rangle [P(x-1, t') - P(x, t')] \right. \\ \left. + (x+1)P(x+1, t') - xP(x, t') \right\}, \quad (3.102)$$

where $t' = \frac{c_2}{6}t = \frac{k_2}{(\Delta V)^2}t$ and

$$R_{ch} = \frac{6}{c_2} \left\{ a_+(x-1)P(x-1, t') + a_-(x+1)P(x+1, t') \right. \\ \left. - [a_+(x) + a_-(x)] P(x, t') \right\}. \quad (3.103)$$

We can seek a solution of the form

$$P(x, t') = P_0(x, t') + \varepsilon_2 P_1(x, t') + \dots \quad (3.104)$$

Since $P(x, t')$ must be normalized independent of ε_2 , we have

$$\sum_x P_0(x, t') = 1 \quad \text{and} \quad \sum_x P_n(x, t') = 0 \quad \text{for } n > 1. \quad (3.105)$$

The solution is obtained by use of a probability generating function defined by

$$F(s, t') = \sum_{x=0}^{\infty} s^x P(x, t'). \quad (3.106)$$

$F(s, t')$ can also be expanded as a series in ε_2

$$F(s, t') = F_0(s, t') + \varepsilon_2 F_1(s, t') + \dots,$$

subject to the conditions

$$F_0(s, t') \Big|_{s=1} = 1 \quad \text{and} \quad F_n(s, t') \Big|_{s=1} = 0 \quad \text{for } n > 1. \quad (3.107)$$

Then the evolution equation becomes

$$\frac{\partial}{\partial t'} F(s, t') = R + \varepsilon_2^{-1} (s-1) \left\{ \langle x \rangle F(s, t') - \frac{\partial}{\partial s} F(s, t') \right\}, \quad (3.108)$$

with $R = \sum_{x=0}^{\infty} s^x R_{ch}$. By expanding $\langle x \rangle$ in powers of ε_2

$$\langle x \rangle = \langle x \rangle_0 + \varepsilon_2 \langle x \rangle_1 + \dots \quad (3.109)$$

and then equating the coefficients of powers of ε_2 in equation (3.108), a set of evolution equations for $F_n(s, t')$ are obtained; these can be solved successively.

As an example, let us determine the stationary distribution for the Schlögl model, which is expected to be different from that obtained from birth and death master equation. For the Schlögl model R is

$$R = (1-s) \left\{ s^2 \frac{d^3 F}{ds^3} - b_1 s^2 \frac{d^2 F}{ds^2} + b_3 \frac{dF}{ds} - b_2 F \right\} \quad (3.110)$$

where

$$b_1 = \frac{k_1}{k_2} b\Delta V = \frac{3c_1}{c_2} b\Delta V,$$

$$b_2 = \frac{k_4}{k_2} (\Delta V)^2 = \frac{6c_4}{c_2},$$

$$b_3 = \frac{k_3}{k_2} b(\Delta V)^3 = \frac{6c_3}{c_2} b\Delta V.$$

At steady state, then

$$\varepsilon_2 \left\{ s^2 \frac{d^3 F}{ds^3} - b_1 s^2 \frac{d^2 F}{ds^2} + b_3 \frac{dF}{ds} - b_2 F \right\} + \frac{dF}{ds} - \langle x \rangle_F = 0. \quad (3.111)$$

Equating the coefficients of ε_2^0 gives

$$\frac{dF_0}{ds} - \langle x \rangle_0 F_0 = 0. \quad (3.112)$$

Solving equation (3.112) subject to the condition $F_0(s=1) = 1$, we get

$$F_0 = e^{\langle x \rangle_0 (s-1)}. \quad (3.113)$$

Equating the coefficients of ε_2^1 gives

$$s^2 \frac{d^3 F_0}{ds^3} - b_1 s^2 \frac{d^2 F_0}{ds^2} + b_3 \frac{dF_0}{ds} - b_2 F_0 + \frac{dF_1}{ds} - \langle x \rangle_0 F_1 - \langle x \rangle_1 F_0 = 0 . \quad (3.114)$$

Setting $s=1$ and using (3.106), we obtain a moment equation

$$\langle x(x-1)(x-2) \rangle_0 - b_1 \langle x(x-1) \rangle_0 + b_3 \langle x \rangle_0 - b_2 = 0 . \quad (3.115)$$

Since F_0 generates a Poisson distribution, $\langle x^n \rangle = \langle x \rangle^n$ and therefore $\langle x \rangle_0$ is the solution of the macroscopic rate equation.

$$\langle x \rangle_0^3 - b_1 \langle x \rangle_0^2 + b_3 \langle x \rangle_0 - b_2 = 0 . \quad (3.116)$$

Thus for the Schlögl model three steady states may exist when $\varepsilon_2 \rightarrow 0$. To find $F_1(s)$, we substitute

$$F_1(s) = F_0(s) \psi_1(s) \quad (3.117)$$

in equation (3.114) to obtain

$$\frac{d\psi_1}{ds} = \langle x \rangle_1 - s^2 \langle x \rangle_0^3 + b_1 s^2 \langle x \rangle_0^2 - b_3 \langle x \rangle_0 + b_2 , \quad (3.118)$$

with $\psi_1(1) = 0$. Solving (3.118) yields

$$\begin{aligned} \psi_1(s) = & \langle x \rangle_1 (s-1) - \frac{1}{3} \langle x \rangle_0^3 (s^3-1) + \frac{1}{3} b_1 \langle x \rangle_0^2 (s^3-1) \\ & - b_3 \langle x \rangle_0 (s-1) + b_2 (s-1) \quad . \quad (3.119) \end{aligned}$$

To find $\langle x \rangle_1$, we equate the coefficients of ϵ_2^2 :

$$\begin{aligned} s^2 \frac{d^3 F_1}{ds^3} - b_1 s^2 \frac{d^2 F_1}{ds^2} + b_3 \frac{dF_1}{ds} - b_2 F_1 + \frac{dF_2}{ds} - \langle x \rangle_0 F_2 \\ - \langle x \rangle_1 F_1 - \langle x \rangle_2 F_0 = 0. \quad (3.120) \end{aligned}$$

Setting $s=1$ and noticing that $\left. \frac{dF_2}{ds} \right|_{s=1} = \langle x \rangle_2$, we find

$$\left\{ \frac{d^3 F_1}{ds^3} - b_1 \frac{d^2 F_1}{ds^2} + b_3 \frac{dF_1}{ds} - b_2 F_1 \right\}_{s=1} = 0. \quad (3.121)$$

Substituting the expressions (3.117) and (3.119) for F_1 and ψ_1 we finally obtain

$$\langle x \rangle_1 = \frac{-6b_3 \langle x \rangle_0^2 + \langle x \rangle_0 [6b_2 + 2b_1 b_3 - 2b_3] - 2b_2 (b_1 - 1)}{3 \langle x \rangle_0^2 - 2b_1 \langle x \rangle_0 + b_3}. \quad (3.122)$$

This procedure clearly breaks down at the marginal stability points where the denominator in (3.122) vanishes.

A more satisfactory, but more difficult treatment is the multivariate master equation approach.⁴³ In this approach too, the entire system volume is divided into a number of cells of equal volume ΔV . A birth and death process is assumed to occur in each cell, in addition to migration between adjacent cells. In contrast with the mean field approach, the equation of motion for the detailed distribution $P(\underline{x}, t)$ is considered, where the j -th component of \underline{x} is the number of X molecules in the j -th cell. $P(\underline{x}, t)$ is a n -dimensional joint distribution when there are n cells and only one chemical component is allowed to vary. The multivariate master equation for the Schlögl model is

$$\begin{aligned} \frac{\partial}{\partial t} P(\underline{x}, t) = & \sum_r \left\{ a_+(x_r-1)P(\underline{x}-\underline{\delta}_r, t) + a_-(x_r+1)P(\underline{x}+\underline{\delta}_r, t) \right. \\ & - [a_+(x_r) + a_-(x_r)] P(\underline{x}, t) \\ & \left. + D \sum_{\ell} [(x_r+1)P(\underline{x}+\underline{\delta}_\ell-\underline{\delta}_r, t) - x_r P(\underline{x}, t)] \right\} \end{aligned} \quad (3.123)$$

for all \underline{x} in Z^n where $Z = \{ 0, 1, \dots \}$, $\underline{\delta}_r$ is a row vector with r -th component unity and all other components zero, ℓ runs over all nearest neighbours of the r -th cell, and D is the diffusion coefficient of X . The generating function for the joint distribution is

$$F(\underline{s}, t) = \sum_{\underline{x}} \prod_r s_r^{x_r} P(\underline{x}, t) \quad (3.124)$$

Since the variables in the Schlögl model can be scaled leaving only two parameters we may define the parameters ω and ω' by

$$\omega = \frac{k_4}{k_2} - 3 = \frac{6c_4}{c_2(\Delta V)^2} - 3, \quad (3.125)$$

$$\omega' = \frac{k_3 b}{k_2} - 1 = \frac{6c_3 b}{c_2(\Delta V)^2} - 1, \quad (3.126)$$

and we may select $[A]$ such that

$$\frac{k_1 [A]}{k_2} = 3 \quad (3.127)$$

without loss of generality. Then $\omega = \omega' = 0$ is the critical point. The steady-state equation for the generating function becomes

$$\begin{aligned} \sum_r (1-s_r) s_r^2 & \left(\frac{1}{(\Delta V)^2} \frac{\partial^3 F}{\partial s_r^3} - \frac{3}{\Delta V} \frac{\partial^2 F}{\partial s_r^2} \right) \\ & + \sum_r (1-s_r) \left[(3+\omega) \frac{\partial F}{\partial s_r} - (1-\omega') \Delta V F \right] \\ & + D \sum_r \sum_{\ell} (s_\ell - s_r) \frac{\partial F}{\partial s_r} = 0. \end{aligned} \quad (3.128)$$

Nicolis et al have assumed that the steady state distribution is of the form

$$F = Z \exp \left\{ \Delta V \sum_r (s_r - 1) \right\}, \quad (3.129)$$

and that the volume of the cells is sufficiently large that the solution can be obtained as a perturbation expansion in

$$\varepsilon = (\Delta V)^{-1} \ll 1. \quad (3.130)$$

Considering the approach to the critical point along the line $\omega = \omega'$, we scale the quantities ω and D near the critical point. Since the generating function and its derivatives are needed only at $\underline{s} = \underline{1}$, we also put

$$s_r = \varepsilon^e \xi_r + \dots \quad 0 < e < 1 \quad (3.131)$$

along with

$$\omega = \varepsilon^j \omega_1 + \dots \quad (3.132)$$

$$\text{and } D = \varepsilon^f D_1 + \dots \quad (3.133)$$

Substituting equations (3.129)-(3.133) into equation (3.128) shows that the steady state equation has the leading terms

$$\sum_r -\xi_r \epsilon^{2(1-e)} \frac{\partial^3 Z}{\partial \xi_r^3} + \sum_r 4\xi_r^2 \epsilon^{2e-1} Z + \sum_r -\xi_r \epsilon^j \omega_1 \frac{\partial Z}{\partial \xi_r} + \sum_r \sum_\ell \xi_r \epsilon^f D_1 \left(\frac{\partial Z}{\partial \xi_\ell} - \frac{\partial Z}{\partial \xi_r} \right) + \dots = 0. \quad (3.134)$$

The applicability of different kinds of theories near the critical point is determined by the relative importance of these four terms. Thus, for

$$f > \max \{j, 2(e-1), 2e-1\}$$

$$\text{and } j = 2(1-e) = 2e-1, \quad (3.135)$$

the birth and death description neglecting spatial fluctuations is valid. On the other hand, for

$$j < \min \{j, 2(1-e), 2e-1\}, \quad (3.136)$$

diffusion dominates and chemical reaction effects appear as perturbations. All terms have equal importance if

$$e = 3/4 \text{ and } j = f = 1/2. \quad (3.137)$$

The resulting third-order equation in this case has the solution

$$Z(\{\xi_r\}) = \int_{-\infty}^{\infty} \dots \int_{-\infty}^{\infty} \{d\theta_r\} [\exp(\sum_r \xi_r \theta_r)] R(\{\theta_r\}),$$

where

$$R(\{\theta_r\}) = \exp \left\{ -\frac{1}{4} \sum_r \left(\omega_1 \frac{\theta_r^2}{2} + \frac{\theta_r^4}{4} + \frac{D_1}{4} \sum_{\ell} (\theta_{\ell} - \theta_r)^2 \right) \right\}.$$

(3.138)

The functional in the exponential is the Ginzburg-Landau potential. If

$$e < 3/4 \quad \text{and} \quad 2e-1 = j = f, \quad (3.139)$$

the third order term can be dropped and consequently the θ_r^4 term is missing in the solution. This corresponds to the Gaussian approximation.

3.6 CRITICAL PHENOMENA

The steady state structure of the Schlögl model is similar to that of a van der Waals gas or a ferromagnetic material. A close analogy exists between the parameters of these systems. The transition between multiple steady states of the Schlögl model is similar to the gas-liquid transition. For the Schlögl model the pump parameter B plays the role

of pressure and a change in the ratio of rate constants affects the shape of the X versus B curve as a change in temperature affects pV curves. The order parameters are the concentration of X and the density respectively. A less complete analogy can be drawn with the magnetization of a ferromagnetic material where the pump parameter and the rate-constant ratio correspond to external field strength and temperature respectively. Because of this similarity, the observed critical phenomena in the case of gas-liquid and magnetic systems⁴⁴ are expected to be manifest in the Schlögl model also.

Inhomogeneous spatial fluctuations are very important in critical phenomena. So, the birth-and-death description is not sufficient for this study. Including the diffusion process the deterministic rate equation can be written as^{45,46}

$$\frac{\partial}{\partial t} X(\underline{r}, t) = -X^3 + 3AX^2 - (3+\delta)A^2X + (1+\delta')A^3 + D\nabla^2 X, \quad (3.140)$$

where A, δ and δ' are defined by

$$\begin{aligned} A &= \frac{k_1 B}{3k_3} = \frac{c_1 B}{c_2}, \\ 3 + \delta &= \frac{9k_2 k_4 B^2 V^2}{k_1^2} = \frac{6c_2 c_4 B^2}{c_1^2}, \\ 1 + \delta' &= \frac{27k_2^2 k_3 V^2}{k_1^3 B^2} = \frac{6c_2^2 c_3}{c_1^3}, \end{aligned} \quad (3.141)$$

and $t' = \frac{k_2}{v^2} = \frac{c_2}{6}t$. $x(\underline{r}, t')$ is related to its Fourier

components $x_{\underline{q}}(t')$ by

$$x(\underline{r}, t') = L^{-d/2} \sum_{\underline{q}} x_{\underline{q}}(t') e^{i\underline{q} \cdot \underline{r}}$$

$$\text{and } x_{\underline{q}}(t') = L^{-d/2} \int_{-L/2}^{L/2} dr_1 \dots \int_{-L/2}^{L/2} dr_d x(\underline{r}, t') e^{-i\underline{q} \cdot \underline{r}},$$

where L is the side of the d -dimensional cubic reaction vessel.

In terms of the Fourier components, the rate equation is

$$\begin{aligned} \frac{\partial}{\partial t'} x_{\underline{q}}(t') &= [(3+\delta)A^2 + q^2 D] x_{\underline{q}} + L^{-d/2} 3A \sum_{\underline{k}} x_{\underline{q}-\underline{k}} x_{\underline{k}} \\ &\quad - L^{-d} \sum_{\underline{k}} \sum_{\underline{k}'} x_{\underline{k}} x_{\underline{k}'} x_{\underline{q}-\underline{k}-\underline{k}'} + L^{d/2} (1+\delta') A^3 \delta_{\underline{q}, \underline{0}} \end{aligned} \quad (3.142)$$

using

$$\int_{-L/2}^{L/2} e^{ik_1 r_1} dr_1 = L. \quad (3.143)$$

It is difficult to study the corresponding stochastic equations in completely general form. The first improvement on the

deterministic equation is the Langevin equation obtained by simply adding uncorrelated uniformly fluctuating ("white") noise terms $\eta_{\underline{q}}$ to the deterministic equations; the averaged $\eta_{\underline{q}}$ and correlations satisfy

$$\langle \eta_{\underline{q}}(t) \rangle = 0$$

$$\text{and } \langle \eta_{\underline{q}_1}(t_1) \eta_{\underline{q}_2}(t_2) \rangle = 2\Gamma \delta_{\underline{q}_1 - \underline{q}_2} \delta(t_1 - t_2). \quad (3.144)$$

Making the change of variable to $\sigma_{\underline{q}}$

$$\sigma_{\underline{q}} = X_{\underline{q}}/A - \delta_{\underline{q},0}, \quad (3.145)$$

and adding the noise terms transforms equation (3.142) into

$$\begin{aligned} \frac{\partial}{\partial t''} \sigma_{\underline{q}} &= - [\delta + q^2 D'] \sigma_{\underline{q}} + L^{d/2} (\delta' - \delta) \sigma_{\underline{q},0} \\ &+ L^{-d} \sum_{\underline{k}} \sum_{\underline{k}'} \sigma_{\underline{k}} \sigma_{\underline{k}'} \sigma_{\underline{q} - \underline{k} - \underline{k}'} + \eta_{\underline{q}}(t''), \end{aligned} \quad (3.146)$$

where $t'' = A^2 t'$ and $D' = D/A^2$.

The corresponding Fokker-Planck equation giving the time evolution of the probability distribution for $\{\sigma_{\underline{q}}\}$ is a second-order partial differential equation. Its stationary solution is

$$P_s(\{\sigma_{\underline{k}}\}) = N \exp[-F(\{\sigma_{\underline{k}}\})], \quad (3.147)$$

where N is a normalization constant and

$$\begin{aligned}
 F(\{\sigma_{\underline{k}}\}) &= \Gamma^{-1} \left\{ \sum_{\underline{k}} [\delta/2 + D'k^2/2] |\sigma_{\underline{k}}|^2 \right. \\
 &\quad + \frac{1}{4} L^{-d} \sum_{\underline{k}} \sum_{\underline{k}'} \sum_{\underline{k}''} \sigma_{\underline{k}} \sigma_{\underline{k}'} \sigma_{\underline{k}''} \sigma_{-\underline{k}-\underline{k}'-\underline{k}''} \\
 &\quad \left. + L^{d/2} (\delta - \delta') \sigma_{\underline{0}} \right\}. \tag{3.148}
 \end{aligned}$$

This has the form of the Ginzburg-Landau Hamiltonian in the Ising model of a ferromagnet.

Many physical properties diverge as the critical point is approached. The strength of this divergence is characterized by critical exponents. For example, when the critical point $\delta = \delta' = 0$ is approached along the line $\delta = \delta'$

$$\langle \sigma_0 \rangle \sim (-\delta)^{\gamma_1} \quad \text{for } \delta = \delta' < 0 \tag{3.149}$$

where γ_1 is a critical exponent. Similarly other exponents are defined by^{45,46}

$$\langle \sigma_0 \rangle \sim (\delta')^{1/\gamma_2} \quad \text{for } \delta = 0, \tag{3.150}$$

$$\langle \sigma_0^2 \rangle \sim \delta^{-\gamma_3} \quad \text{for } \delta = \delta', \tag{3.151}$$

$$\text{and } \langle \sigma_{\underline{q}} \sigma_{-\underline{q}} \rangle \sim \delta^{-\gamma_3} D(q^2 \delta^{-2\gamma_4}). \tag{3.152}$$

These exponents can be calculated using renormalization

group techniques.

Renormalization is a coarse graining transformation followed by a change of scale.⁴⁷ Suppose we have a joint probability distribution over the microstates of the system. From this we construct another distribution whose spatial (and time) resolution is lower. To do this we have combined several microstates together losing details within a single collection. Let us parametrize the extent of this coarse graining and scale change by s . Then the set $\{R_s : s > 1\}$ of all such transformations is called the renormalization group (even though it does not satisfy all the axioms of group algebra). The basic hypothesis of renormalization group theory is that at the critical point all length scales are equivalent; that is, the system behaves identically at all levels intermediate between microscopic and macroscopic scales except close to the microscopic scale. This principle is an observed fact in magnetization and condensation processes. Accordingly the probability distribution corresponding to the critical point becomes invariant asymptotically under a renormalization transformation; i.e.,

$$\lim_{s \rightarrow \infty} R_s P = P^* \quad (3.153)$$

where P^* is a fixed point of R_s for all s . Asymptotically the distribution corresponding to a point in the neighborhood of the critical point (but not on the critical surface) moves

away from P^* . The functional dependence of this movement on the parameters of the system can be related to the rate of divergence of physical properties. Thus the critical exponents can be calculated.

When we apply a renormalization to equation (3.148), we find that the result has the same form with the coefficient s^{4-d} appearing in front of the quartic term. Since we are interested in large s behaviour, we can neglect the quartic term in the potential when $4-d < 0$ and obtain a Gaussian distribution. The fixed point of the class of Gaussian distributions and the class of Ginzburg-Landau distributions are identical only at $d = 4$. The Gaussian distribution is valid for $d > 4$. When d decreases from 4, this approximation becomes increasingly inaccurate. Thus $d_c = 4$ is a critical dimension. This suggests a perturbation expansion in a parameter with exponent $4-d$. If the quartic term in the potential is treated as a perturbation, then an expansion is obtained in powers of δ^{ε_3} where $\varepsilon_3 = 4-d$. Thus even when $d < 4$, there is a region (designated "the critical region") around the critical point outside which the Gaussian approximation is valid. As d increases the critical region shrinks and finally disappears when d reaches 4. The Ginzburg criterion qualitatively governs the size of the critical region.

From the perturbation expansion we obtain the following critical exponents:

$$\gamma_1 = \frac{1}{2} - \frac{\epsilon_3}{6} + \frac{\epsilon_3^2}{18} + O(\epsilon_3^3), \quad (3.154)$$

$$\gamma_2 = 3 + \epsilon_3 + \frac{25}{54}\epsilon_3^2 + O(\epsilon_3^3), \quad (3.155)$$

$$\gamma_3 = 1 + \frac{1}{6}\epsilon_3 + \frac{25}{36}\epsilon_3^2 + O(\epsilon_3^3), \quad (3.156)$$

$$\text{and } \gamma_4 = \frac{1}{2} + \frac{1}{12}\epsilon_3 + \frac{1}{142}\epsilon_3^2 + O(\epsilon_3^3). \quad (3.157)$$

In equilibrium critical phenomena the heat capacity diverges at the critical point. A property analogous to the heat capacity exists in nonequilibrium systems. The entropy (S) and entropy deficiency (K) functions defined by (see equation (3.72))

$$S(\{P_i\}) = - \sum_i P_i \ln P_i \quad (3.158)$$

$$K(\{P_i\}, \{P_i^e\}) = \sum_i P_i \ln (P_i/P_i^e) \quad (3.159)$$

(in appropriate units) can be viewed as the averages of the random variables

$$b_i = - \ln P_i \quad (3.160)$$

$$r_i = b_i^e - b_i = \ln (P_i/P_i^e), \quad (3.161)$$

called the bit number and relative bit number respectively.

Roughly speaking, b_i is proportional to the number of binary digits necessary to represent P_i . In information theory, $-S$ is called the Shannon information measure and K is called the Kullback measure of information gain. In equilibrium statistical thermodynamics, the probability distributions are of the form (cf. equation (3.69))

$$P_i = \exp \left[- \sum_r \Delta\mu_r X_{ir} \right]. \quad (3.162)$$

The heat capacity of a system is related to the variance of energy in the canonical distribution. Since the bit number corresponds to the energy of the microstates, (e.g.,

$$b_i = - \ln P_i = \frac{E_i}{k_B T} \quad (3.163)$$

for a canonical ensemble), a generalized heat capacity can be defined in terms of the bit number variance, as

$$C_r = (\langle b^2 \rangle - \langle b \rangle^2) / \Delta\mu_r. \quad (3.164)$$

The divergence of bit number variance of the Schlögl model has been studied by Schlögl.⁴⁸ When diffusion is effective and $\delta = \delta'$, the stationary distribution for the homogeneous mode has the form

$$P(x) \sim \exp [- V (x^{2+\sigma})^2] \quad (3.165)$$

where σ is a derived constant. When the bit number variance is calculated from this distribution and plotted, it is found that it dramatically changes at the critical point and that this change approaches a divergence as $V \rightarrow \infty$.

CHAPTER IV

A STUDY OF ASYMPTOTIC RELAXATION IN THE SCHLÖGL MODEL USING EIGENVECTORS OF THE TRANSITION MATRIX.

It is well known that deterministic methods of chemical kinetics are not adequate for treating reacting systems exhibiting chemical instability.^{8,49-52} In particular stochastic methods are needed to analyze transitions between multiple steady states in such systems. The Schlögl model has been widely used for studying phenomena associated with multiple steady states. Schlögl⁴ analyzed the model deterministically and showed that for certain sets of parameter values the model has two stable steady states and an unstable steady state (section 2.1). Matheson et al⁵ compared the stationary distribution from a stochastic treatment with the deterministic steady state results (section 2.2). Procaccia and Ross³³ have discussed the question of relative stability of the two stable steady states (section 3.4). Gillespie⁹ studied the time-dependent features of this model using first passage times (section 3.4). Here the time-dependent probability distributions are displayed for long times at which transitions from one stable steady state to another are expected to occur.

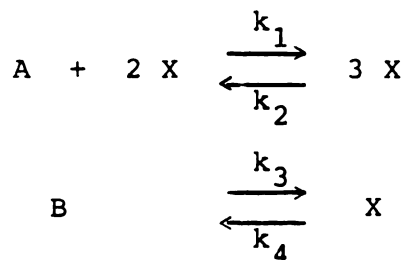
The stochastic time evolution of the system is described by a birth-and-death master equation (section 2.2). Since it is a first-order linear equation, its solution is in principle known in terms of the eigenvalues and the eigenvectors of the

transition matrix⁸ (section 2.3). A criterion for the validity of the Kramers rule is given and results for the Schlögl model are presented in this chapter.

Creel and Ross⁵³ have reported experimental observations of transitions between multiple steady states of an $\text{NO}_2/\text{N}_2\text{O}_4$ mixture illuminated with an argon-ion laser.

4.1 THE SCHLÖGL MODEL AND ITS STOCHASTIC FORMULATION

In the Schlögl model the chemical reactions



occur in a homogeneous open system. The particle numbers of species A and B (denoted by A and B) are assumed to be kept constant by contact with external reservoirs or by appropriate feeding into or removal from the reactor. Thus X is the only variable, while A and B are external parameters. For convenience we will also assume the numbers of A and B to be equal. When the reaction parameter η defined by

$$\eta = \frac{k_1 k_4}{k_2 k_3} \quad (4.1)$$

exceeds a critical value $\eta_c = 9$, there is a range of B values

for which the system has three possible steady states, $X_1 < X_2 < X_3$, of which X_1 and X_3 are stable and X_2 is unstable. Outside this range of B and below the critical point, there is only one stable steady state. The boundary separating these two regions consists of the marginal stability points.

In the stochastic formulation $X(t)$ is viewed as a random variable taking integer values in $\{x:0 < x < \infty\}$. The state of the system at a specified time t is then given by a probability vector $\underline{P}(t)$ whose x -th component is the probability that $X(t) = x$. The dynamics of the system are described by the time evolution of $P(x,t)$ [$P(x,t) \equiv P_x(t)$] according to the master equation,

$$\begin{aligned} \frac{\partial}{\partial t} P(x,t) = & a_+(x-1)P(x-1,t) + a_-(x+1)P(x+1,t) \\ & - a(x)P(x,t), \quad x > 0, \end{aligned} \quad (4.2)$$

where

$$a_+(x) = \frac{c_1}{2} Bx(x-1) + c_3 B, \quad (4.3)$$

$$a_-(x) = \frac{c_2}{6} x(x-1)(x-2) + c_4 x, \quad (4.4)$$

$$\text{and } a(x) = a_+(x) + a_-(x). \quad (4.5)$$

The parameters c_i are related to the rate constants k_i by

$$c_i = k_i n_i! V^{1-m_i}, \quad (4.6)$$

where n_i is the molecularity of the i -th step in X , m_i is the total molecularity of the i -th step (e.g., $n_1 = 2$, $m_1 = 3$), and V is the volume of the system. The stationary distribution $P_s(x)$ is obtained by setting the right-hand side of the master equation equal to zero. $P_s(x)$ has local maxima corresponding to stable steady states and a minimum at the X -value for the unstable steady state.

The master equation in matrix form is

$$\frac{\partial \underline{P}}{\partial t} = \underline{A} \underline{P}, \quad (4.7)$$

where

$$A_{xy} = a_+(y) \delta_{x-1,y} + a_-(y) \delta_{x+1,y} + a(y) \delta_{xy}. \quad (4.8)$$

Its solution is (section 2.3)

$$P(x,t) = P_s(x) + \sum_{j=1}^{\infty} \alpha_j P_j(x) e^{\lambda_j t}, \quad (4.9)$$

where

$$\alpha_j = \sum_x \frac{P_j(x) P(x,0)}{P_s(x)}, \quad (4.10)$$

and λ_j and \underline{P}_j are the nonzero eigenvalues and the corresponding right eigenvectors of \underline{A} respectively. In particular, if $P(x,0) = \delta_{xy}$, then

$$\alpha_j = P_j(y) / P_s(y). \quad (4.11)$$

4.2. TRANSITION BETWEEN THE TWO STABLE STEADY STATES

For numerical studies the following values of the rate constants used by Gillespie³⁶ are selected:

$$c_1 = 3 \times 10^{-7} \text{ (molecule}^{-3} \text{ time}^{-1}\text{),}$$

$$c_2 = 1 \times 10^{-4} \text{ (molecule}^{-3} \text{ time}^{-1}\text{),}$$

$$\text{and } c_3 = 1.5 \times 10^{-3} \text{ (molecule}^{-1} \text{ time}^{-1}\text{);}$$

then $c_4 = 1.5 \text{ (molecule}^{-1} \text{ time}^{-1}\text{)}$ corresponds to the critical point. To illustrate the transition between the two stable steady states, consider $c_4 = 3.33333$ and $B = 1.01 \times 10^5$ as an example. Figure 4.1 shows the stationary distribution and the eigenvectors corresponding to the three eigenvalues closest to zero. As seen in section 2.3, $\lambda_0 = 0$ and all other eigenvalues are negative. Let the eigenvalues and eigenvectors be arranged such that $\lambda_0 > \lambda_1 > \lambda_2 \dots$. In the example illustrated in Figure 4.1 the first two nonzero eigenvalues

Figure 4.1 Eigenvectors of the transition matrix A for the Schlögl model, when the parameters correspond to a point in the interior of the multiple steady-state region. ($c_4 = 3.33333$ and $B = 1.01 \times 10^5$).

The eigenvalues are:

- a) $\lambda_0 = 0,$
- b) $\lambda_1 = -3.8404 \times 10^{-8},$
- c) $\lambda_2 = -1.0537,$
- d) $\lambda_3 = -1.5619.$

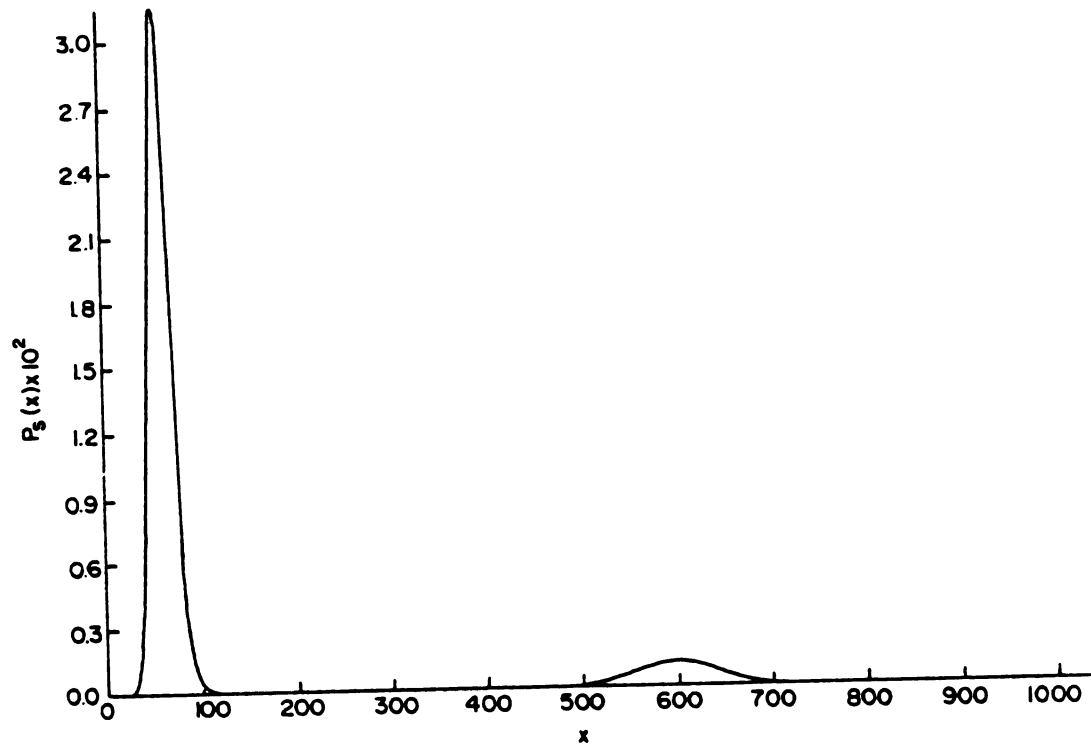


Figure 4.1.a The stationary mode \underline{P}_s .

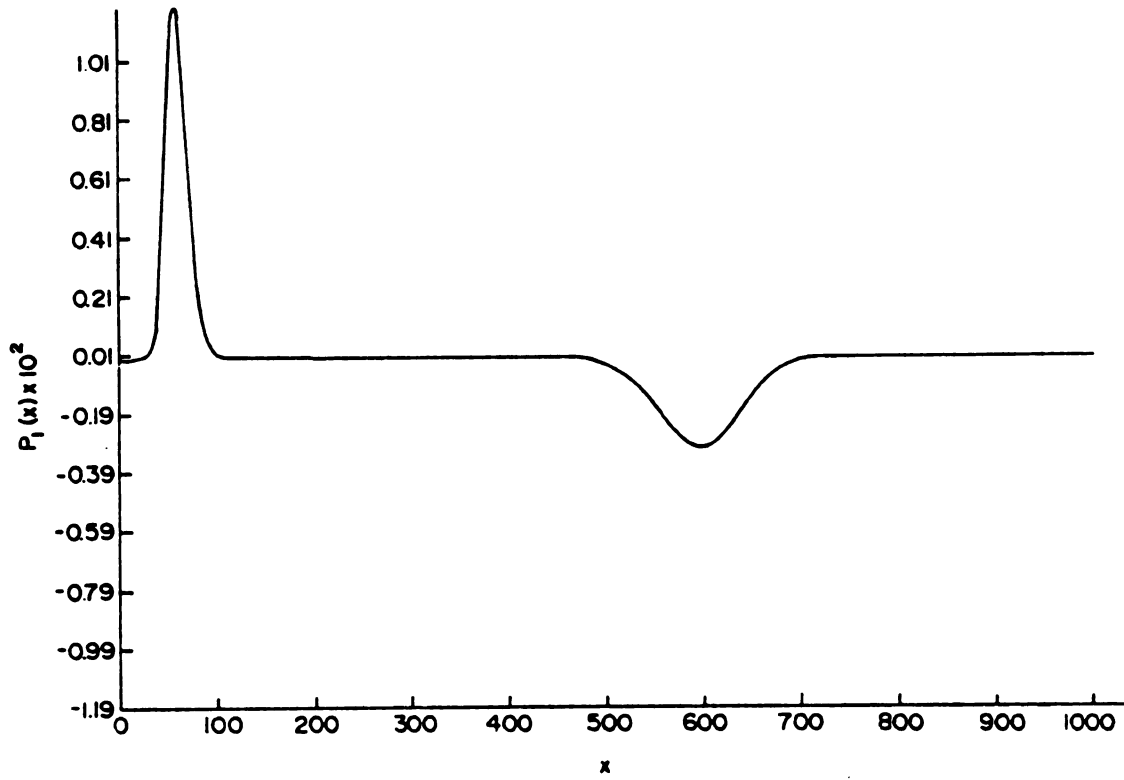


Figure 4.1. b The transition mode \underline{P}_1 .

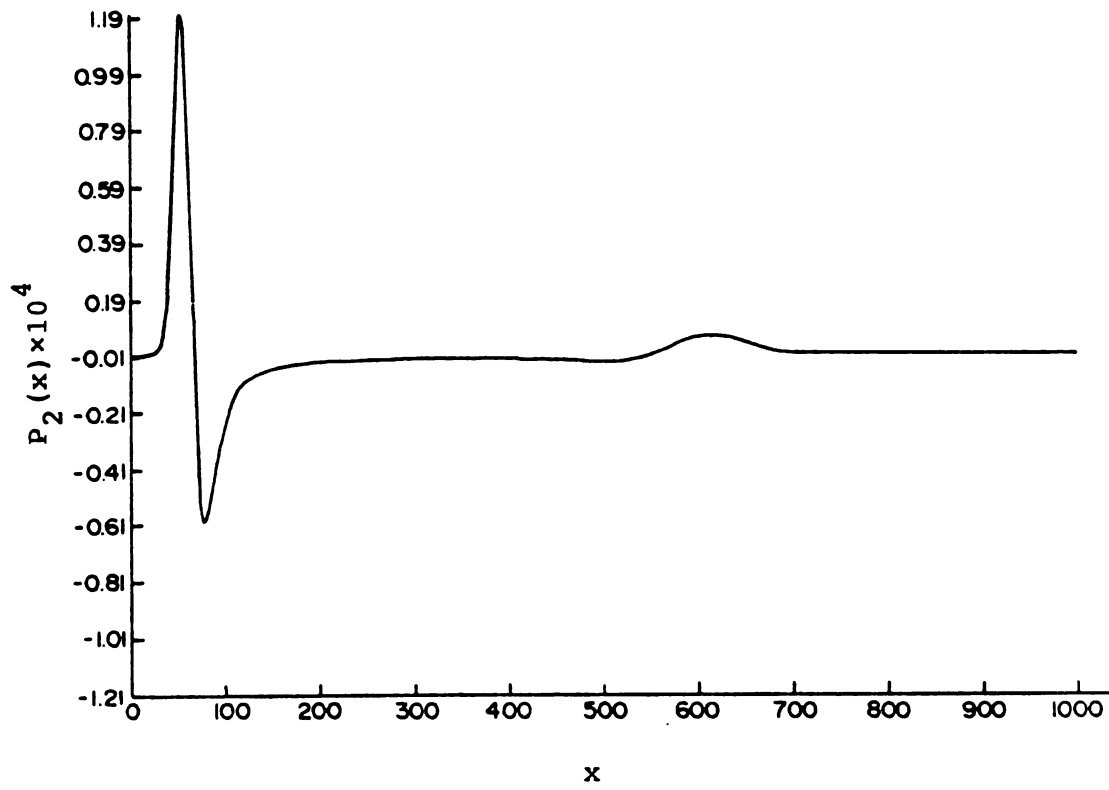


Figure 4.1.c The eigenvector \underline{P}_2 corresponding to λ_2 .

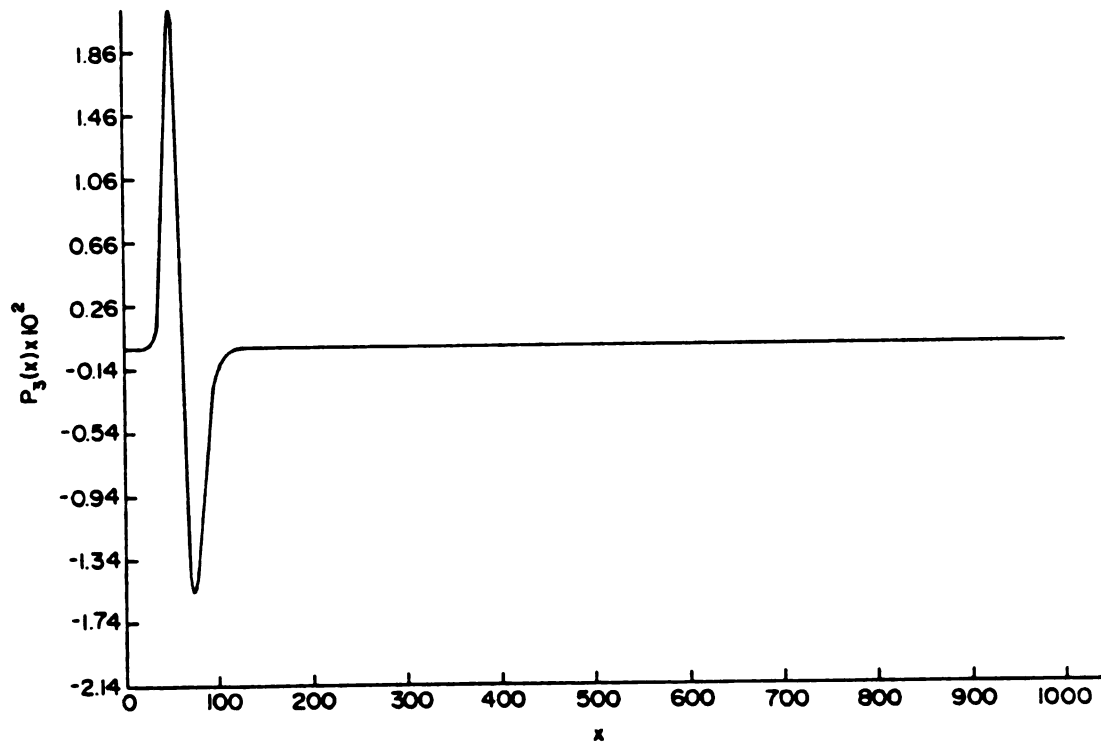


Figure 4.1.d The eigenvector \underline{P}_3 corresponding to λ_3 .

($\lambda_1 = -3.8404 \times 10^{-8}$ and $\lambda_2 = -1.0537$) differ by several orders of magnitude. This means that the eigenmode \underline{P}_1 persists for a long time after all other modes have decayed. Therefore, after a sufficiently long time, $P(x,t)$ has significant contributions only from \underline{P}_s and \underline{P}_1 . Moreover, \underline{P}_1 has a positive peak corresponding to one of the peaks in the stationary distribution \underline{P}_s and a negative peak corresponding to the other (see Figures 4.1.a and 4.1.b). As \underline{P}_1 decays, $P(x,t)$ decreases in one steady-state region and grows in the other. Let \underline{P}_1 be called the transition mode.

Figures 4.2 - 4.5 show the time evolution of the probability distribution for various initial values of x . A quasi-stationary distribution is established on a short time scale. Then this distribution slowly relaxes to the stationary distribution in accordance with the Kramers rule (explained in section 4.3). In general the quasi-steady distribution is determined by the initial distribution. If the initial distribution is a delta function peaked at an x -value close to one of the stable steady states, then the quasi-stationary distribution is peaked almost exclusively at that steady state. This behavior was noted by Oppenheim *et al*³¹. When the initial x -value is close to the unstable steady state, however, the quasi-steady distribution has contributions from both stable regions. (Figure 4.4)

The direction in which the transition occurs depends on the sign of α_1 in equation (4.9), which in turn depends

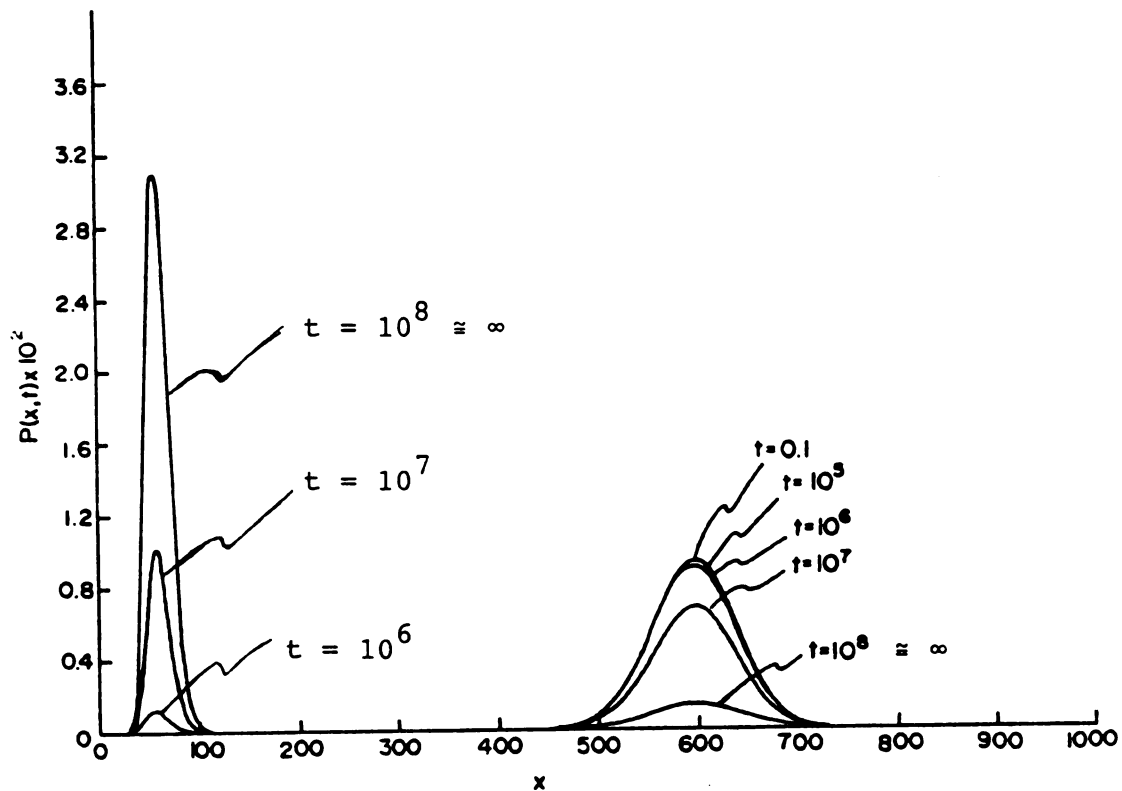


Figure 4.2 Time evolution of probability distribution when the parameters correspond to a point in the interior of the multiple steady-state region. $c_4 = 3.333333$ and $B = 1.01 \times 10^5$ (same as in Figure 4.1). Initial distribution is $\delta(x-500)$.

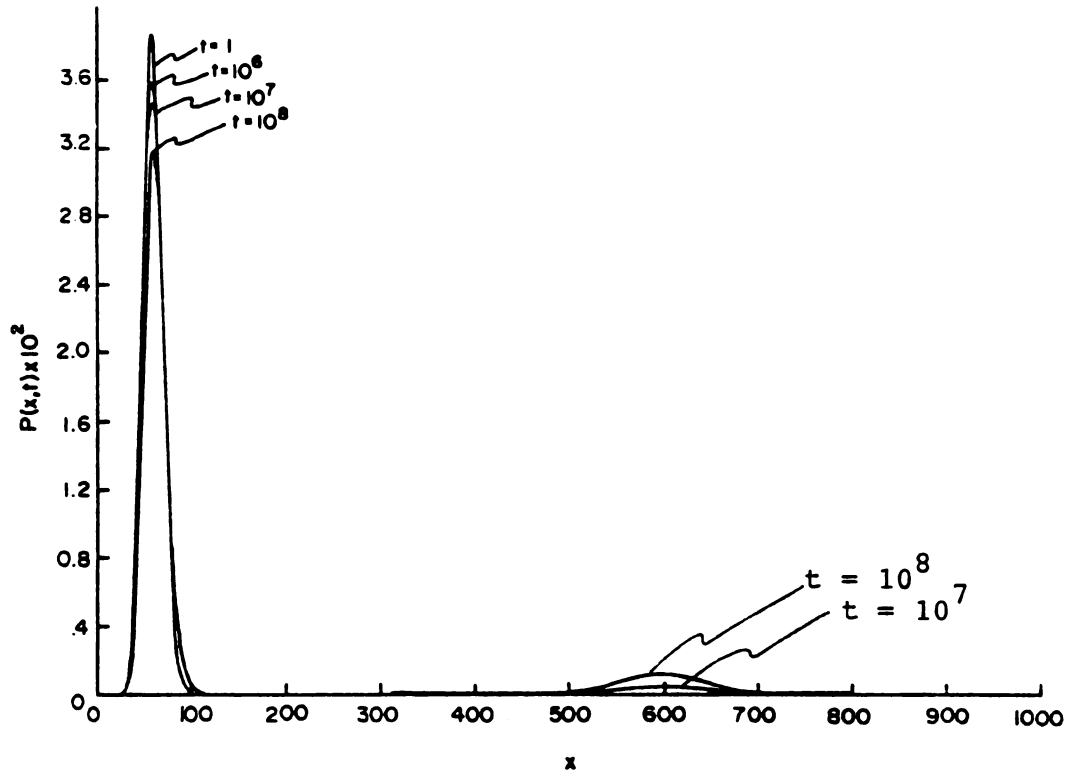


Figure 4.3 Time evolution of probability distribution.
 $c_4 = 3.33333$ and $B = 1.01 \times 10^5$.
 Initial distribution is $\delta(x-50)$.

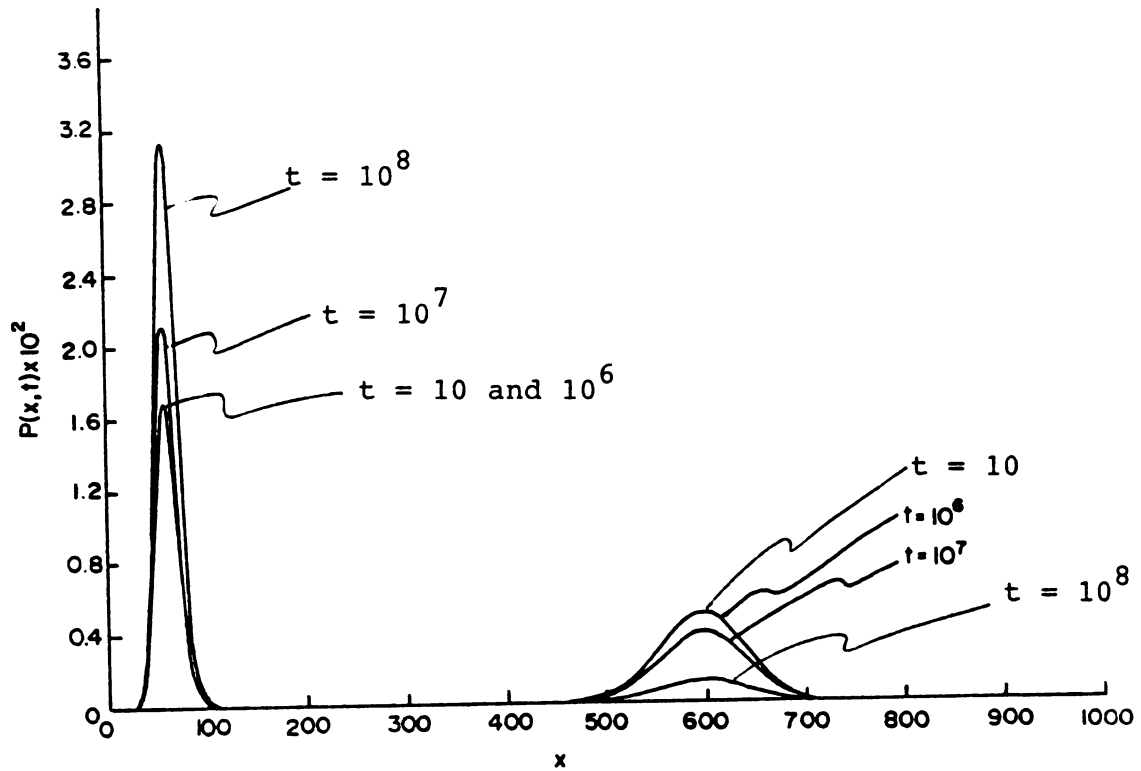


Figure 4.4 Time evolution of probability distribution.

$$c_4 = 3.33333 \text{ and } B = 1.01 \times 10^5.$$

Initial distribution is $\delta(x-253)$, peaked at the unstable steady-state X -value.

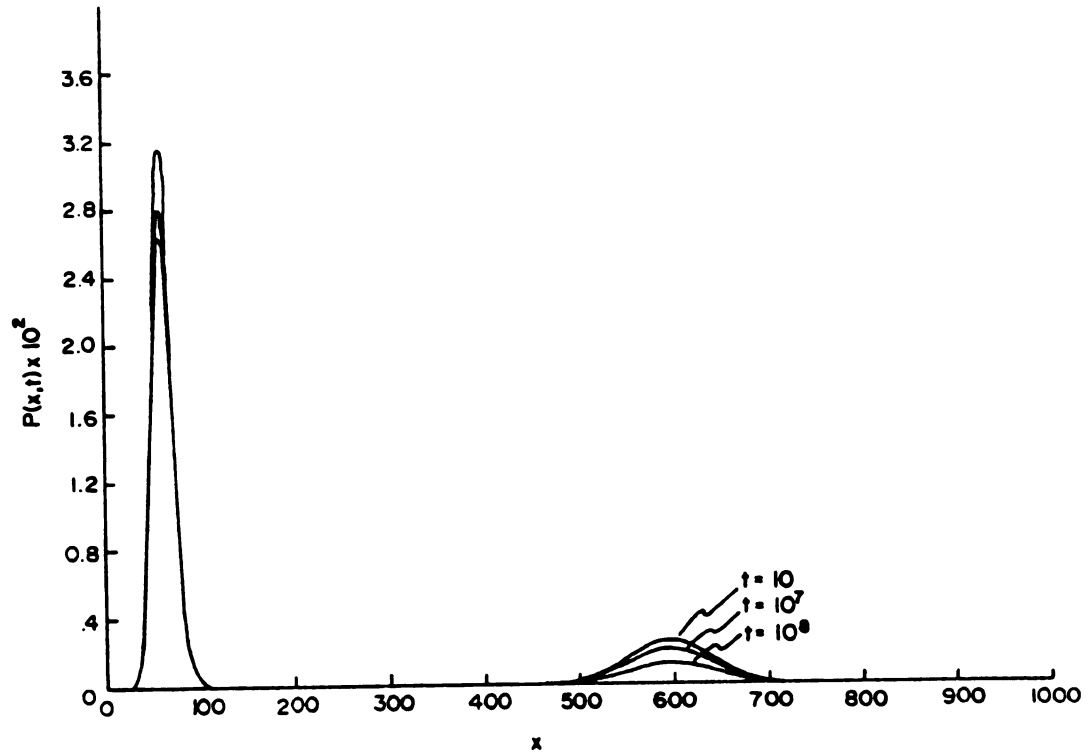


Figure 4.5 Time evolution of probability distribution.

$$c_4 = 3.33333 \text{ and } B = 1.01 \times 10^5.$$

Initial distribution is $\delta(x-230)$.

on the sign of $P_1(x_0)$ if the initial distribution is a delta function at x_0 . Further, the two regions between which the transition occurs are separated by the zero of \underline{P}_1 and not by the minimum of \underline{P}_s . These points differ significantly in some cases as will be seen below.

4.3. THE VALIDITY OF KRAMERS RELAXATION

A bistable system is said to undergo Kramers relaxation⁵⁴ if the probability distribution equilibrates within each region rapidly and then diffuses slowly from one region to another thereby effecting a pure transition. Gardiner⁵⁵ has reformulated the Kramers rule based on a one-dimensional Fokker-Planck equation. Similar results can be derived from a birth-and-death master equation describing a bistable system. For this purpose, let us define

$$M(x,t) = \sum_{y=0}^x P(y,t), \quad (4.13)$$

$$N_1(t) = M(X_2-1,t), \quad (4.14)$$

$$N_2(t) = P(X_2,t), \quad (4.15)$$

$$N_3(t) = \sum_{x=X_2+1}^{\infty} P(x,t), \quad (4.16)$$

$$n_1 = \sum_{x=0}^{X_2-1} P_S(x), \quad (4.17)$$

$$n_2 = P_S(X_2), \quad (4.18)$$

$$\text{and } n_3 = \sum_{x=X_2+1}^{\infty} P_S(x). \quad (4.19)$$

From the master equation (4.2) and from the detailed balance relation (2.23) satisfied by $P_S(x)$, it follows that

$$\frac{\partial}{\partial t} M(x,t) = a_+(x)P_S(x) \left[\frac{P(x+1,t)}{P_S(x+1)} - \frac{P(x,t)}{P_S(x)} \right]. \quad (4.20)$$

Dividing by $a_+(x)P_S(x)$ and summing over x from X_1 to X_2-1 , we obtain

$$\sum_{x=X_1}^{X_2-1} [a_+(x)P_S(x)]^{-1} \frac{\partial}{\partial t} M(x,t) = \frac{P(X_2,t)}{P_S(X_2)} - \frac{P(X_1,t)}{P_S(X_1)}. \quad (4.21)$$

If Kramers relaxation is followed, then we can set

$$P(x,t) \cong P_S(x) \frac{N_1(t)}{n_1} \quad \text{for } x < X_2,$$

$$P(x,t) \cong P_S(x) \frac{N_3(t)}{n_3} \quad \text{for } x > X_2. \quad (4.22)$$

With these, equation (4.21) becomes

$$\sum_{x=X_1}^{X_2-1} [a_+(x)P_S(x)]^{-1} \frac{\partial}{\partial t} M(x,t) = \frac{N_2(t)}{n_2} - \frac{N_1(t)}{n_1}. \quad (4.23)$$

To calculate the left-hand side:

$$M(x,t) = \frac{N_1(t)}{n_1} \sum_{y=0}^x P_S(y) = \frac{N_1(t)}{n_1} \left(n_1 - \sum_{y=x+1}^{X_2-1} P_S(y) \right)$$

$$= N_1(t) [1 - \phi(x)] \quad \text{for } x < X_2, \quad (4.24)$$

where

$$\phi(x) = \begin{cases} n_1^{-1} \sum_{y=x+1}^{X_2-1} P_S(y) & \text{for } x < X_2, \\ n_3^{-1} \sum_{y=X_2+1}^x P_S(y) & \text{for } x > X_2. \end{cases} \quad (4.25)$$

Substituting (4.24) in (4.23), we get

$$\kappa \frac{d}{dt} N_1(t) = \frac{N_2(t)}{n_2} - \frac{N_1(t)}{n_1}, \quad (4.26)$$

where

$$\kappa = \sum_{x=X_1}^{X_2-1} \frac{1 - \phi(x)}{a_+(x) P_S(x)}. \quad (4.27)$$

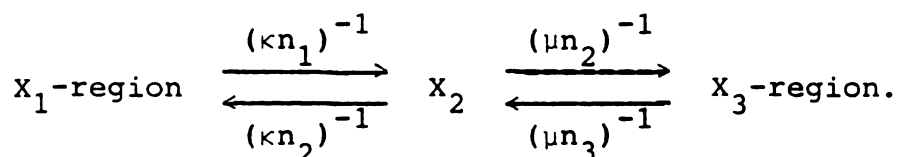
Similarly by summing equation (4.20) from X_2+1 to X_3 , we can obtain

$$\mu \frac{d}{dt} N_2(t) = \frac{N_2(t)}{n_2} - \frac{N_3(t)}{n_3} \quad (4.28)$$

where

$$\mu = \sum_{x=X_2+1}^{X_3} \frac{1 - \phi(x)}{a_+(x)P_s(x)}. \quad (4.29)$$

Equations (4.26) and (4.28) permit a three-state interpretation similar to Eyring's transition state theory.



The probability distribution for the Schlögl model satisfies equation (4.22) if the following conditions are met:

- 1) The eigenvalue corresponding to the transition mode must be sufficiently smaller in magnitude than all other nonzero eigenvalues. A quantitative criterion is given below.
- 2) The zero of the transition mode must match the minimum of the stationary mode. Moreover, $P_s(x)$ and $P_1(x)$ should be proportional in $0 < x < X_2$; and similarly for $x > X_2$. In other words, the shapes of the transition mode and the stationary mode should match in each region separately.

A transition between stable steady states is well defined if there exists a time τ when a considerable fraction of the transition mode remains after all faster modes have decayed almost completely. It is possible to find a relation between λ_1 and λ_2 such that the coefficient of \underline{P}_1 has decayed to a fraction f_1 of its initial value and the

coefficient of \underline{p}_2 to a fraction f_2 of its initial value ,

$$\text{i.e., } e^{\lambda_1} = f_1,$$

$$\text{and } e^{\lambda_2} = f_2. \quad (4.30)$$

The required relation is

$$\frac{\lambda_2}{\lambda_1} > \log f_2 / \log f_1. \quad (4.31)$$

Thus the coefficient of the transition mode will remain at 90% (50%) of its initial value after the coefficient for the faster mode has decayed to 1% of its initial value, if the ratio of the eigenvalues exceeds 43 (6.6 respectively). This condition differs from that given by Oppenheim et al⁸ in terms of the difference $|\lambda_2 - \lambda_1|$. Their criterion allows the possibility that the transition mode itself is negligible compared to the stationary mode by the time the next faster mode has decayed substantially.

The first three nonzero eigenvalues have been plotted versus B in various regions of the parameter space (Figures 4.6 - 4.8). Decay of the transition mode is very slow well inside the multiple steady-state region, but it becomes faster as either the critical point or a marginal stability point is approached. Figure 4.9 shows the region in which

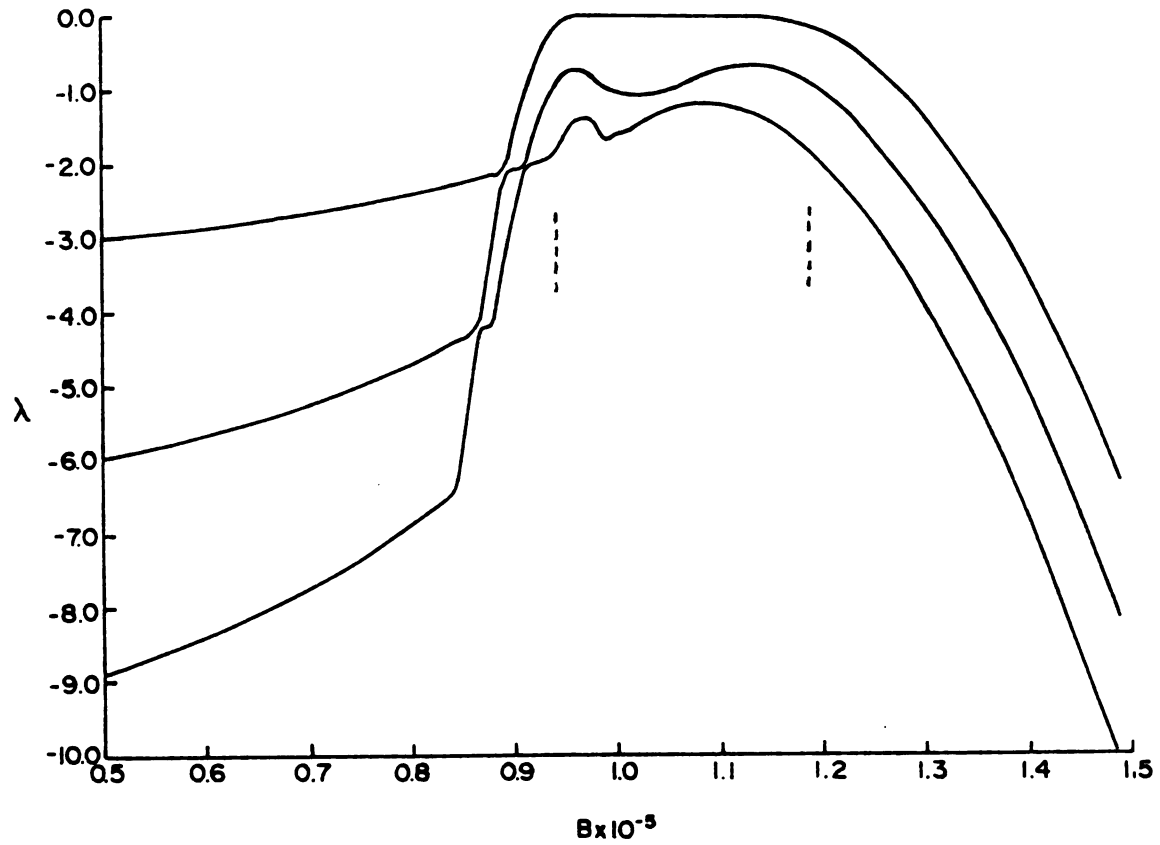


Figure 4.6 The first three nonzero eigenvalues of the transition matrix \underline{A} . $c_4 = 3.33333$. The dashed lines enclose the B-range in which there are three steady states.

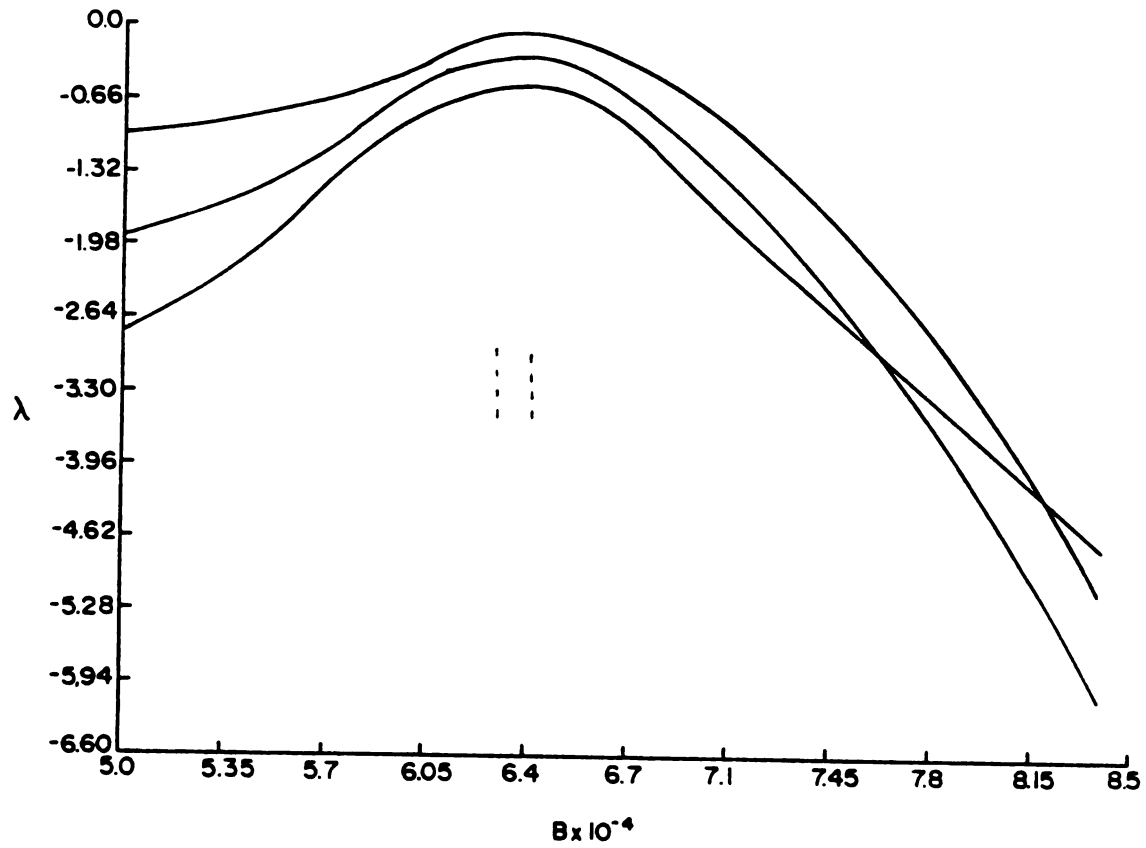


Figure 4.7 The first three nonzero eigenvalues of the transition matrix \underline{A} . $c_4 = 1.7$. The dashed lines enclose the B-range in which there are three steady states.

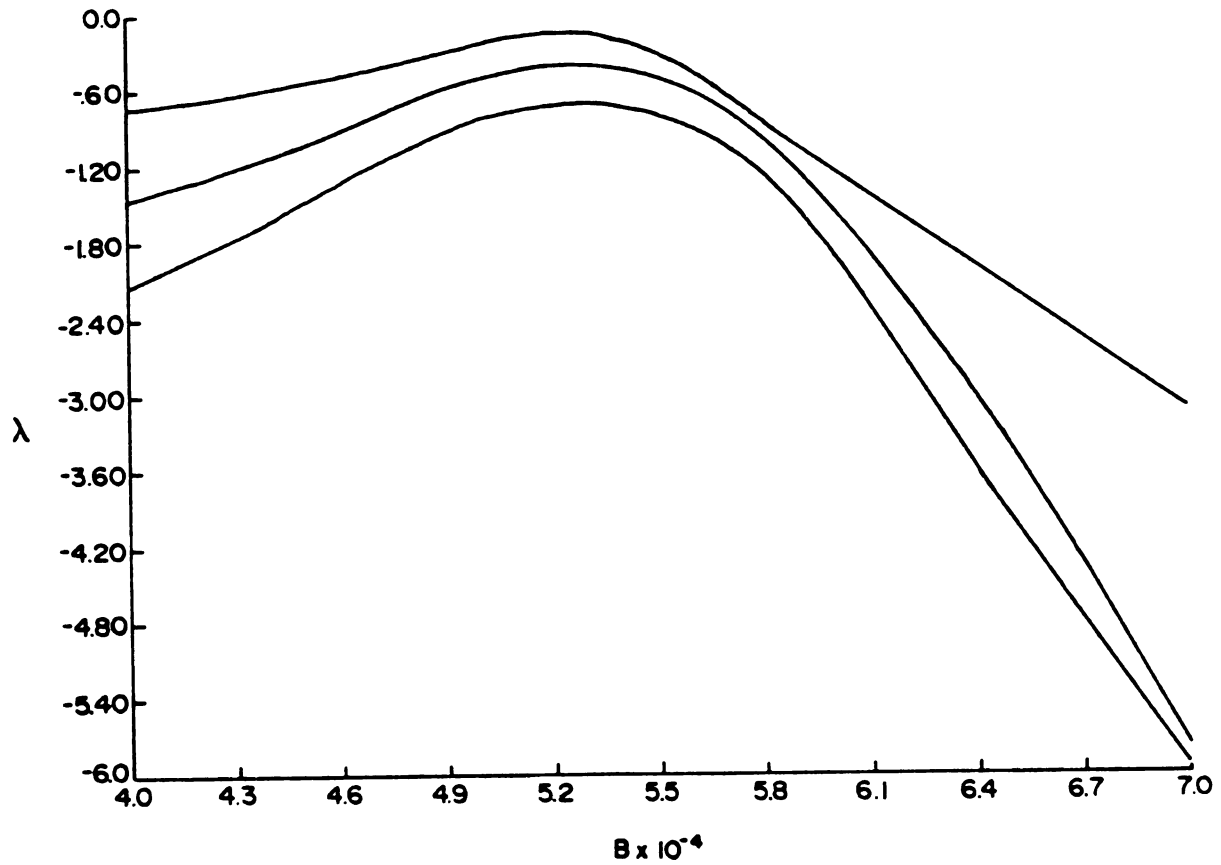


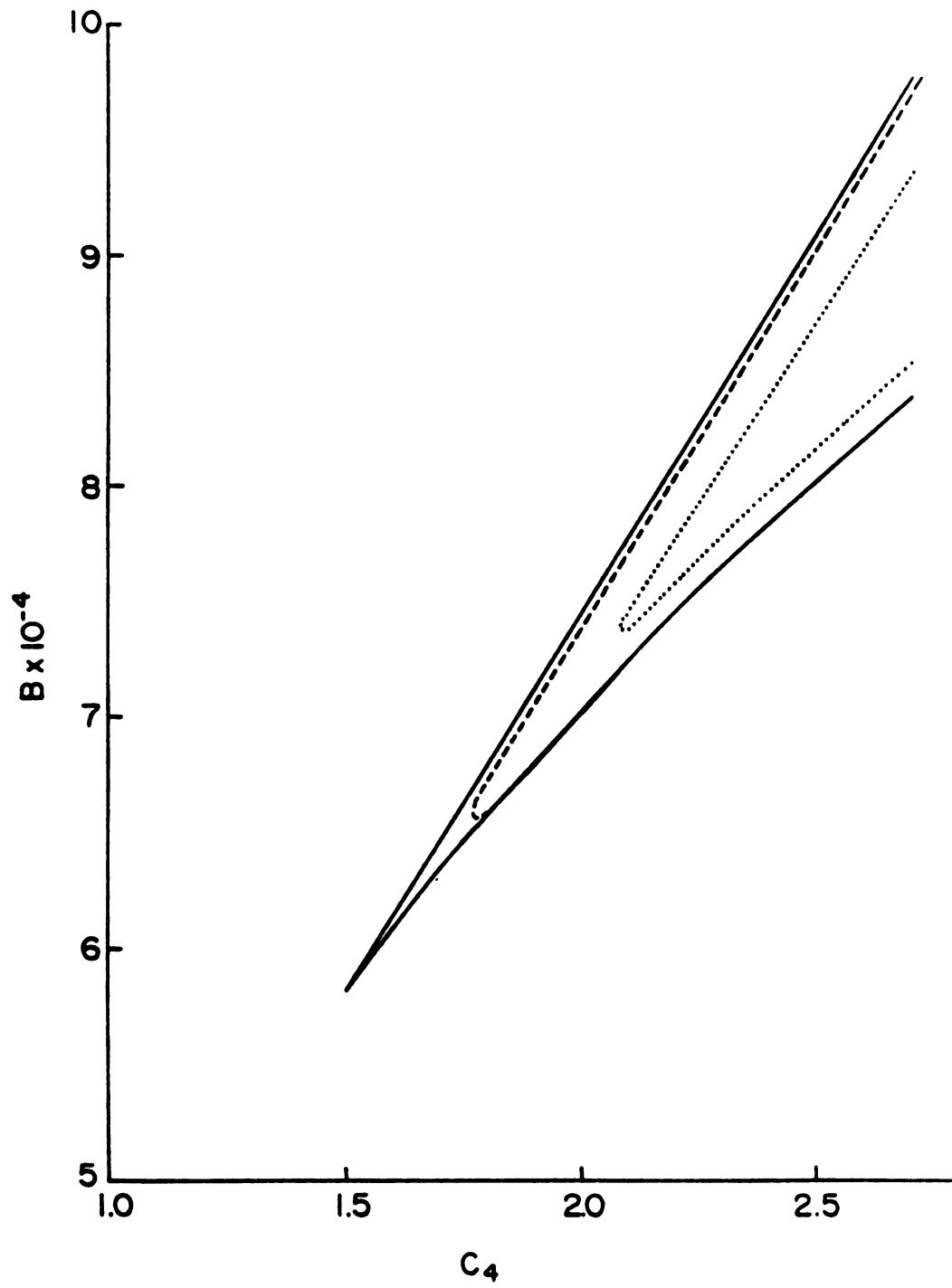
Figure 4.8 The first three nonzero eigenvalues of the transition matrix \underline{A} . $c_4 = 1.3$ (no multiple steady states).

Figure 4.9 Regions of the parameter space where the conditions on the eigenvalues (equation (4.31)) is satisfied. The solid lines consist of the marginal stability points.

$$f_2 = 0.01$$

$$f_1 = 0.9 \text{ for the dotted line.}$$

$$f_1 = 0.5 \text{ for the dashed line.}$$



condition (4.31) on the eigenvalues is satisfied.

Figures 4.10 and 4.11 show the stationary distribution, the first three eigenvectors with nonzero eigenvalues, and the time-dependent distributions near a marginal stability point. It is interesting to note that the stationary distribution does not have a significant peak near the higher steady state, but the transition mode does. Consequently, the intermediate probability distributions are peaked at both steady states. However, the relaxation to the lower steady state is fast and there is no quasi-stationary distribution.

Figures 4.12 - 4.14 illustrate situations near the critical point. In this region the zero of the transition mode differs considerably from the unstable steady state X -value. In Figure 4.14.b, for example, a transition occurs between two regions of approximately equal size, even though the stationary distribution is asymmetric.

Although the deterministic analysis sharply divides the parameter space into single and multiple steady state regions, the stochastic analysis reveals that in the multiple steady state region close to the boundary, the behavior is similar to that in the single steady state region, i.e., transition between multiple steady states and equilibration in the vicinity of a single steady state are similar near the boundary. Thus there is no abrupt change in the qualitative behavior at the boundary separating the single and multiple steady-state regions.

Figure 4.10 Eigenvectors of the transition matrix A
near a marginal stability point.

($c_4 = 3.33333$ and $B = 9.6 \times 10^4$).

The eigenvalues are:

a) $\lambda_0 = 0,$

b) $\lambda_1 = -1.6732 \times 10^{-2},$

c) $\lambda_2 = -7.3902 \times 10^{-1},$

d) $\lambda_3 = -1.4365 .$

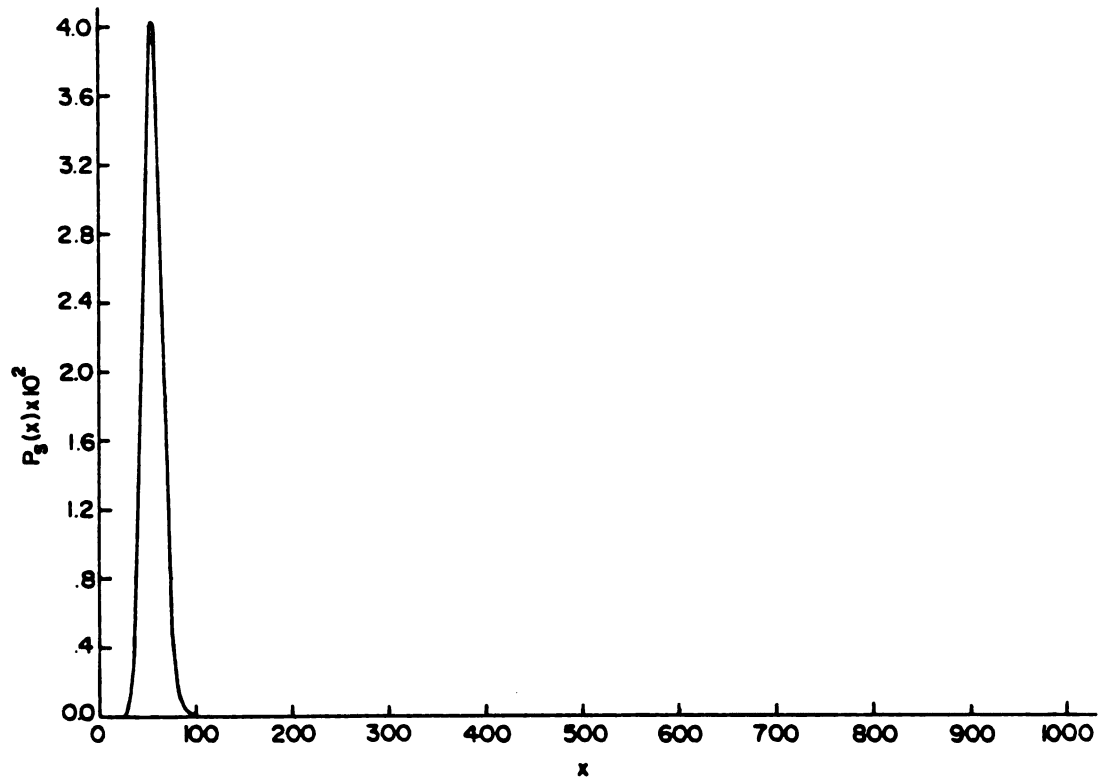


Figure 4.10.a The stationary mode \underline{P}_s .

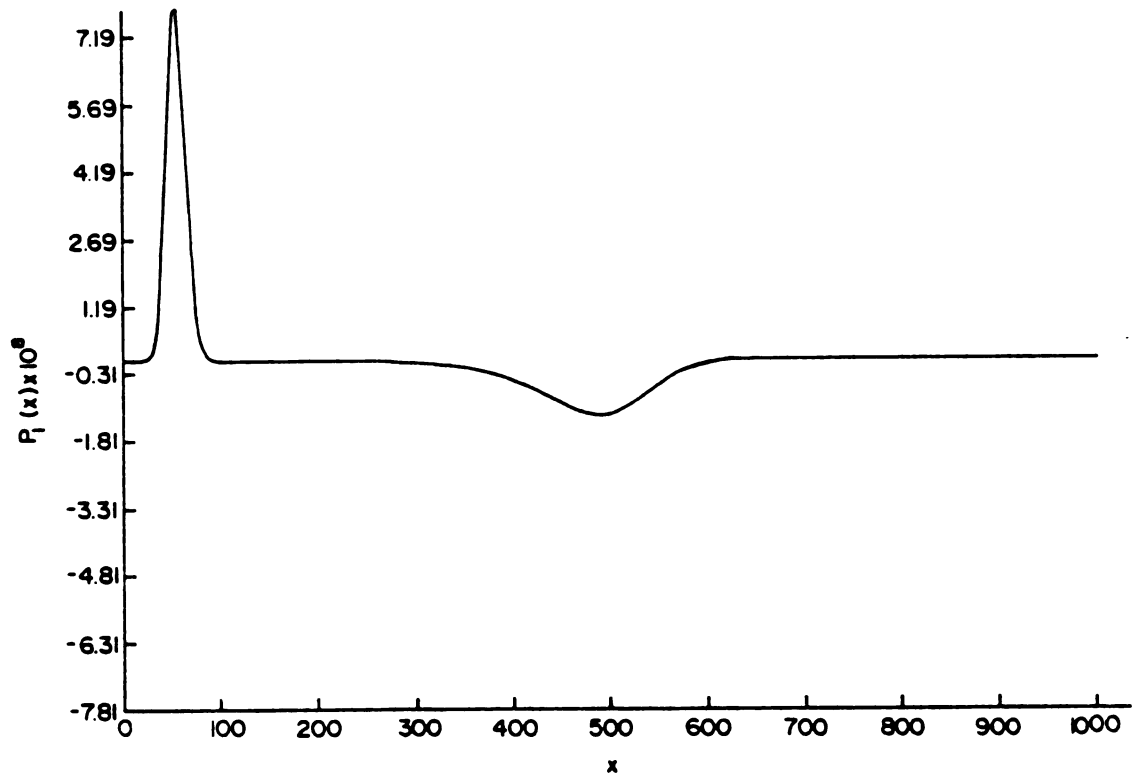


Figure 4.10.b The transition mode \underline{P}_1 .

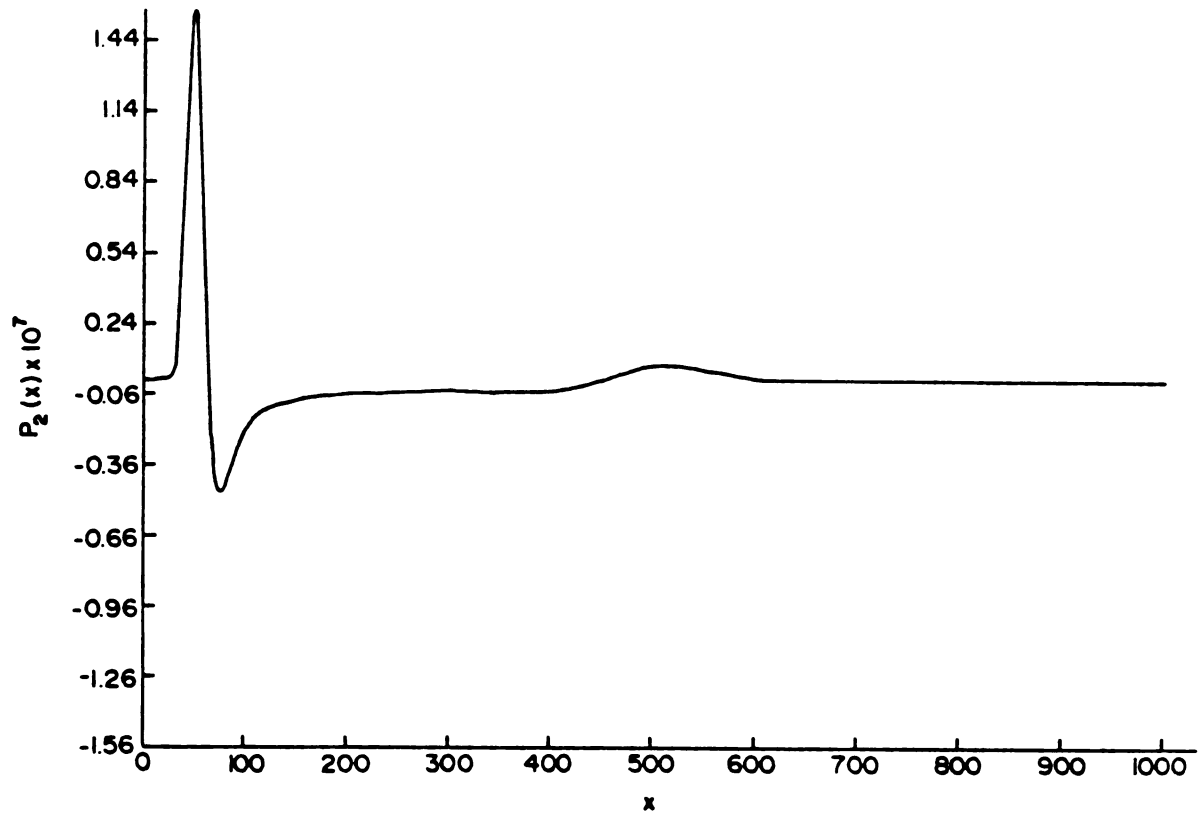


Figure 4.10.c The eigenvector \underline{P}_2 corresponding to λ_2 .

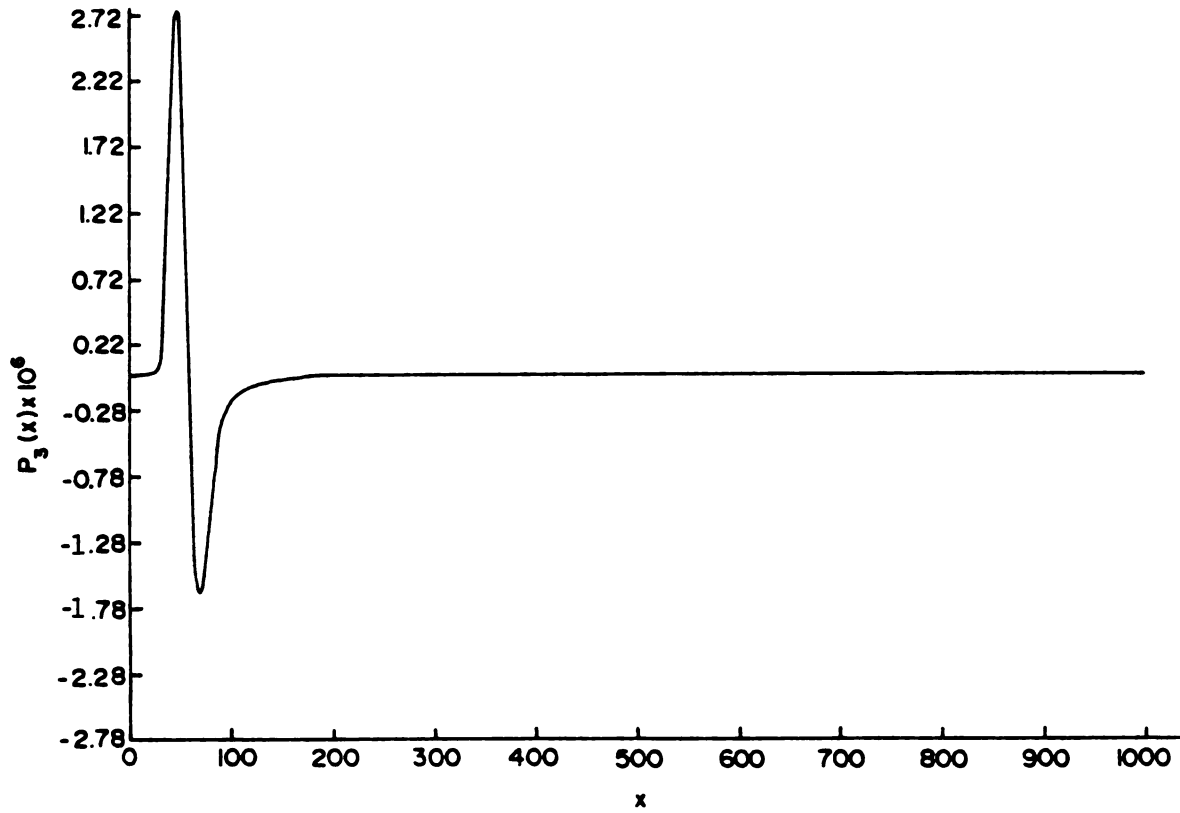


Figure 4.10.d The eigenvector \underline{P}_3 corresponding to λ_3 .

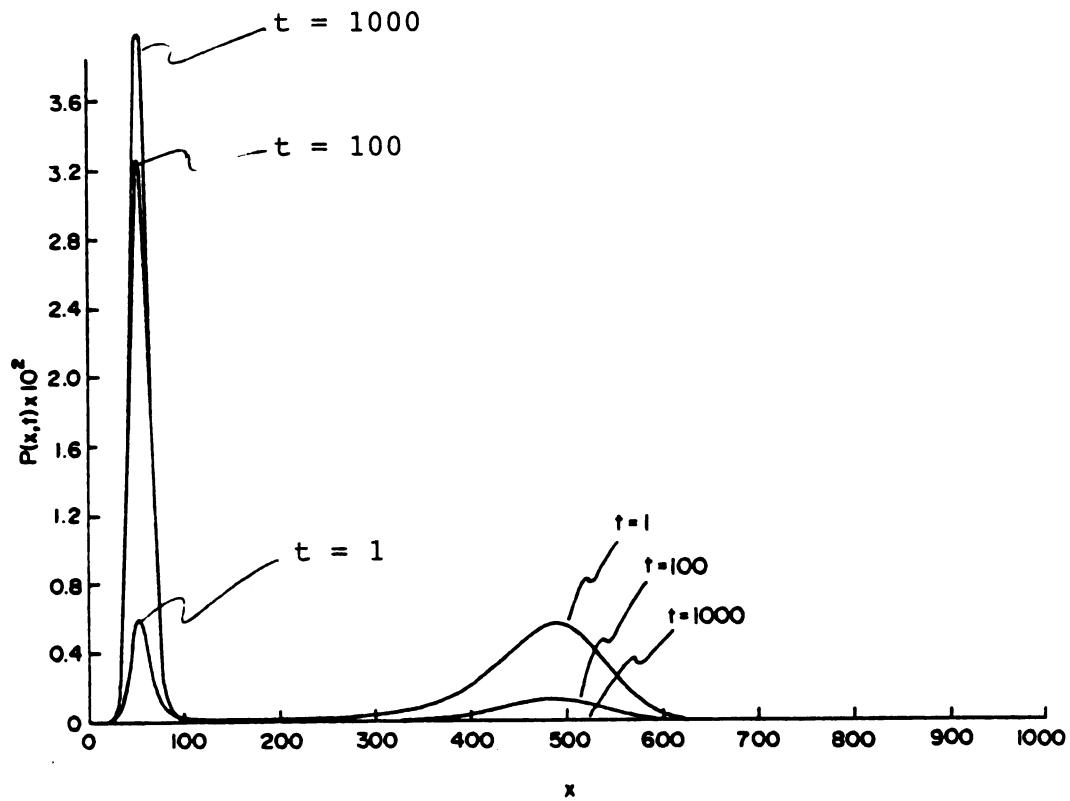


Figure 4.11 Time evolution of the probability distribution near a marginal stability point. $c_4 = 3.33333$
 $B = 9.6 \times 10^4$. Initial distribution is $\delta(x-400)$.

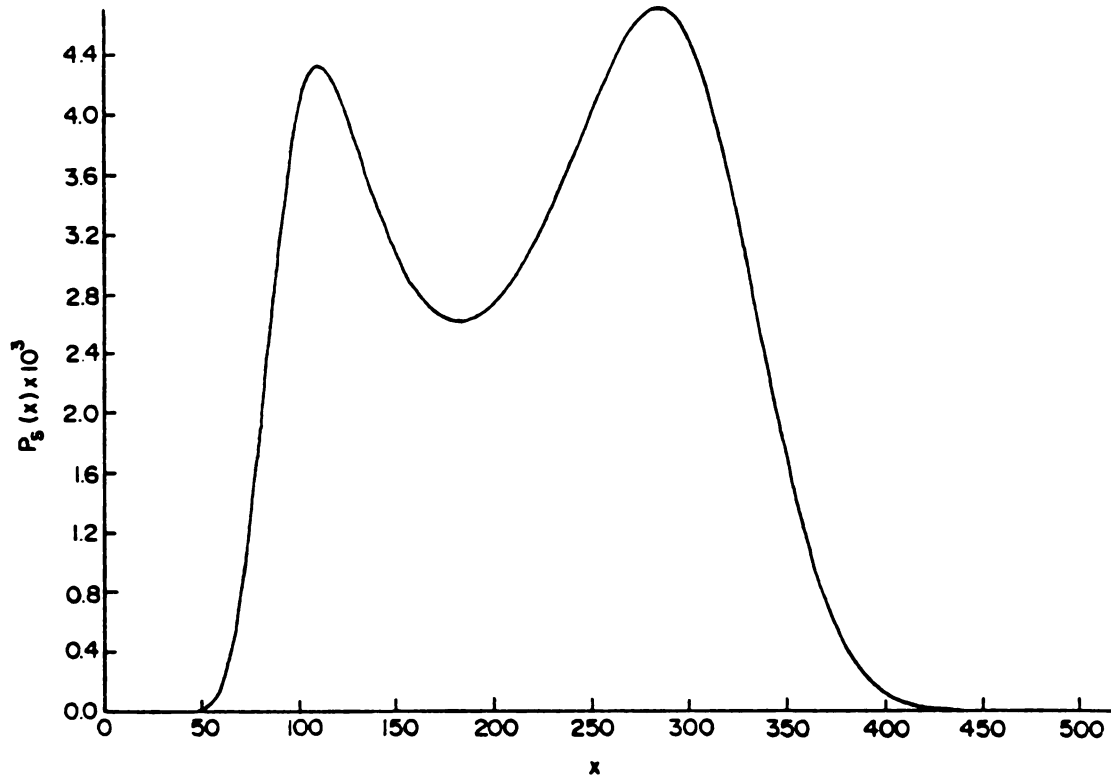


Figure 4.12.a

Figure 4.12 Eigenvectors of the transition matrix near the critical point. $c_4 = 1.7$ and $B = 6.39 \times 10^4$. The eigenvalues are a) 0, b) -4.9051×10^{-2} , c) -2.7271×10^{-1} , and d) -5.3060×10^{-1} .

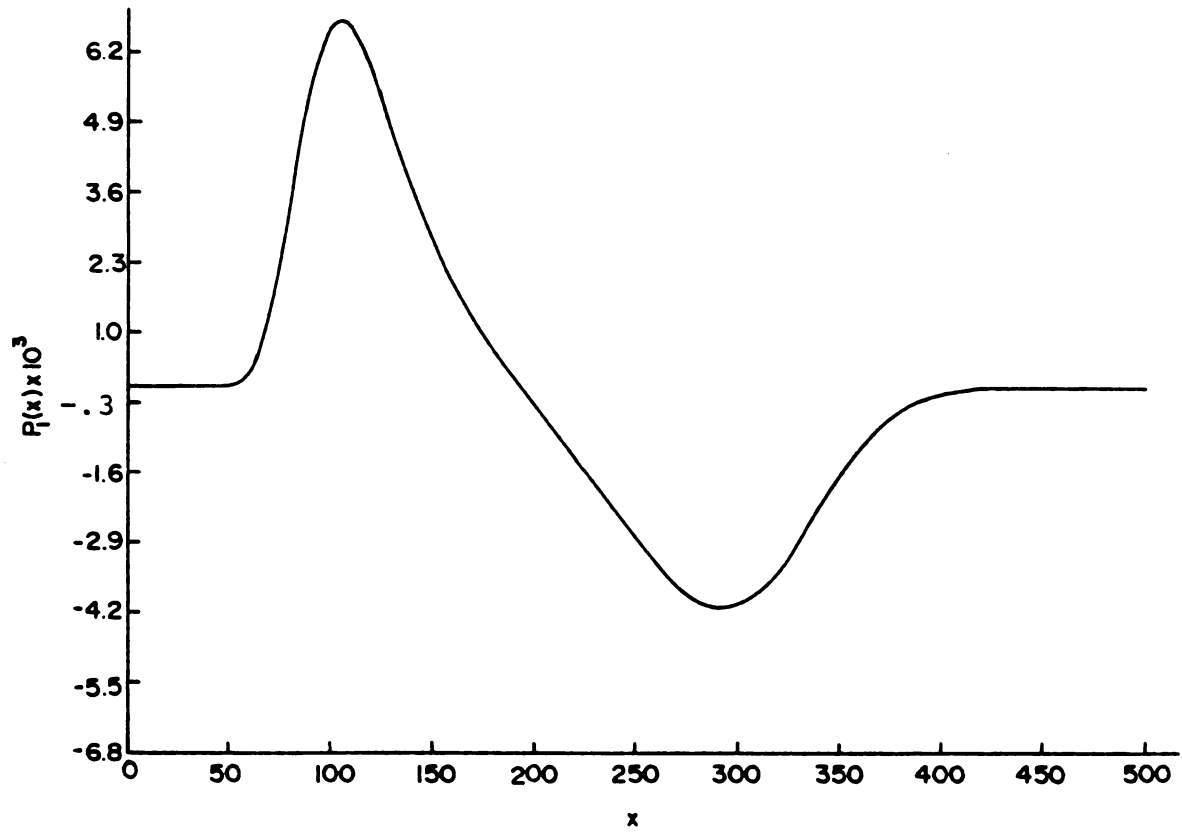


Figure 4.12.b

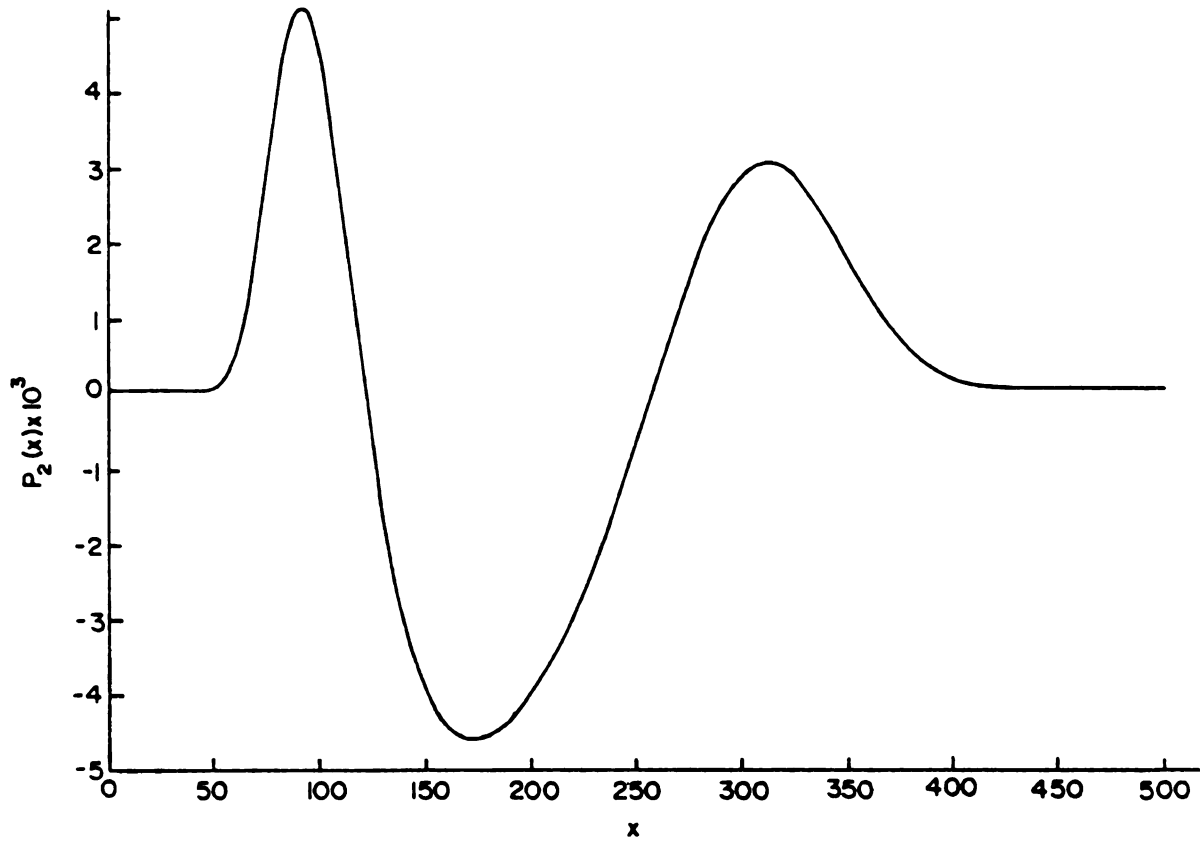


Figure 4.12.c

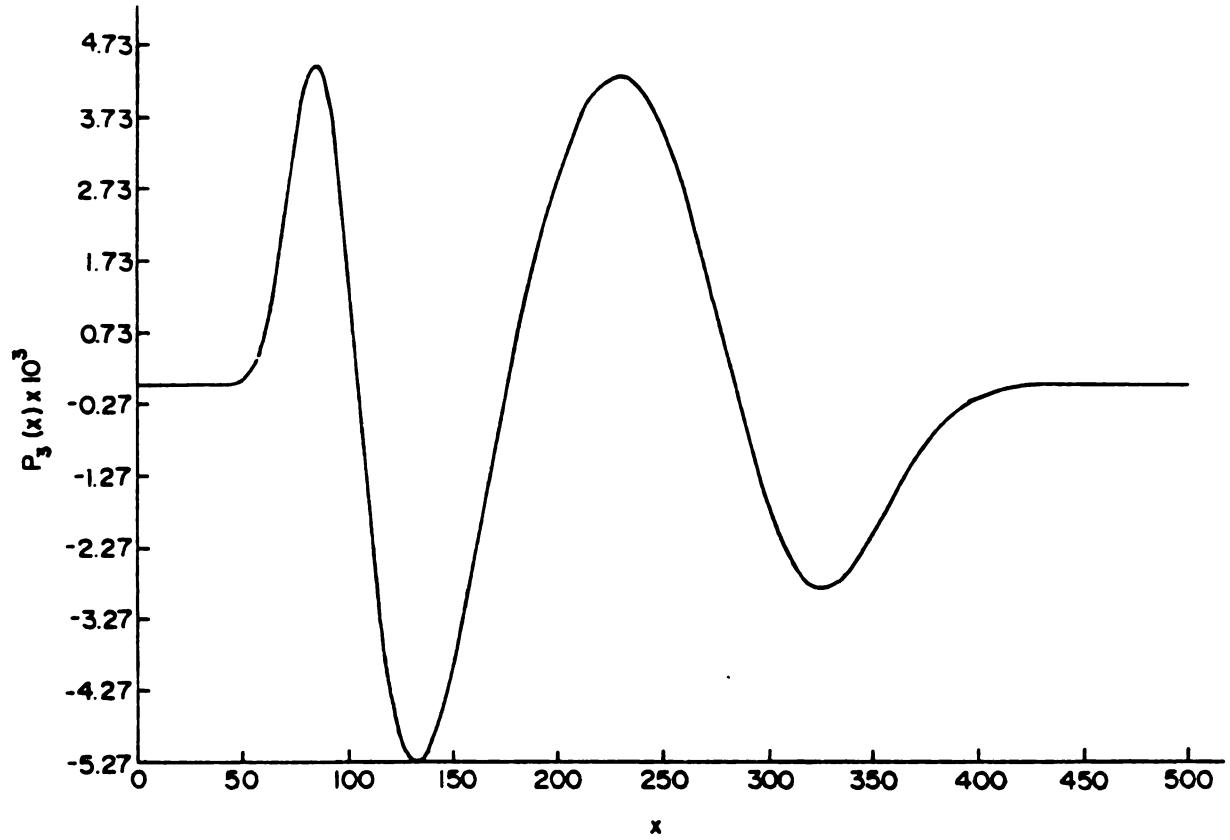


Figure 4.12.d

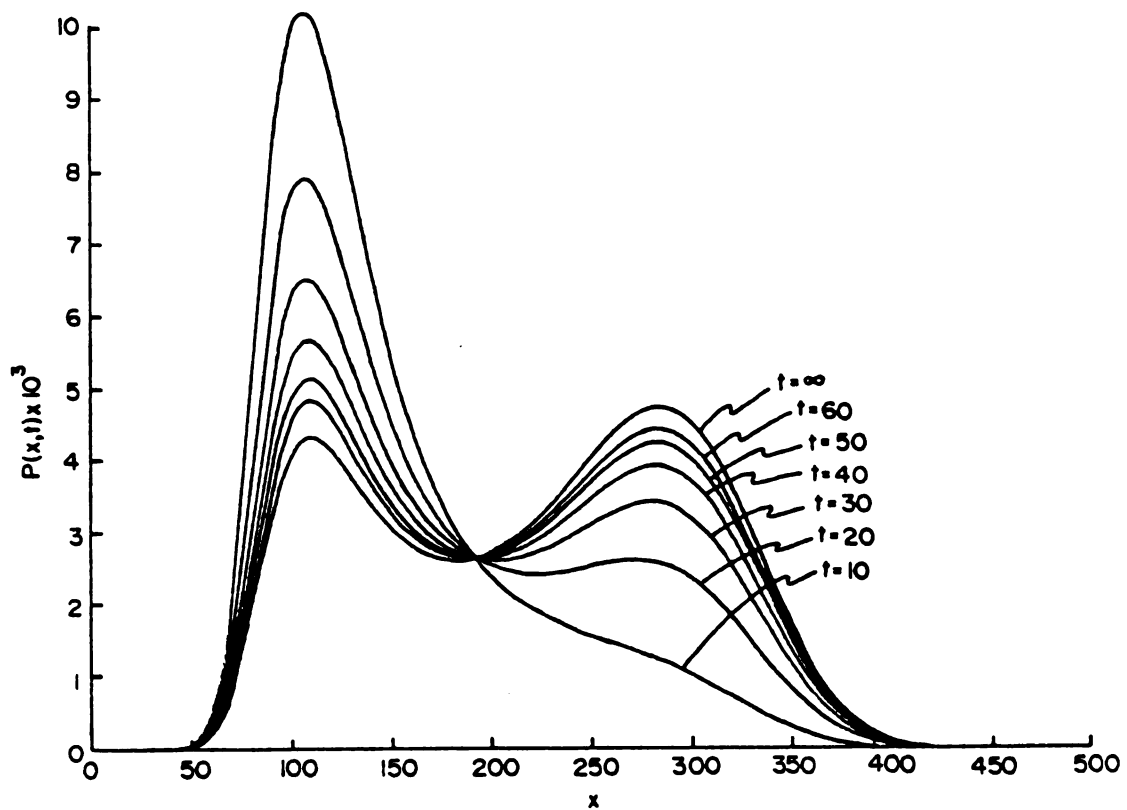


Figure 4.13.a

Figure 4.13 Time evolution of probability distribution near the critical point. $c_4 = 1.7$ and $B = 6.39 \times 10^4$. Initial distributions are a) $\delta(x-120)$, b) $\delta(x-300)$, and c) $\delta(x-182)$.

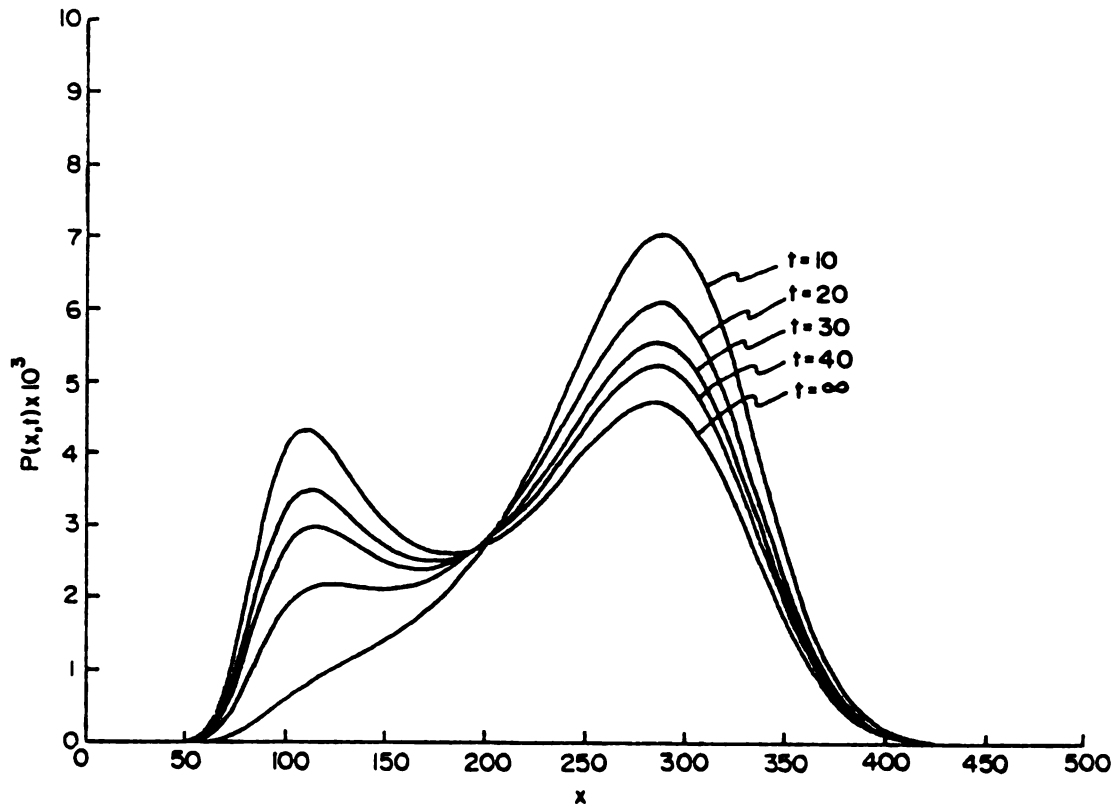


Figure 4.13.b

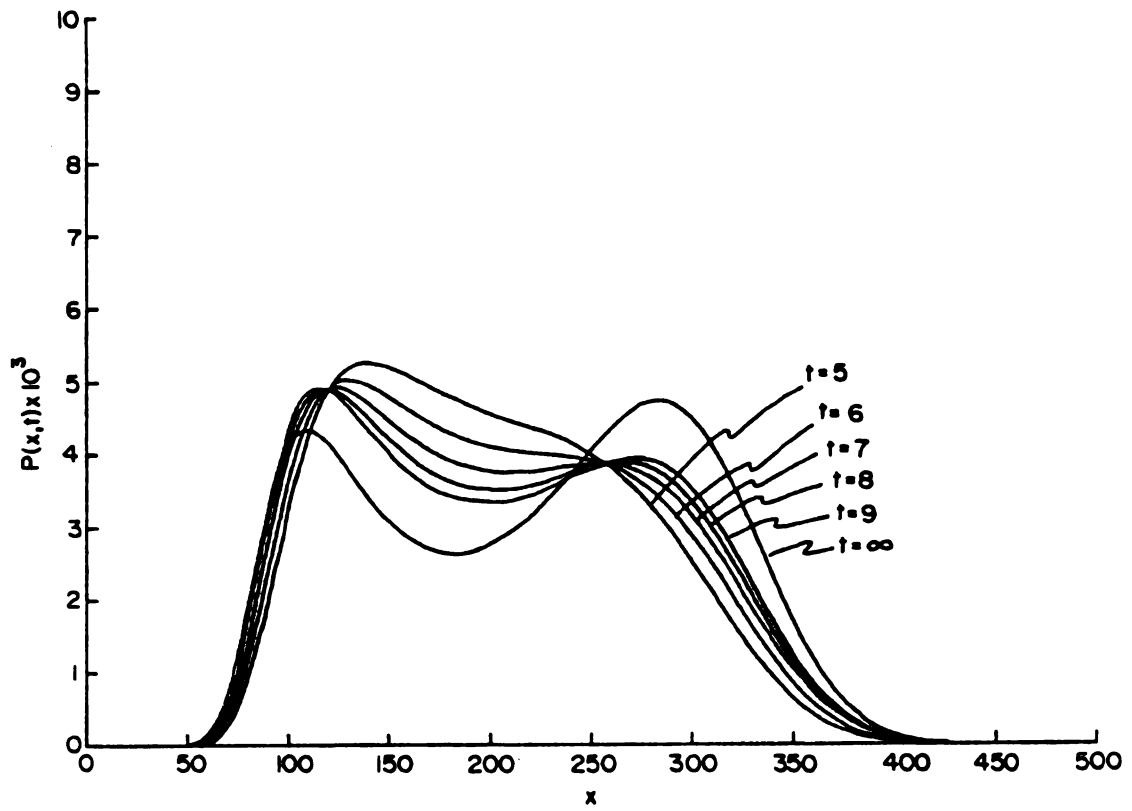


Figure 4.13.c

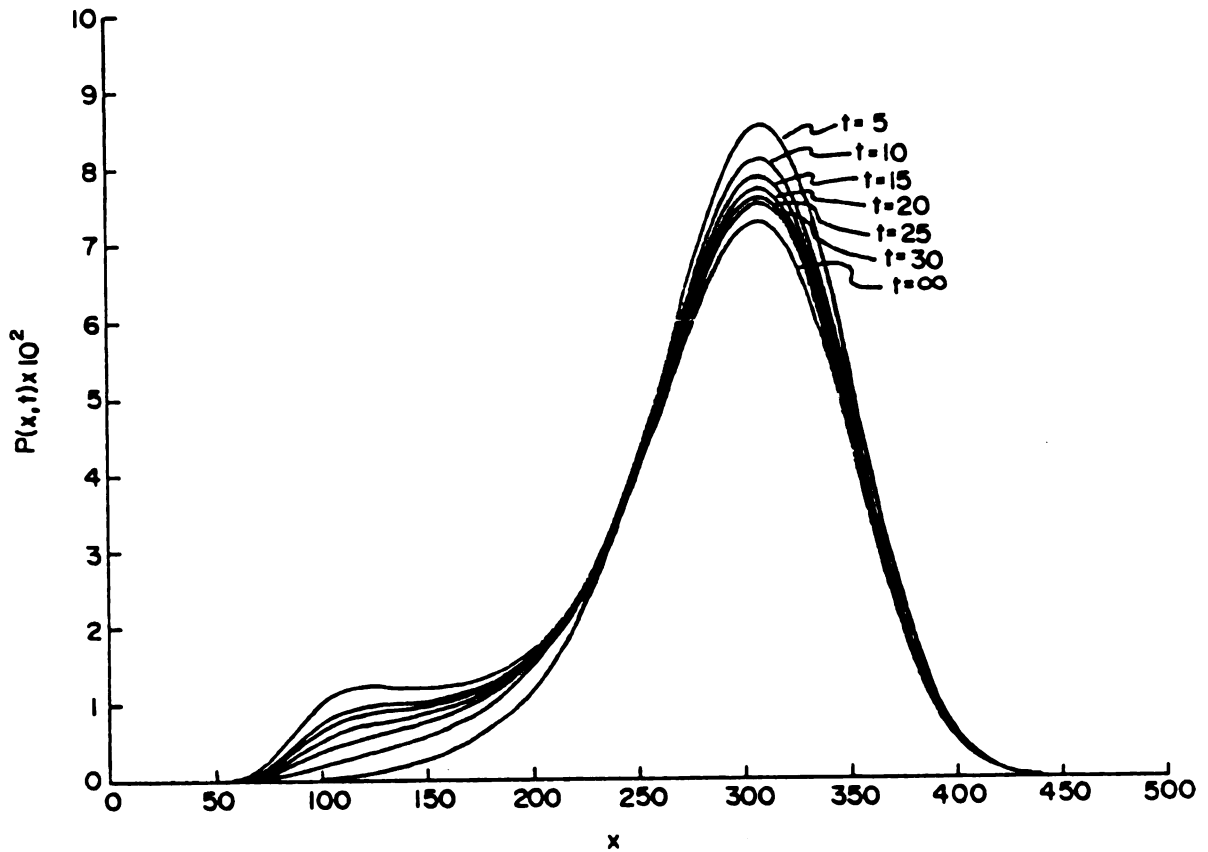


Figure 4.14.a

Figure 4.14 Time evolution of probability distribution near the critical point and near a marginal stability point. $c_4 = 1.7$ and $B = 6.45 \times 10^4$. Initial distributions are a) $\delta(x-300)$, b) $\delta(x-100)$, and c) $\delta(x-190)$.

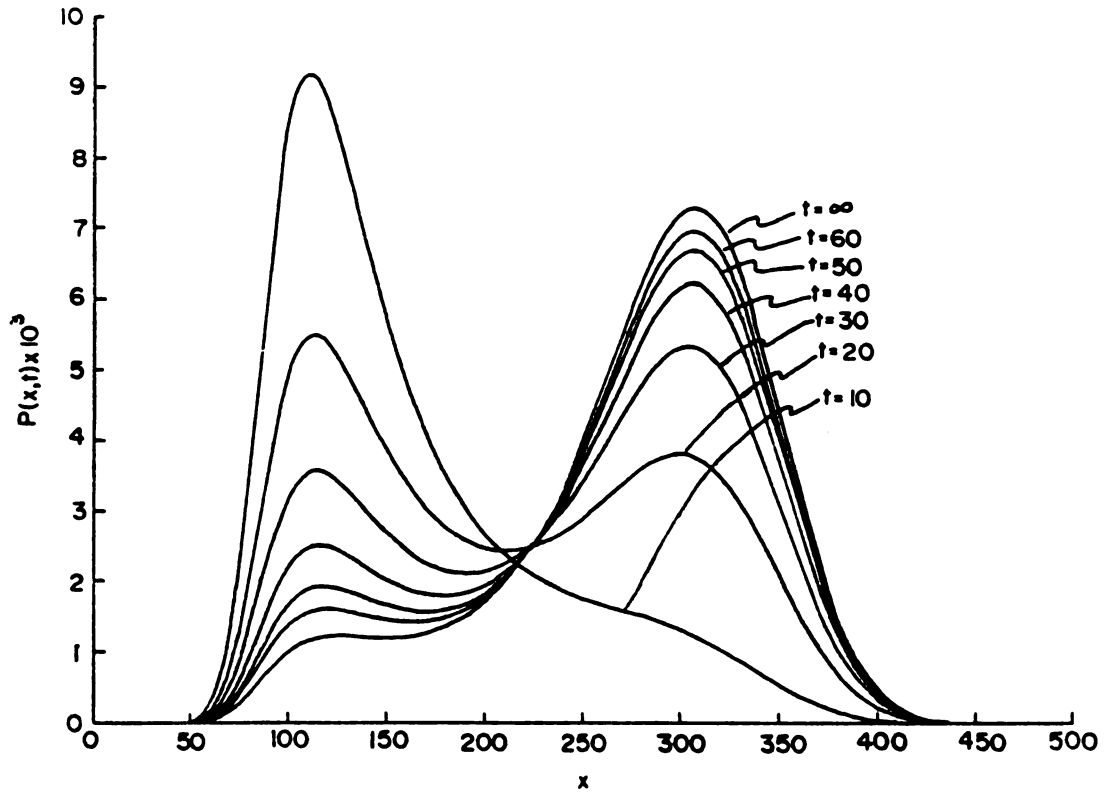


Figure 4.14.b

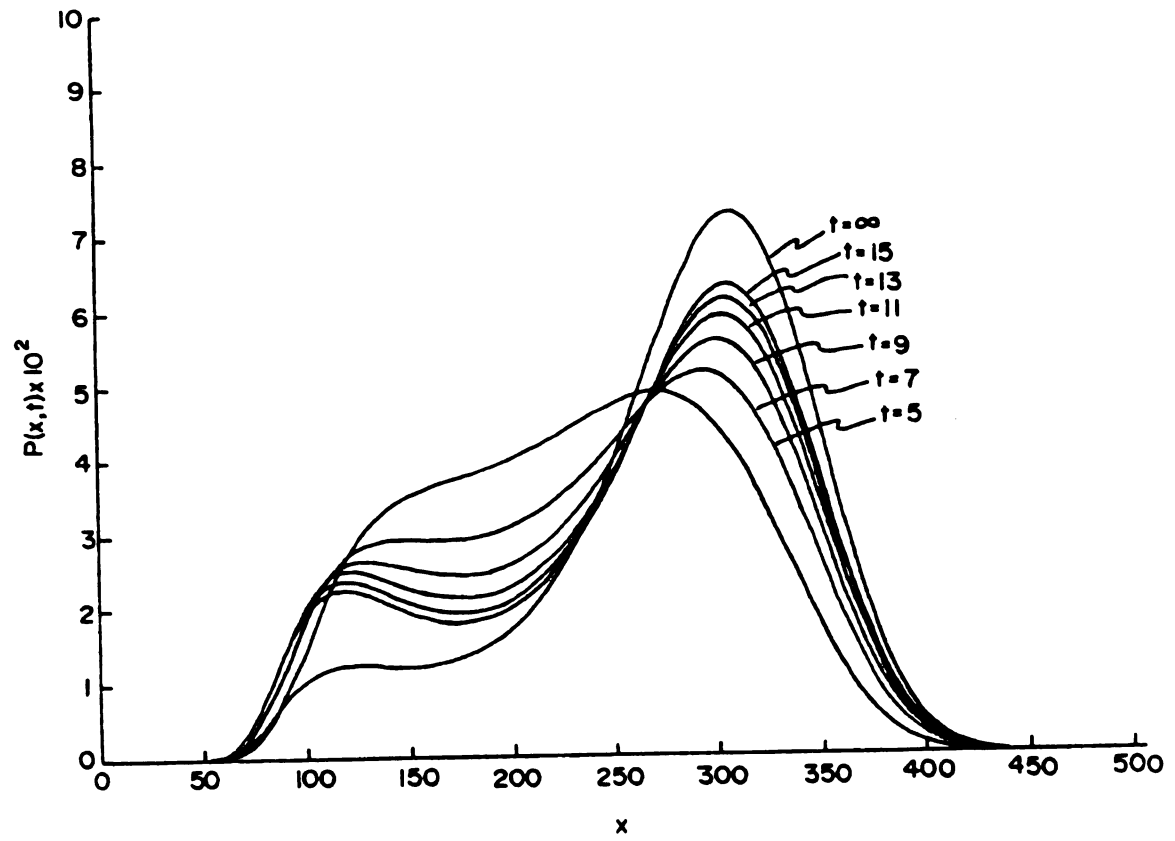


Figure 4.14.c

In summary, the asymptotic solutions of the master equation for the Schlögl model have been constructed from the eigenvectors of the transition matrix. In the cases studied, deviations from the Kramers rule are attributable not only to the similarity of the decay times of various modes, but also to distortions in the shape of the slowest mode.

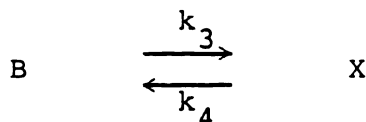
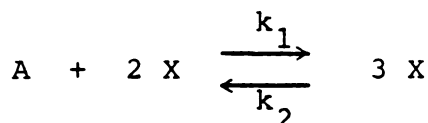
CHAPTER V

HYSTERESIS IN TRANSITIONS BETWEEN MULTIPLE NONEQUILIBRIUM STEADY STATES OF THE SCHLÖGL MODEL

Many models have been proposed and studied with the aim of understanding regulatory phenomena such as chemical oscillations and pattern formation in chemically reacting open systems far from equilibrium.^{1,3-5,56-60} One interesting phenomenon associated with the presence of multiple steady states in reacting systems far from equilibrium is hysteresis in transitions between the steady states. Hysteresis can be viewed as a special kind of oscillation caused by an external variation of a system parameter. I have simulated hysteresis in the Schlögl model system both deterministically and stochastically. Hysteresis has been observed by Creel and Ross⁵³ in the dissociation of N_2O_4 when irradiated with an argon-ion laser. The steady state patterns of the chemical system are similar to those of the model system.

5.1 SCHLÖGL MODEL AND ITS STEADY STATES

In the Schlögl model the chemical reactions



occur in a homogeneous open system; the numbers of molecules of A and B (denoted by A and B) are assumed to be externally controllable and they are constrained to be equal. Thus the number of molecules of X (denoted by X) is the only system variable. When the reaction parameter η defined by

$$\eta = \frac{k_1 k_4}{k_2 k_3}$$

exceeds a critical value $\eta_c = 9$, there is a range of B values for which the system has three possible steady states, $X_1 < X_2 < X_3$, of which X_1 and X_3 are stable and X_2 is unstable. Outside this range of B and below the critical point there is only one stable steady state. The boundary separating these two regions consists of the marginal stability points.

In the stochastic formulation $X(t)$ is viewed as a random variable taking integer values in $\{x: 0 < x < \infty\}$. The state of the system at a specified time t is then given by a probability vector $\underline{P}(t)$ whose x -th component is the probability that $X(t) = x$. The dynamics of the system are described by the time evolution of $P(x,t)$ [$P(x,t) \equiv P_x(t)$] according to the master equation for the Schlögl model^{5,9}

$$\begin{aligned} \frac{\partial}{\partial t} P(x,t) &= a_+(x-1,t)P(x-1,t) + a_-(x+1,t)P(x+1,t) \\ &\quad - a(x,t)P(x,t), \end{aligned} \tag{5.1}$$

where

$$a_+(x,t) = \frac{c_1}{2} B(t)x(x-1) + c_3 B(t), \quad (5.2)$$

$$a_-(x,t) = \frac{c_2}{6} x(x-1)(x-2) + c_4 x, \quad (5.3)$$

$$\text{and } a(x,t) = a_+(x,t) + a_-(x,t). \quad (5.4)$$

This equation allows for time dependence of B . The parameters c_i are related to the rate constants k_i by

$$c_i = k_i n_i! V^{1-m_i} \quad (5.5)$$

where n_i is the molecularity of the i -th step in X , m_i is the total molecularity of the i -th step (e.g., $n_1 = 2$ and $m_1 = 3$), and V is the volume of the system.¹⁰

5.2 DETERMINISTIC SIMULATION OF HYSTERESIS

For numerical studies we select the following values of the rate constants used by Gillespie:³⁶

$$\begin{aligned} c_1 &= 3 \times 10^{-7} \text{ (molecule}^{-3} \text{ time}^{-1}\text{)}, \\ c_2 &= 1 \times 10^{-4} \text{ (molecule}^{-3} \text{ time}^{-1}\text{)}, \\ c_3 &= 1.5 \times 10^{-3} \text{ (molecule}^{-1} \text{ time}^{-1}\text{)}; \end{aligned} \quad (5.6)$$

then $c_4 = 1.5$ (molecule⁻¹ time⁻¹) corresponds to the critical point. For c_4 values greater than this, the steady state curve is S-shaped (see Figure 5.1). If we first prepare the system at a single steady state in the lower branch and then slowly increase B, X follows close to the steady state value until near a marginal stability point and then it jumps to the vicinity of the other steady state branch. If B is slowly decreased, a downward jump occurs near the other marginal stability point. This generates a hysteresis loop, shown as the curves marked with arrows in Figure 5.1. The curves are the solutions of the equations of evolution

$$\frac{dX}{dt} = \frac{c_1}{2} B X (X-1) + c_3 B - \frac{c_2}{6} X(X-1)(X-2) - c_4 X$$

$$\frac{dB}{dt} = \pm \beta . \quad (5.7)$$

Hysteresis occurs to some extent below the critical point also, i.e., where there are no multiple steady states at all. This is shown by the curves with arrows in Figure 5.2.

The area enclosed by the hysteresis loop is a measure of the extent of hysteresis. In Figure 5.3, the area obtained from the deterministic treatment (equations (5.7)) is plotted versus the rate of change of B for various values of the critical parameter, c_4 . This increases with an increase in β indicating the dynamic contribution to the hysteresis effect.

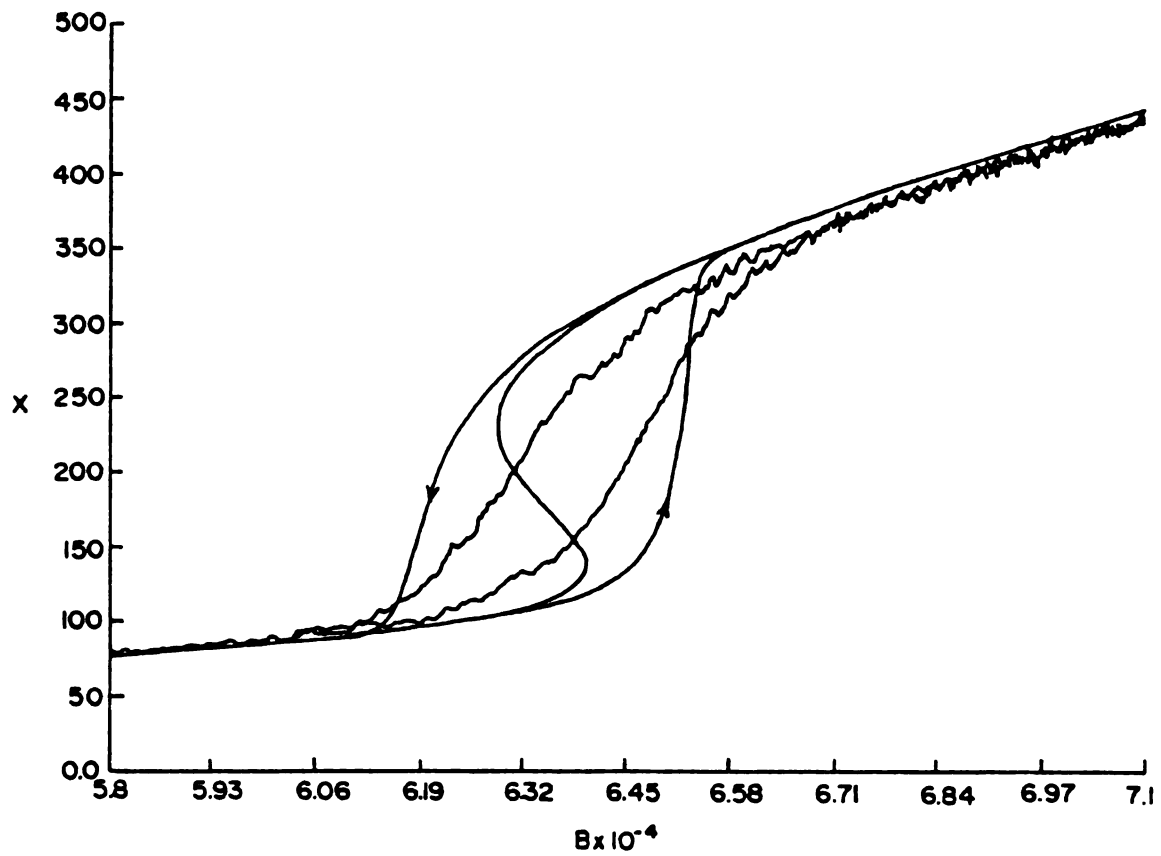


Figure 5.1 Results from deterministic (curves with arrows) and stochastic (noisy curves) simulations of hysteresis in the multistable region ($c_4 = 1.7$). The S-shaped curve is the set of steady states. $\beta = 50$.

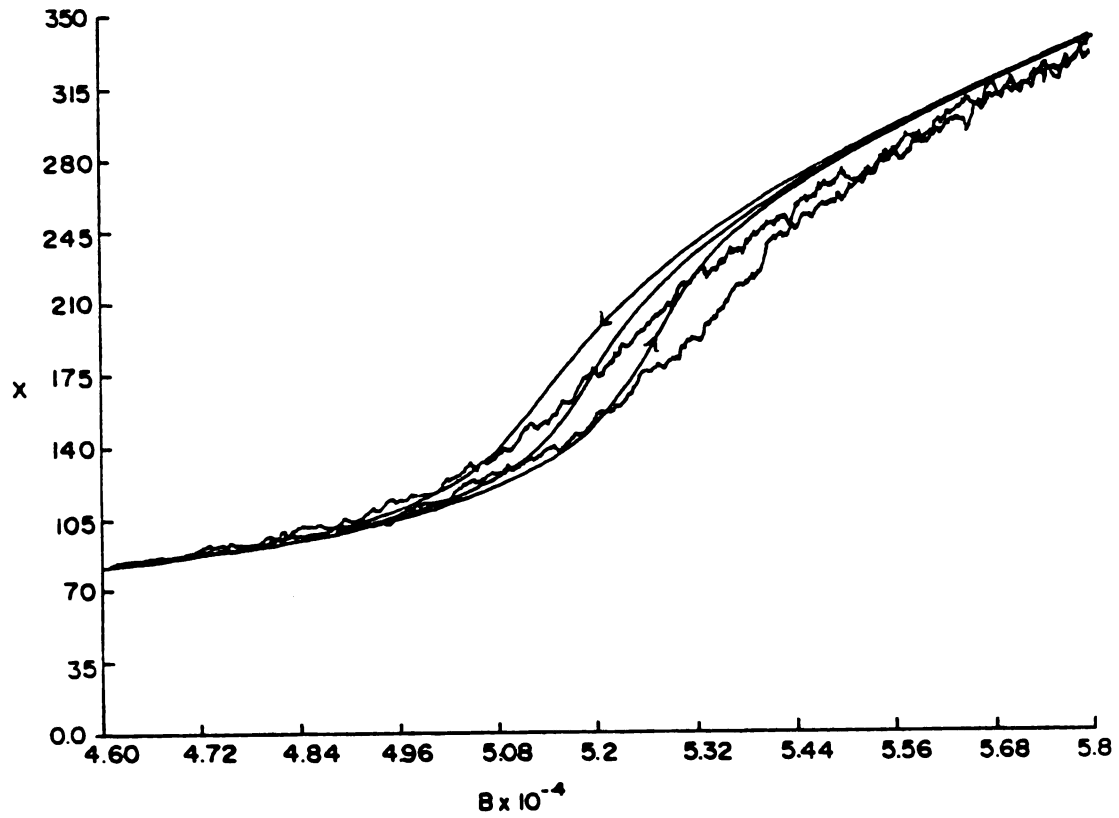


Figure 5.2 Results from deterministic (curves with arrows) and stochastic (noisy curves) simulations of hysteresis in the single steady-state region ($c_4 = 1.3$). $\beta = 50$.

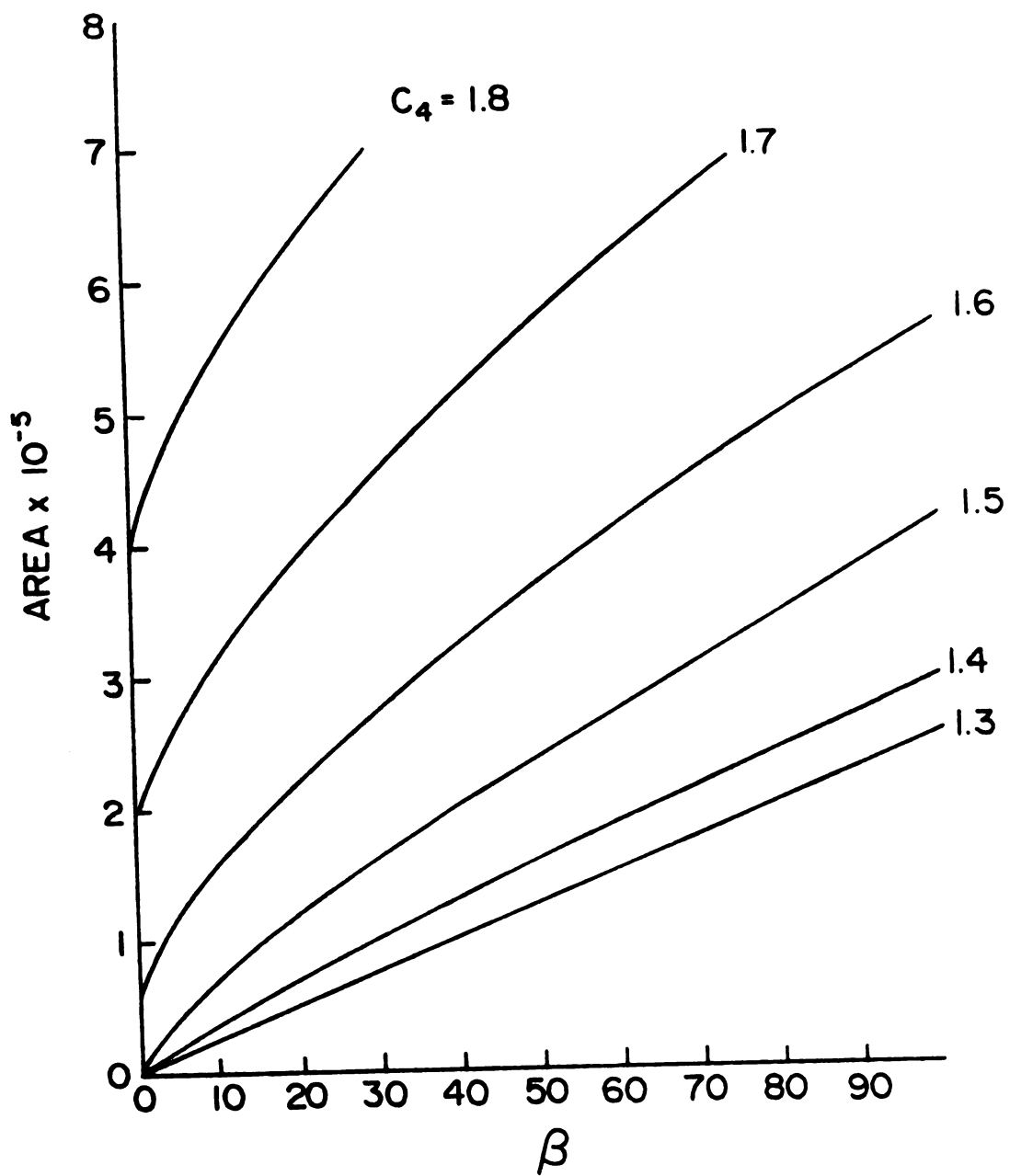


Figure 5.3 Area inside the hysteresis loop versus the rate of change of B. (Deterministic results)

In the figure, the points corresponding to $\beta = 0$ were obtained by integrating the area enclosed between the two branches of stable steady states. This is the area obtained when vertical transitions (transitions with $dX/dB \rightarrow \pm\infty$) occur exactly at the marginal stability points. It is interesting to note that the area of the hysteresis loop extrapolates to this finite value as β tends to zero in the multiple steady state region, and it extrapolates to zero in the single steady state region. The finite limit indicates a static contribution to the hysteresis effect from the multi-state region, but below the critical point the hysteresis is purely dynamic.

5.3 STOCHASTIC SIMULATION

Gillespie has devised an algorithm to simulate chemical reaction systems stochastically¹⁰ and has extended it to include time dependent transition rates²⁰ (section 2.3). This algorithm first randomly selects the time of the next reaction and then draws another random number to determine which of the various reaction steps should be carried out. If a reaction step has occurred at time t , bringing the system to state x , then the probability $P_1(\tau; x, t)d\tau$ that the next reaction step will occur in the time interval $(t+\tau, t+\tau+d\tau)$ is given by

$$P_1(\tau; x, t) = a(x, t+\tau) \exp \left\{ - \int_t^{t+\tau} a(x, s) ds \right\}. \quad (5.8)$$

The conditional probability that the next reaction is a forward (or backward) step given that the next reaction occurs after an interval τ , is

$$P_2(\pm|\tau;x,t) = \frac{a_{\pm}(x,t+\tau)}{a(x,t+\tau)}. \quad (5.9)$$

The simulation algorithm starts by selecting two random numbers r_1 and r_2 with uniform probability from the unit interval. The distribution function corresponding to $P_1(\tau;x,t)$ is

$$\begin{aligned} F_1(\tau;x,t) &= \int_0^{\tau} P_1(s;x,t) ds \\ &= \int_0^{\tau} a(x,t+s) \exp [A(t) - A(t+s)] ds \end{aligned} \quad (5.10)$$

where

$$A(t) = \int_0^t a(x,s) ds \quad (5.11)$$

After performing the integral we obtain

$$F_1(\tau;x,t) = 1 - \exp \left\{ - \int_0^{\tau} a(x,t+s) ds \right\}. \quad (5.12)$$

We need to select τ such that

$$r_1 = F_1(\tau),$$

$$\text{i.e., } \int_0^{\tau} a(x, t+s) ds = -\ln(1-r_1). \quad (5.13)$$

In equation (5.13) we can replace $1-r_1$ by r_1 since both are statistically equivalent. For the Schlögl model $a_-(x, t)$ is independent of B and $a_+(x, t)$ depends linearly on B . When B is varied linearly with time,

$$a(x, t+s) = a(x, t) + \frac{a_+(x, t)}{B(t)} \beta s. \quad (5.14)$$

Therefore,

$$\int_0^{\tau} a(x, t+s) ds = a(x, t)\tau + \frac{a_+(x, t)}{B(t)} \beta \frac{\tau^2}{2}. \quad (5.15)$$

Combining equations (5.13) and (5.15), we obtain a quadratic equation for τ :

$$\frac{a_+(x, t)}{2B(t)} \tau^2 + a(x, t)\tau + \ln r_1 = 0. \quad (5.16)$$

Solving the quadratic equation and selecting the solution that

is continuous in r_1 and gives a nonnegative value for τ , we have the following relation between r_1 and τ :

$$\tau = \begin{cases} \frac{-a(x,t) + [a(x,t)^2 - \frac{2\beta}{B(t)} a_+(x,t) \ln r_1]^{\frac{1}{2}}}{a_+(x,t)\beta / B(t)} \\ \text{if } \beta > 0 \quad \text{or} \quad -\ln r_1 < -\frac{B(t)}{\beta} [\frac{1}{2}a_+(x,t) - a_-(x,t)] \\ \\ \frac{1}{a_-(x,t)} \left(\frac{B(t)}{2\beta} a_+(x,t) - \ln r_1 \right) \\ \text{if } \beta < 0 \quad \text{and} \quad -\ln r_1 > -\frac{B(t)}{\beta} [\frac{1}{2}a_+(x,t) - a_-(x,t)] \end{cases} \quad (5.17)$$

From equation (2.65) we also have a relation between r_2 and m :

$$m = \begin{cases} +1 & \text{if } r_2 < a_+(x,t+\tau) / a(x,t+\tau) \\ -1 & \text{if } r_2 > a_+(x,t+\tau) / a(x,t+\tau). \end{cases} \quad (5.18)$$

The time variable is advanced by τ and the particle number for X is incremented or decremented by one depending on whether m is positive or negative. This procedure is then repeated for the new state. The iteration produces a random path of the system in time. This approach yields results equivalent to those obtained by the master equation. Two hundred sample paths have been simulated and the averaged paths are shown in Figures 5.1 and 5.2.

In the deterministic simulation, the transition cannot

occur before the marginal stability point is reached (Appendix A); but as seen in Figure 5.1 (noisy curves), fluctuations induce the transition within the multiple steady state region. The areas obtained from the stochastic simulations A_s and the corresponding deterministic areas A_d are plotted versus β and c_4 in Figures 5.4 and 5.5 respectively. The error bars indicate expected deviations from the mean; they were calculated from the standard deviations using the central limit theorem.¹⁷ In general the area A_s obtained from stochastic simulation is less than that from the deterministic integration (A_d), though the qualitative behaviour is the same in both cases. Another important difference between the two kinds of simulation is that as the rate of change of B tends to zero, A_d tends to a finite value in the multiple steady state region, but A_s tends to zero.

When B is changed at an infinitesimal rate, the deterministic analysis predicts that the forward and backward transitions occur at two different marginal stability points whereas the stochastic analysis predicts a unique transition point on the average in the multiple steady state region. This point was noticed and emphasized by Turner.⁶¹ However this result should not be interpreted as a complete absence of hysteresis effects in the stochastic simulation; rather, our results show that hysteresis in the Schlögl model is a dynamic effect and that the static contribution predicted by a deterministic analysis disappears when fluctuations are taken into account.

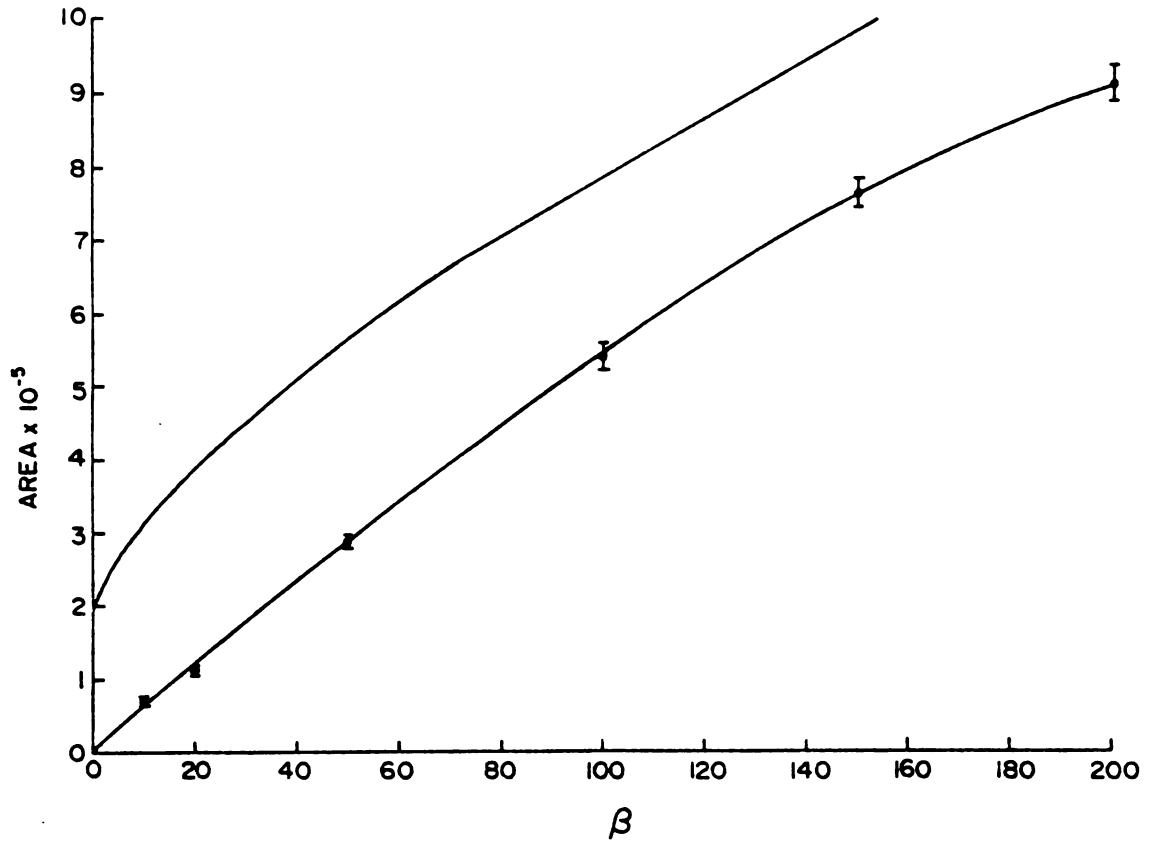


Figure 5.4 Comparison of deterministic (upper line) and stochastic simulation (lower line) results.

$$c_4 = 1.7$$

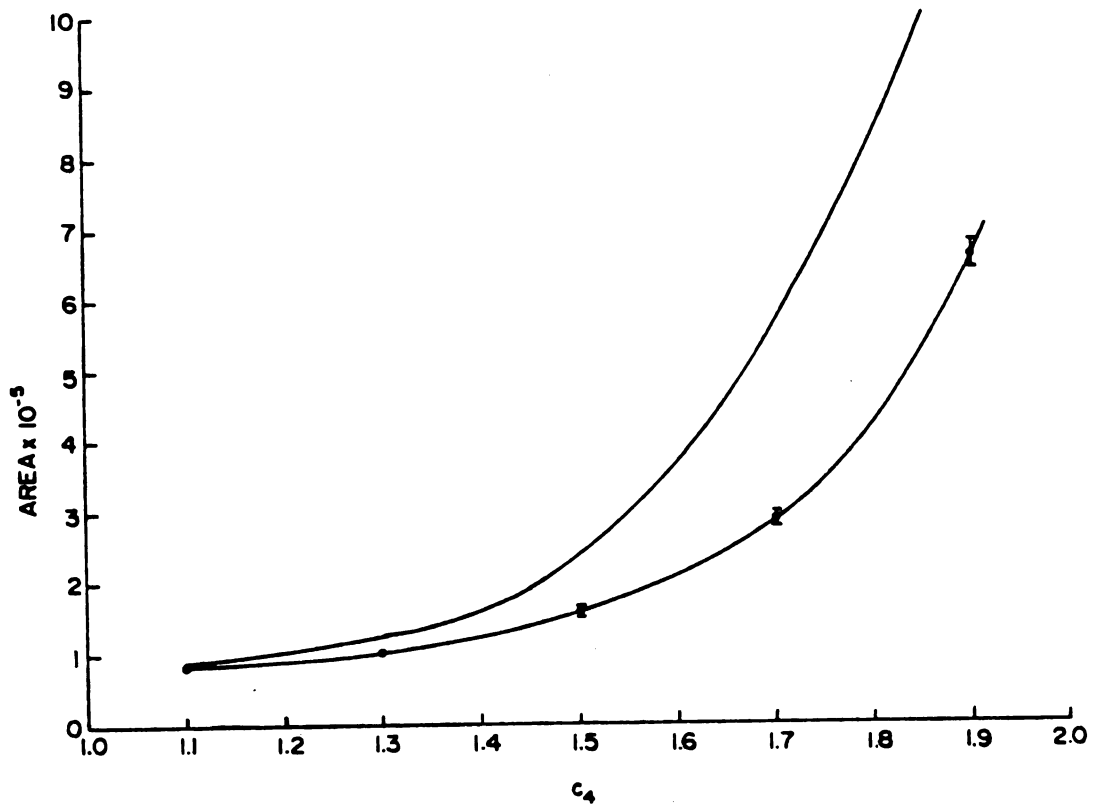


Figure 5.5 Comparison of deterministic (upper line) and stochastic simulation (lower line) results.

$\beta = 50.$

CHAPTER VI
DETERMINISTIC STUDY OF MULTIPLE STEADY STATES IN COUPLED
FLOW TANK REACTORS

The question of relative stability of different steady states arises when two or more of the steady states compatible with fixed fluxes, fixed elemental composition of the system and external conditions are asymptotically stable to small concentration fluctuations. Resolutions have been proposed on the basis of stochastic analysis³⁶, thermodynamic analysis³⁰⁻³², and mixing experiments²⁹ (section 3.4).

The purpose of this chapter is to describe the new steady states and dynamical behavior of coupled systems when each exhibits multiple steady states. It is also shown how the outcome of mixing experiments with exchange of material between two continuously stirred flow tank reactors can be predicted from a deterministic analysis; the results obtained differ from those predicted by Noyes²⁹, except for simple cubic reaction rate laws. It is shown that deterministic studies of coupled tanks do not yield information about the relative stabilities of single tank steady states, even when the outcome of a mixing experiment is independent of the mixing method, i.e., independent of the changes made in the coupled rate constant as a function of time.

6.1 MULTIPLE STEADY STATES IN A SINGLE CONTINUOUSLY STIRRED FLOW-TANK REACTOR.

A model continuously stirred flow tank reactor (CSTR) is characterized by two assumed operating conditions:

1. The volume of material in the tank reactor is fixed and there is a negligible change in the density of material as a consequence of reaction.

2. Mixing is assumed to be sufficiently rapid that the material is uniform in composition throughout the tank.

The concentration of reactant i in the input is R_0^i , and if product j is present in the input stream, its concentration is P_0^j . The reactant concentration in the output stream is identical to that in the tank. The flow of material through the tank is characterized by a flow rate constant k_0 , the inverse of the average residence time for material in the tank; equivalently k_0 is the ratio of the volume of material entering the reactor per unit time to the total reactor volume.

In the following development we restrict attention to the case where there is a single reactant R and a single product P in the tank, as in the work by Noyes²⁹. With a single reactant and product, if $R_T = R_0 + P_0$, and if the tank is flushed with material from the input stream so that the total reaction plus product concentration is equal to R_T initially, then deterministically $R + P = R_T$ at all times.

In the tank, reactant R is converted into product P by reaction according to the rate law

$$dP/dt = - dR/dt = v(R,P) = v(R,R_T), \quad (6.1)$$

where the last equality is valid because P can be replaced by $R_T - R$. With the addition of the rate of change of R due to flow through the tank, the total rate of change of reactant concentration is

$$dR/dt = k_0(R_0 - R) - v(R,R_T). \quad (6.2)$$

Three different polynomial forms for $v(R,R_T)$ and the deterministic steady states associated with these models are used as explicit examples in this chapter. The forms for $v(R,R_T)$ are

1. Noyes' cubic model. For this model

$$v(R,P) = a(R-P/K) (1 - bR + cR^2), \quad (6.3)$$

and the variables have values $a = 8.97 \times 10^{-4} \text{ s}^{-1}$, $ab = 5.985 \times 10^{-2} \text{ M}^{-1} \text{ s}^{-1}$, $ac = 1.00 \times 10^{-2} \text{ M}^{-2} \text{ s}^{-1}$, $K = 10^6$ and $R + P = R_T = 0.1 \text{ M}$

2. Noyes' quartic model. For this model,

$$v(R,P) = a' (R-P/K) (1 - b'R + c'R^3), \quad (6.4)$$

with $a' = 10^{-3} \text{ s}^{-1}$, $b' = 50 \text{ M}^{-1}$, $c' = 1.87 \times 10^4 \text{ M}^{-3}$, $K = 10^6$ and $R_0 = R_T = 0.1 \text{ M}$.

3. Two quintic forms Q_1 and Q_2 , for which

$$v = (R-P/K) (a + bP + cP^2 + dP^3 + eP^4), \quad (6.5)$$

$K = 10^6$ and $R_T = 0.2 M$. The quintic expressions are aphysical as reaction rates, but they are useful in illustrating the difference between mathematical results valid without restrictions on $v(R, R_T)$ and those steady-state and dynamical results applicable when $v(R, R_T)$ is any cubic polynomial. For models Q_1 and Q_2 , the constant sets take the following values:

Q_1 :

$$\begin{aligned} a &= 3.028222 \times 10^{-9} \text{ s}^{-1} \\ b &= 3.822292 \times 10^{-3} \text{ M}^{-1} \text{ s}^{-1} \\ c &= 1.984543 \times 10^{-2} \text{ M}^{-2} \text{ s}^{-1} \\ d &= 6.649973 \times 10^{-2} \text{ M}^{-3} \text{ s}^{-1} \\ e &= 0.999999 \text{ M}^{-4} \text{ s}^{-1}, \end{aligned}$$

Q_2 :

$$\begin{aligned} a &= 2.966667 \times 10^{-8} \text{ s}^{-1} \\ b &= 3.788482 \times 10^{-3} \text{ M}^{-1} \text{ s}^{-1} \\ c &= 1.969993 \times 10^{-2} \text{ M}^{-2} \text{ s}^{-1} \\ d &= 6.499974 \times 10^{-2} \text{ M}^{-3} \text{ s}^{-1} \\ e &= 0.999999 \text{ M}^{-4} \text{ s}^{-1}. \end{aligned}$$

Corresponding to a given value of R_0 (less than or equal to R_T),

there is a range of k_0 values for which there are three real positive solutions of $dR/dt = 0$ for Noyes' cubic model and for the two quintics. The three steady state solutions are designated R_α , R_β , and R_γ , with $R_\alpha < R_\gamma < R_\beta < R_T$. In Figure 6.1, the steady-state R concentrations are plotted as functions of k_0 for six different R_0 values in the range from 0.03M to 0.1M, with $R_T = 0.1M$ for Noyes' cubic model (in Noyes' work $R_T \equiv R_0$). For the quintic models, attention is restricted to single values of k_0 , $k_0 = 7.659631 \times 10^{-4} \text{ s}^{-1}$ for model Q_1 and $k_0 = 7.5924 \times 10^{-4} \text{ s}^{-1}$ for model Q_2 . In general, for the quartic model, there are four steady state solutions of the deterministic kinetic equations, but the branch of solutions with the smallest R values is unstable to small concentration fluctuations; Noyes has plotted the remaining three solution branches as functions of k_0 in reference 29.

The stability of the steady-state solutions of equation (6.2) may be determined by a linear stability analysis. If \bar{R} is a steady state solution of the deterministic kinetic equation for reactant concentration, then the time-evolution of a small concentration fluctuation δR about \bar{R} is governed by

$$\frac{d}{dt} \delta R = - \left(k_0 + \left. \frac{\partial v}{\partial R} \right|_{\bar{R}} \right) \delta R, \quad (6.6)$$

on the unidimensional subset of the full concentration space defined by the condition $R + P = R_T$. Therefore a single tank

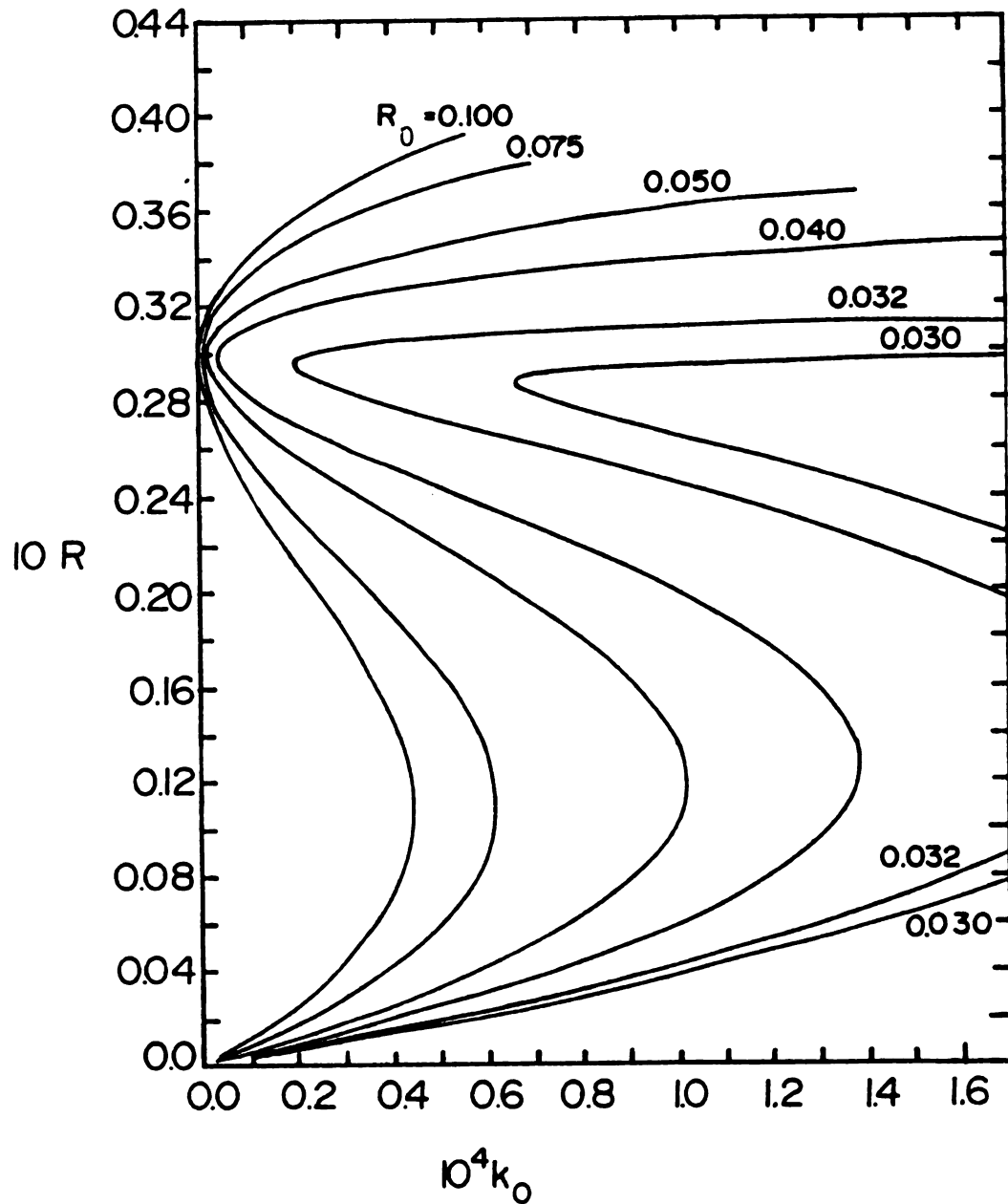


Figure 6.1 Steady states for the cubic model in a single flow tank reactor. The reactant concentration (R) in the tank at steady state is plotted as a function of the flow rate constant (k_0) for various values of reactant concentration (R_0) in the input stream.

state is stable if $k_0 + (\partial v / \partial R)_{\bar{R}} > 0$, marginally stable if $k_0 + (\partial v / \partial R)_{\bar{R}} = 0$, and unstable otherwise. For all of the models (6.3 - 6.5), linear stability analysis shows that the intermediate concentration γ branch is unstable to small concentration fluctuations, while the α and β branches are stable. The points of coalescence of the γ branch with the α or β branch are marginal stability points (see Figure 6.1).

Our aim is to investigate what happens when two tanks, one initially in the α state and the other in the β state, are coupled by exchange of material. As part of this investigation we find the possible steady states of the coupled tank system and their dependence upon the coupling rate constant k_x . This analysis shows that the outcome of mixing experiments is not an indicator of the relative stability of the asymptotically stable steady states.

6.2 COUPLED FLOW-TANK REACTORS

Let us consider two tanks, operated with the same flow rate constant k_0 , the same R_T , and $R_0 = R_T$ (i.e., each has an input stream containing reactant only). Conversion of reactant to product is assumed to proceed according to the same rate law in each tank. If the two tanks are coupled by a mechanical pumping of material from tank 1 to tank 2, while at the same time, material is pumped from tank 2 into tank 1 with the same flow rate constant k_x , then the rate of change of reactant concentrations in the two tanks are

$$dR_1/dt = k_0 (R_0 - R_1) - v(R_1, R_0) + k_x (R_2 - R_1)$$

$$\text{and } dR_2/dt = k_0 (R_0 - R_2) - v(R_2, R_0) + k_x (R_1 - R_2).$$

(6.7)

Thus, independent of the values of k_x , the points $(R_1, R_2) = (R_\alpha, R_\alpha)$, (R_β, R_β) , and (R_γ, R_γ) are always steady-state solutions of the coupled tank equations.

Because the condition $R + P = R_T$ reduces the single-tank problem to a single-variable problem, there is a potential that governs the deterministic time-evolution of the single-tank system, and there is also a potential in the coupled-tank case. If $V(R)$ is defined by the condition

$$V(R) = \int^R v(x, R_0) dx, \quad (6.8)$$

and if ϕ is defined by

$$\begin{aligned} \phi(R_1, R_2; k_0, k_x) = & -k_0 R_0 R_1 + 1/2 k_0 R_1^2 + V(R_1) \\ & -k_0 R_0 R_2 + 1/2 k_0 R_2^2 + V(R_2) \\ & + 1/2 k_x (R_2 - R_1)^2, \end{aligned} \quad (6.9)$$

then ϕ satisfies the conditions

$$dR_1/dt = -\partial\phi/\partial R_1 \quad (6.10)$$

and

$$dR_2/dt = - \partial\phi/\partial R_2. \quad (6.11)$$

For fixed k_0 and k_x , then

$$\frac{d\phi}{dt} = \frac{\partial\phi}{\partial R_1} \frac{dR_1}{dt} + \frac{\partial\phi}{\partial R_2} \frac{dR_2}{dt} \leq 0 \quad (6.12)$$

and $d\phi/dt = 0$ only at steady states.

Figure 6.2 shows the possible steady-state concentrations in tank 1 as a function of k_x for Noyes' cubic model with $k_0 = 1.5 \times 10^{-5} \text{ s}^{-1}$. For $k_x = 0$ and for small k_x , there are nine possible steady-state pairs (R_1, R_2) . These are designated $\alpha_\alpha, \alpha_\gamma, \alpha_\beta, \gamma_\beta, \gamma_\gamma, \gamma_\alpha, \beta_\alpha, \beta_\gamma$ and β_β in order of increasing reactant concentration in the tank. The subscript indicates the corresponding steady-state branch in tank 2; i.e., if both $dR_1/dt = 0$ and $dR_2/dt = 0$, and if tank 1 is in state α_β , then tank 2 is necessarily in state β_α . The steady-state R concentration in tank 2 may be computed from the steady-state concentration in tank 1 since

$$\bar{R}_2 = [v(R_1, R_0) + k_x R_1 - k_0 (R_0 - R_1)] / k_x. \quad (6.13)$$

The number of steady-state solutions of the coupled-tank equations obviously depends upon the value of k_x . It decreases

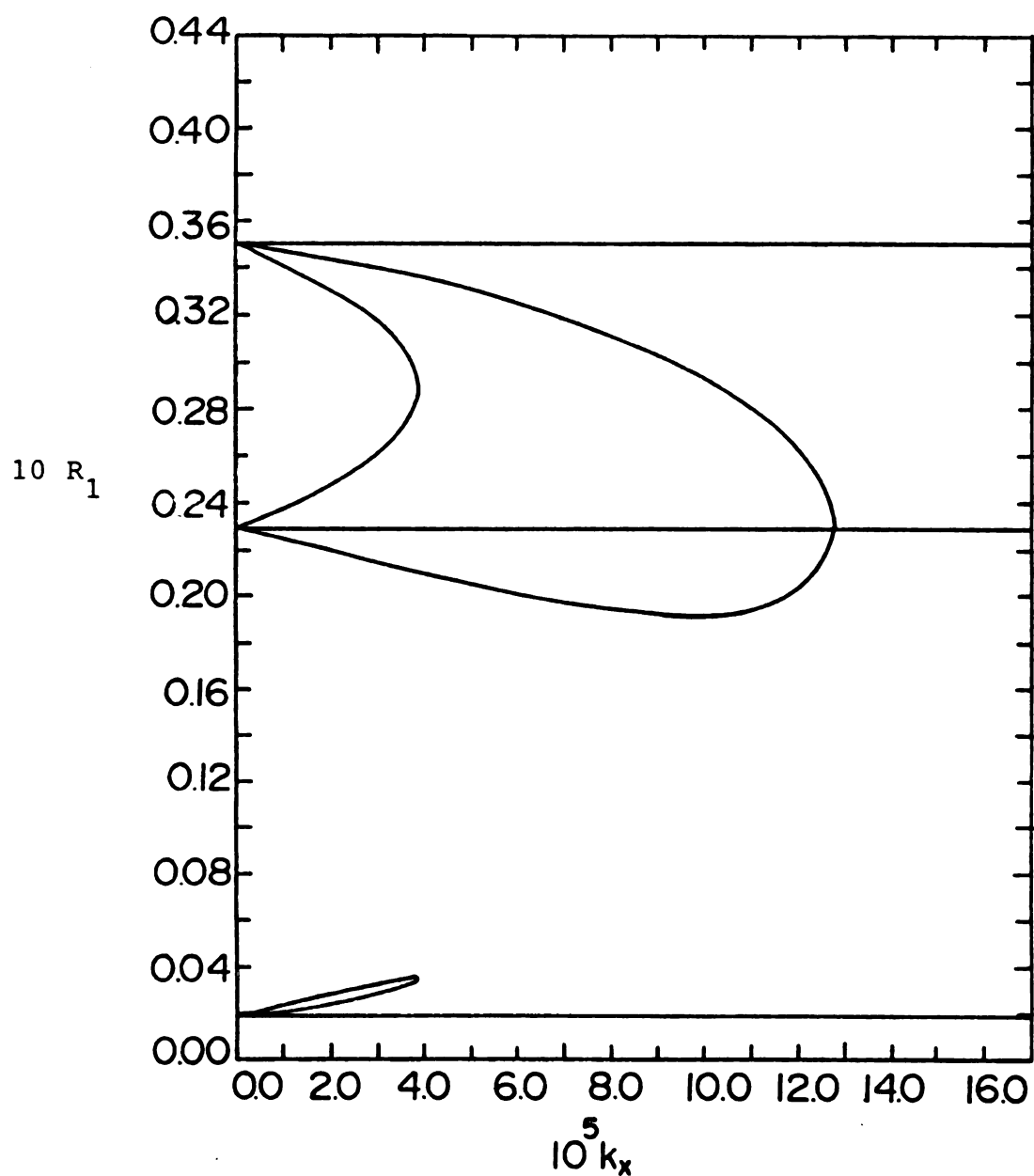


Figure 6.2 Steady states of coupled reactors system for Noyes cubic model. The reactant concentration in one of the tanks (R_1) is plotted versus the mixing rate constant (k_x) for $k_0 = 1.5 \times 10^{-5} \text{ s}^{-1}$.

from nine to five and then to three as k_x is increased. Figures 6.3 and 6.4 show the possible steady-state concentrations in tank 1 for Noyes model, as in Figure 6.2, but for different values of the flow rate constant k_0 ; $k_0 = 2.7 \times 10^{-5} \text{ s}^{-1}$ for Figure 6.3, and $k_0 = 2.516963 \times 10^{-5} \text{ s}^{-1}$ for Figure 6.4.

For the quintic case with the constant set Q_1 , the behaviour of the stationary solutions of equations (6.7) is qualitatively similar to that for Noyes cubic model. For small k_x , nine steady states are found; with an increase in k_x , these coalesce pairwise to leave five states. With a further increase in k_x , only the three steady states for which $\bar{R}_1 = \bar{R}_2$ are found. With the constant set Q_2 , in contrast, new steady state solutions of equations (6.7) are found. Again, for small k_x , there are nine steady states; when k_x is increased, new steady state branches appear. In particular, over the k_x range from $3.688463 \times 10^{-9} \text{ s}^{-1}$ to $4.298794 \times 10^{-9} \text{ s}^{-1}$, there are seventeen possible steady states for equations (6.7) where $v(R, R_0)$ has the quintic form Q_2 . With further increase in k_x , this number decreases to thirteen, then nine, five, and finally three (all three with $\bar{R}_1 = \bar{R}_2$).

Linear stability analysis shows that the stability properties of coupled tank differ from those for single tanks. If (\bar{R}_1, \bar{R}_2) designates a steady state of the coupled tank system, and if we consider a small concentration fluctuation in each tank $(\delta R_1, \delta R_2)$, subject to the

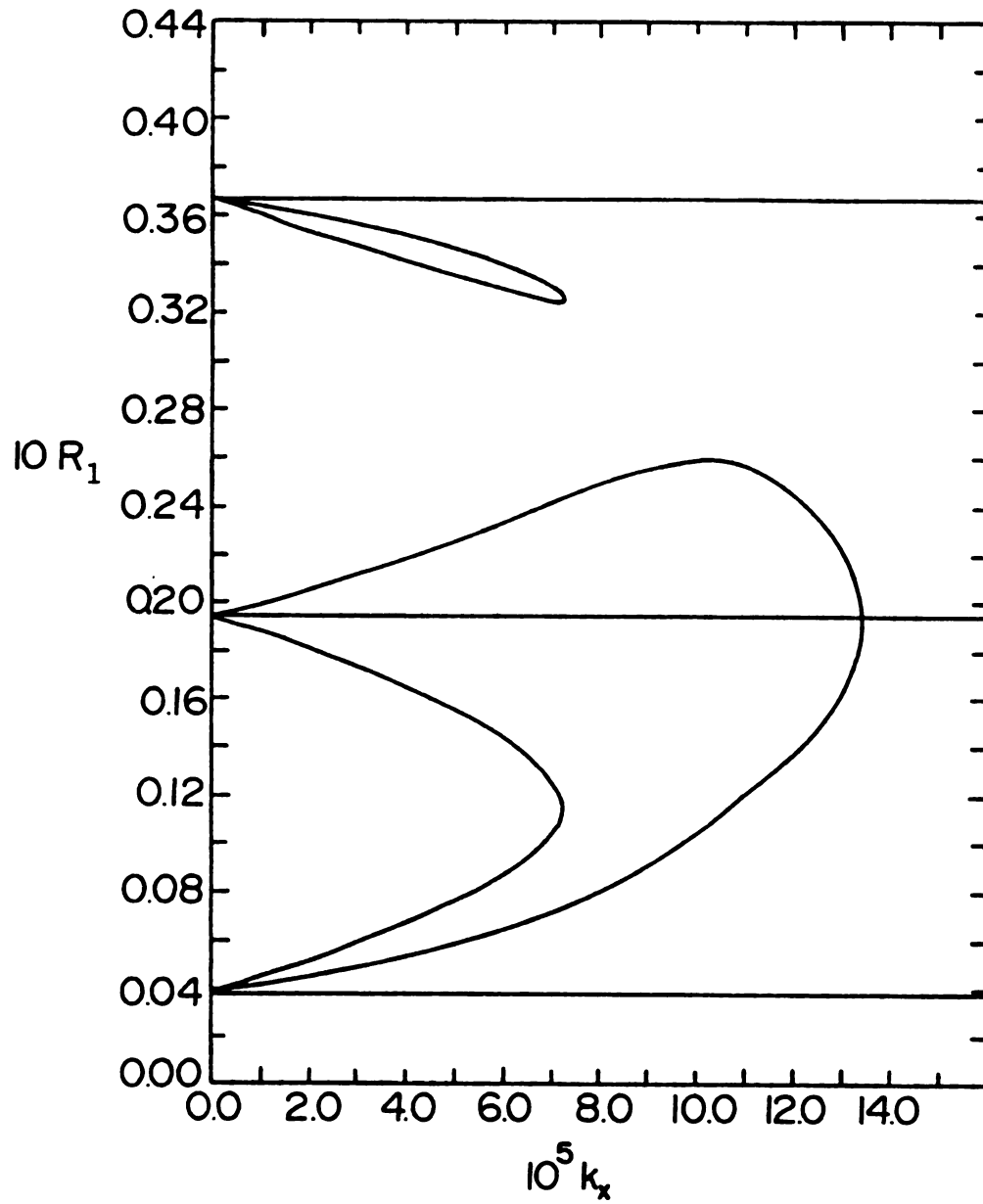


Figure 6.3 Steady states of coupled reactor system for the cubic model. $k_0 = 2.7 \times 10^{-5} \text{ s}^{-1}$.

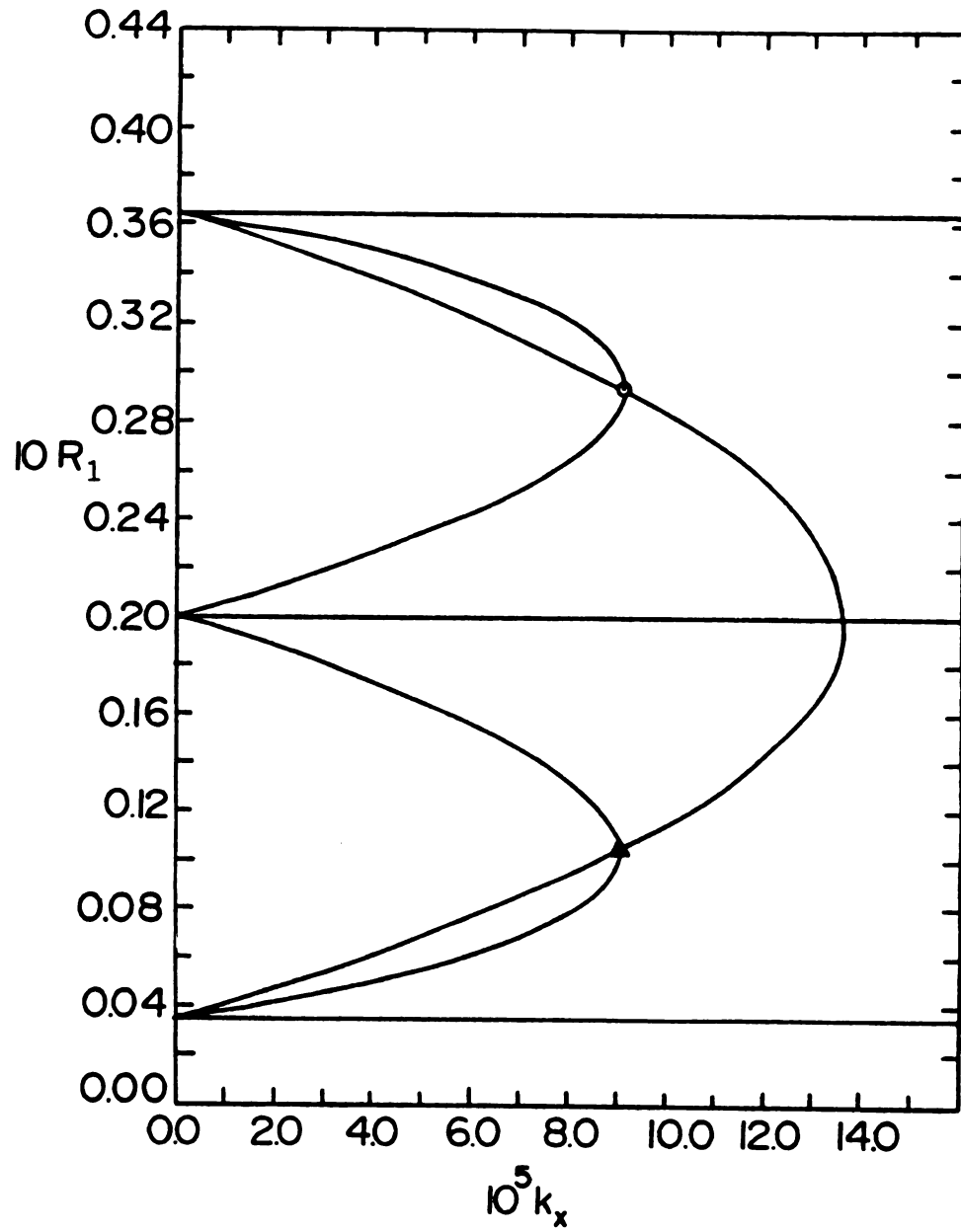


Figure 6.4 Steady states of coupled reactor system for the cubic model. $k_0 = 2.516963 \times 10^{-5} \text{ s}^{-1}$.

conditions $R_1 + P_1 = R_T$ and $R_2 + P_2 = R_T$, then the time-evolution of the fluctuation may be approximated by the linear equations

$$\frac{d}{dt} \begin{pmatrix} \delta R_1 \\ \delta R_2 \end{pmatrix} = - \underline{\underline{M}} \begin{pmatrix} \delta R_1 \\ \delta R_2 \end{pmatrix} \quad (6.14)$$

where

$$\underline{\underline{M}} = \begin{pmatrix} k_0 + \left. \frac{\partial v}{\partial R} \right|_{\bar{R}_1} + k_x & -k_x \\ -k_x & k_0 + \left. \frac{\partial v}{\partial R} \right|_{\bar{R}_2} + k_x \end{pmatrix} \quad (6.15)$$

The stability of the steady state (\bar{R}_1, \bar{R}_2) to small fluctuations depends upon the eigenvalues of the matrix $\underline{\underline{M}}$, λ_1 and λ_2 . If both λ_1 and λ_2 are positive, the state (\bar{R}_1, \bar{R}_2) is stable. Marginal stability occurs when $\det \underline{\underline{M}} = 0$. At this point, at least one of the eigenvalues of $\underline{\underline{M}}$ vanishes, and in the linear regime, a fluctuation of the character of the associated eigenvector is neither damped nor amplified in time. The condition for marginal stability of the $(\alpha_\beta, \beta_\alpha)$ state is

$$\left(k_0 + \left. \frac{\partial v}{\partial R} \right|_{\alpha_\beta} + k_x \right) \left(k_0 + \left. \frac{\partial v}{\partial R} \right|_{\beta_\alpha} + k_x \right) - k_x^2 = 0.$$

(6.16)

Equivalently,

$$\left(k_0 + \frac{\partial v}{\partial R} \Big|_{\alpha_\beta} \right) \left(k_0 + \frac{\partial v}{\partial R} \Big|_{\beta_\alpha} \right) + k_x \left(2k_0 + \frac{\partial v}{\partial R} \Big|_{\alpha_\beta} + \frac{\partial v}{\partial R} \Big|_{\beta_\alpha} \right) = 0. \quad (6.17)$$

If k_x is less than the k_x value at marginal stability, then the inhomogeneous steady state $(\alpha_\beta, \beta_\alpha)$ is stable to small concentration fluctuations.

Each steady state of the coupled-tank system is an extremum point of ϕ . At a stable steady state (\bar{R}_1, \bar{R}_2) ϕ has a local minimum; for a state unstable to any fluctuation, ϕ has a local maximum, and for a state stable to certain perturbations $(\delta R_1, \delta R_2)$ but not to others, ϕ has a saddle point. Contour plots for the potential ϕ for Noyes cubic and quartic models are shown in Figures 6.5 - 6.10. In Figure 6.5 - 6.7, $\phi(R_1, R_2)$ is plotted for Noyes cubic model with $k_0 = 2.517 \times 10^{-5} \text{ s}^{-1}$; the change in potential with change in k_x is illustrated by the sequence of Figure 6.5 with $k_x = 0$ (no coupling between the tanks), Figure 6.6 with $k_x = 4.0 \times 10^{-5} \text{ s}^{-1}$, and Figure 6.7 with $k_x = 9.061 \times 10^{-5} \text{ s}^{-1}$. The k_x value for Figure 6.7 is the point of marginal stability for the coupled-tank state $(\alpha_\beta, \beta_\alpha)$. Figure 6.8 also shows results for the cubic model, but in this case, $k_0 = 1.5 \times 10^{-5} \text{ s}^{-1}$ and $k_x = 3.9 \times 10^{-5} \text{ s}^{-1}$, the marginal stability point of the inhomogeneous coupled-tank steady state for this k_0 value. Figures 6.9 and 6.10 show results for the quartic model obviously lacking the

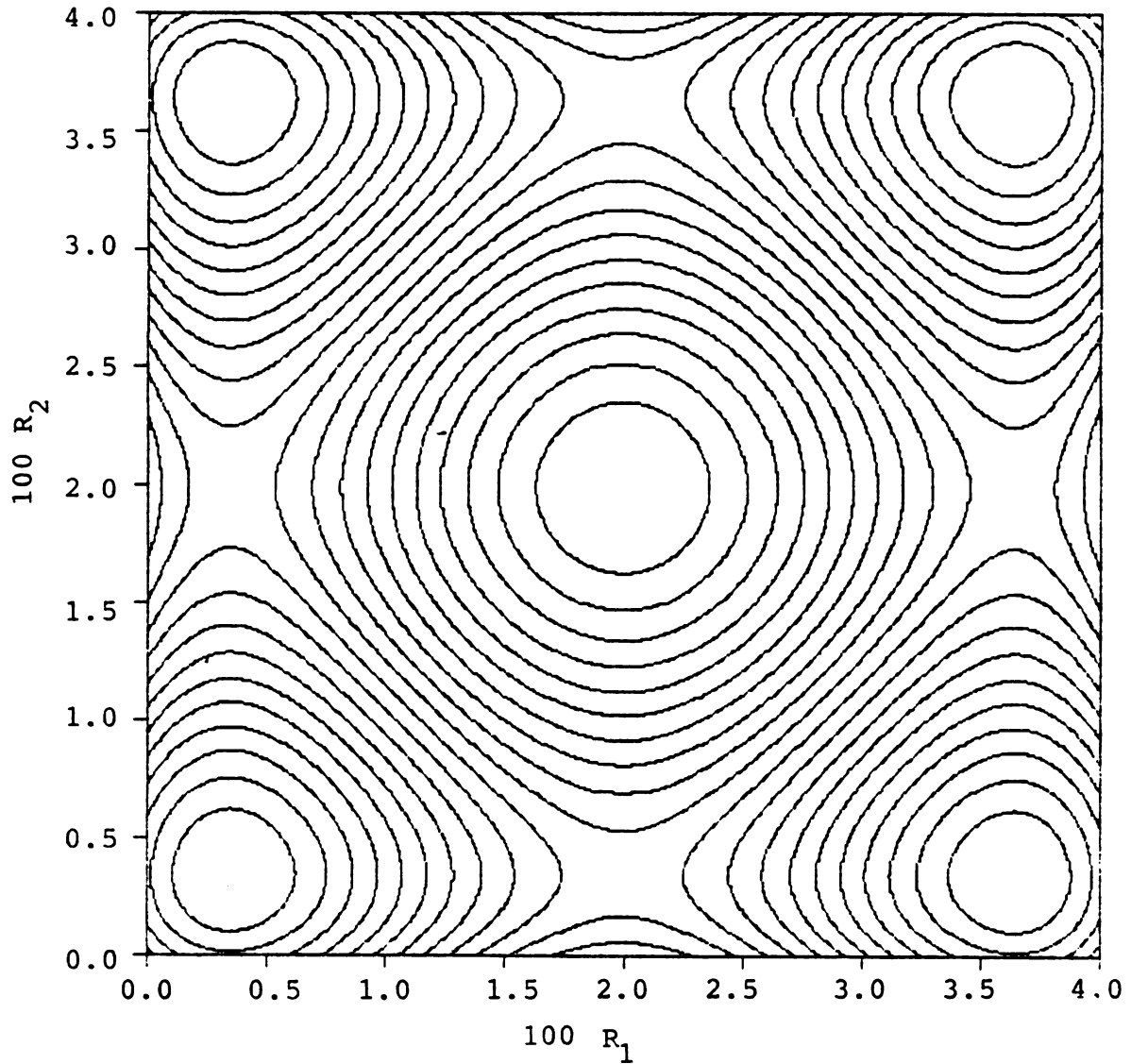


Figure 6.5 The potential function ϕ for the cubic model with $k_0 = 2.517 \times 10^{-5} \text{ s}^{-1}$ and $k_x = 0$. The extremum points of ϕ correspond to the steady states (\bar{R}_1, \bar{R}_2) of the coupled tank system.

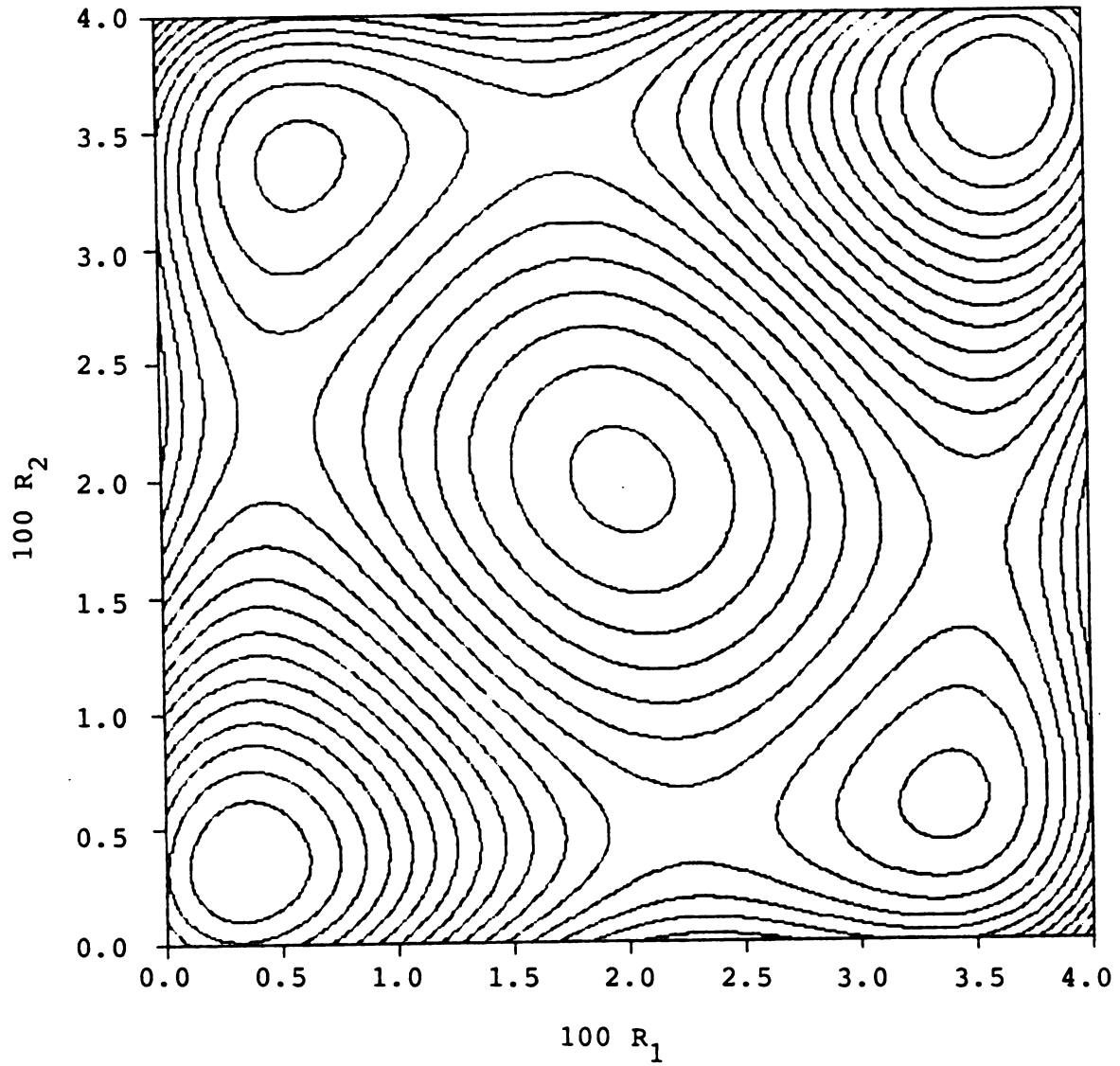


Figure 6.6 The potential function ϕ for the cubic model with $k_0 = 2.517 \times 10^{-5} \text{ s}^{-1}$ and $k_x = 4.0 \times 10^{-5} \text{ s}^{-1}$.

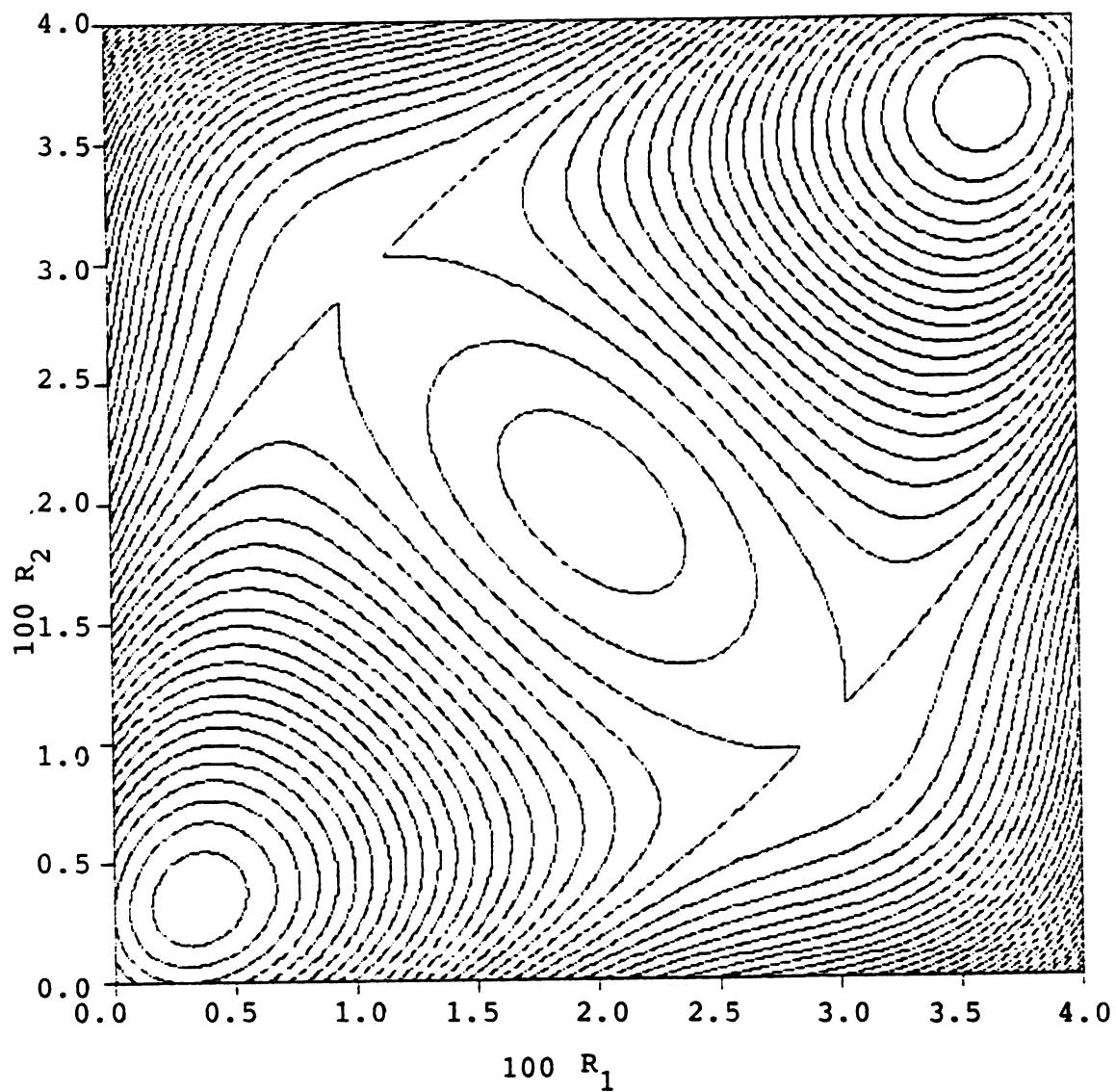


Figure 6.7 The potential ϕ for the cubic model.

$$k_0 = 2.517 \times 10^{-5} \text{ s}^{-1} \text{ and } k_x = 9.061 \times 10^{-5} \text{ s}^{-1}.$$

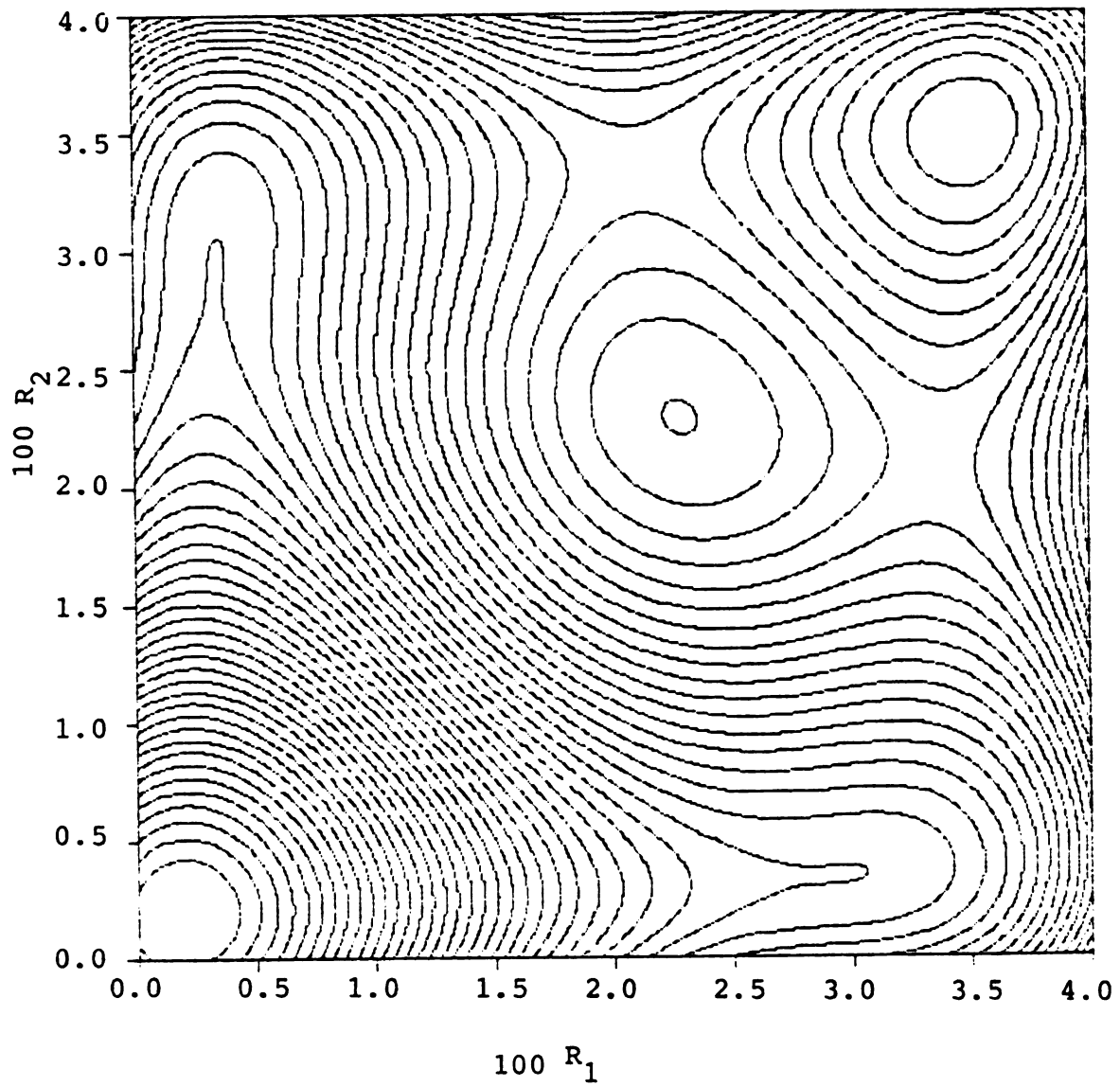


Figure 6.8 The potential ϕ for the cubic model.

$$k_0 = 1.5 \times 10^{-5} \text{ s}^{-1} \text{ and } k_x = 3.9 \times 10^{-5} \text{ s}^{-1}.$$

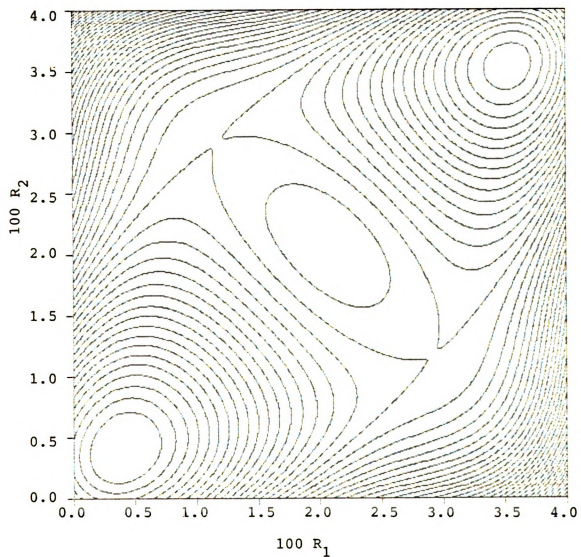


Figure 6.9 The potential ϕ for the quartic model.

$$k_0 = 3.374 \times 10^{-5} \text{ s}^{-1} \text{ and } k_x = 1.28 \times 10^{-5} \text{ s}^{-1}.$$

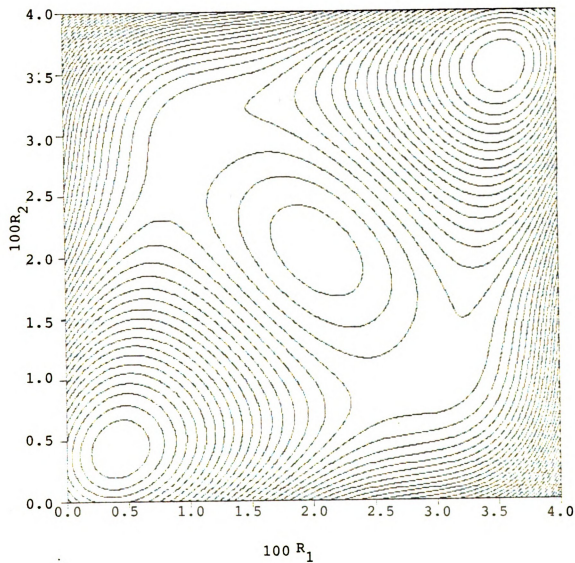


Figure 6.10 The potential ϕ for the cubic model.

$$k_0 = 3.5 \times 10^{-5} \text{ s}^{-1} \text{ and } k_x = 1.1 \times 10^{-4} \text{ s}^{-1}.$$

symmetry present for the cubic model. Figure 6.9 shows the potential for $k_0 = 3.374 \times 10^{-5} \text{ s}^{-1}$ and $k_x = 1.28 \times 10^{-4} \text{ s}^{-1}$, again the marginal stability point of the inhomogeneous coupled-tank state; Figure 6.10 shows results for $k_0 = 3.5 \times 10^{-5} \text{ s}^{-1}$ and $k_x = 1.1 \times 10^{-4} \text{ s}^{-1}$.

Next the effect of changes in the coupling constant k_x are considered. First we consider gradual increases in the coupling constant, beginning with the tanks uncoupled ($k_x=0$) and in different steady states. If k_x is increased sufficiently slowly, the coupled tanks will always be found at time t in the inhomogeneous steady state appropriate for $k_x(t)$, until the marginal stability point is reached. The equation of motion for the system point in the (R_1, R_2) plane is derived as follows: Let (\bar{R}_1, \bar{R}_2) be a steady state solution of the coupled-tank equations

$$\begin{aligned} 0 &= k_0 (R_0 - \bar{R}_1) - v(\bar{R}_1, R_0) + k_x (\bar{R}_2 - \bar{R}_1) \\ 0 &= k_0 (R_0 - \bar{R}_2) - v(\bar{R}_2, R_0) + k_x (\bar{R}_1 - \bar{R}_2), \end{aligned} \quad (6.18)$$

and consider the changes in \bar{R}_1 and \bar{R}_2 produced by an infinitesimal change in k_x to $k_x + \delta k_x$. The new steady state $(\bar{R}_1 + \delta R_1, \bar{R}_2 + \delta R_2)$ satisfies

$$\begin{aligned} 0 &= k_0 (R_0 - \bar{R}_1 - \delta R_1) - v(\bar{R}_1 + \delta R_1, R_0) + (k_x + \delta k_x) \\ &\quad \times (\bar{R}_2 + \delta R_2 - \bar{R}_1 - \delta R_1) \end{aligned}$$

$$\begin{aligned}
0 = & k_0 (R_0 - \bar{R}_2 - \delta\bar{R}_2) - v(\bar{R}_2 + \delta R_2, R_0) \\
& + (k_x + \delta k_x) (\bar{R}_1 + \delta R_1 - \bar{R}_2 - \delta R_2).
\end{aligned}
\tag{6.19}$$

Away from marginal stability points of the coupled-tank system, the changes in steady-state concentrations in the tanks can be expanded as series in powers of δk_x . To first order in δk_x , δR_1 and δR_2 satisfy

$$\begin{aligned}
0 = & -k_0 \delta R_1 - \left. \frac{\partial v}{\partial R} \right|_{\bar{R}_1} \delta R_1 + k_x (\delta R_2 - \delta R_1) + k_x (\bar{R}_2 - \bar{R}_1) \\
0 = & -k_0 \delta R_2 - \left. \frac{\partial v}{\partial R} \right|_{\bar{R}_2} \delta R_2 + k_x (\delta R_1 - \delta R_2) + k_x (\bar{R}_1 - \bar{R}_2);
\end{aligned}
\tag{6.20}$$

i.e.,

$$-\underline{\underline{M}} \begin{pmatrix} \delta R_1 \\ \delta R_2 \end{pmatrix} = \begin{pmatrix} \bar{R}_1 - \bar{R}_2 \\ \bar{R}_2 - \bar{R}_1 \end{pmatrix} \delta k_x,
\tag{6.21}$$

where the same matrix $\underline{\underline{M}}$ determines the damping of concentration fluctuations. The equation has a solution for δR_1 and δR_2 linear in δk_x , provided that $\det \underline{\underline{M}} \neq 0$.

If k_x is increased sufficiently slowly that the coupled-tank system initially in the state $(\bar{R}_1^0, \bar{R}_2^0)$ satisfies the steady-state conditions for coupled tanks with coupling constant $k_x(t)$ at all times t , then the values of \bar{R}_1 and \bar{R}_2

satisfy the differential equation

$$\frac{d}{dk_x} \begin{pmatrix} \delta \bar{R}_1 \\ \delta \bar{R}_2 \end{pmatrix} = - \underline{\underline{M}}^{-1} \begin{pmatrix} \bar{R}_1 - \bar{R}_2 \\ \bar{R}_2 - \bar{R}_1 \end{pmatrix} \quad (6.22)$$

If $k_x = 0$ at $t = 0$, the initial conditions are $\bar{R}_1^0 = R_\alpha, R_\beta$, or R_γ and $\bar{R}_2^0 = R_\alpha, R_\beta$, or R_γ . The matrix $\underline{\underline{M}}$ depends upon k_0, k_x, \bar{R}_1 , and \bar{R}_2 and it is singular when the state (\bar{R}_1, \bar{R}_2) is marginally stable.

In addition to the case of adiabatic mixing treated above, it is also interesting to consider the limit of instantaneous mixing, with k_x approaching infinity. In this limit, only solutions with $\bar{R}_1 = \bar{R}_2$ can be found for the coupled-tank steady-state equations. When the single-tanks exhibit three steady states $R_\alpha < R_\gamma < R_\beta$, with R_α and R_β stable to small concentration fluctuations and R_γ unstable, tanks with reactant concentrations R_1 and R_2 prior to coupling lie in the domain of attraction of the (R_α, R_α) state if $R_1 + R_2 < 2 R_\gamma$, and in the domain of attraction of (R_β, R_β) state if $R_1 + R_2 > 2 R_\gamma$. This result applies to all systems with a single reactant and a single product independent of the form of $v(R,P)$, provided that the system shows the steady-state pattern specified above.

Next, we consider the position of separatrices between the domains of attraction of different stable steady states, and show how these move as the value of k_x is changed. When $k_x = 0$, there are four stable steady states for the coupled

tanks, (R_α, R_α) , (R_α, R_β) , (R_β, R_α) , and (R_β, R_β) . The domains of attraction of these steady states are separated by the perpendicular lines $R_1 = R_\gamma$ and $R_2 = R_\gamma$. As k_x is increased, these separatrices shift. If no new inhomogeneous steady states appear with increasing k_x , these separatrices coalesce when the $(\alpha_\beta, \beta_\alpha)$ state reaches marginal stability; the state $(\alpha_\beta, \beta_\alpha)$ lies on the degenerate separatrix at that point. In the limit as k_x goes to infinity, there is a single separatrix for the domains of attraction of the (R_α, R_α) and (R_β, R_β) states, and as discussed above, it has the equation $R_1 + R_2 = 2 R_\gamma$.

The cubic case shows several special features. If $v(R, R_T)$ is a cubic with multiple steady states in a single flow tank, then for some flow rate constant k_0 , the three steady states satisfy $R_\beta - R_\gamma = R_\gamma - R_\alpha$. For this value of k_0 , the potential $\phi(R_1, R_2; k_0, k_x)$ is symmetric with respect to the line $R_1 + R_2 = 2 R_\gamma$ for any value of k_x (see Appendix F). If R_+ and R_- denote the solutions of the quadratic equation

$$k_0 + \left. \frac{\partial v}{\partial R} \right|_{R_\pm} = 0, \quad (6.23)$$

then $R_+ + R_- = 2 R_\gamma$, (R_+, R_-) is a possible inhomogeneous steady state solution of the coupled tank equations (see Appendix F). If c is defined by the relation

$$k_0 (R_0 - R) - v(R, R_0) = c (R - R_\alpha) (R - R_\gamma) (R - R_\beta) \quad (6.24)$$

for this selected k_0 value, then there is a single separatrix between the domains of attraction of the steady states (R_α, R_α) and (R_β, R_β) when

$$k_x > -\frac{c}{3} (R_\beta - R_\gamma)^2. \quad (6.25)$$

Because of the symmetry of the potential, in this particular case, the separatrix remains fixed as k_x is increased. Hence the point (R_+, R_-) lies on the separatrix for every value of k_x greater than or equal to $-\frac{c}{3}(R_\beta - R_\gamma)^2$.

For the cubic mechanism with any other choice of k_0 , the marginal stability point of the inhomogeneous state lies on the separatrix when k_x takes on the marginal stability value, but with an increase in k_x , the separatrix sweeps past this point.

To illustrate the contrast between the cubic case and the general case, let k_x^{MS} denote the k_x value at which the inhomogeneous (α, β) state is marginally stable, and designate the R concentrations at marginal stability by $\bar{\alpha}$ and $\bar{\beta}$. The values of $\bar{\alpha}$ and $\bar{\beta}$ obviously depend upon k_0 . For a particular k_0 value, denoted k_0^* , $(\bar{\alpha}, \bar{\beta})$ lies on the separatrix of the domains of attraction of the (R_α, R_α) and (R_β, R_β) states, and it remains on the separatrix when the coupling constant is increased to $k_x^{MS} + \delta k_x$. For another k_0 , denoted $k_0^\#$, $(\bar{\alpha}, \bar{\beta})$ lies on the separatrix of the domains of attraction of the (R_α, R_α) and (R_β, R_β) states in the limit as k_x goes to infinity.

In the cubic case $k_0^* = k_0^\#$, but in general this equality does not hold. For the quartic model and the first quintic form, it is possible to find marginal stability points $(\bar{\alpha}, \bar{\beta})$ that lie in the domain of attraction of the (R_α, R_α) state if k_x is increased suddenly to $k_x^{MS} + \Delta k_x$, but that lie in the domain of attraction of (R_β, R_β) if k_x is increased to $k_x^{MS} + 2\Delta k_x$. Further, if new inhomogeneous steady states appear with an increase in k_x , as for the second quintic form, the state $(\alpha_\beta, \beta_\alpha)$ still lies on a degenerate separatrix at its marginal stability point, but this is a separatrix between a homogeneous state and a new inhomogeneous $(\tilde{\alpha}_\beta, \tilde{\beta}_\alpha)$ state, rather than the $(R_\alpha, R_\alpha) - (R_\beta, R_\beta)$ separatrix.

The analysis above essentially explains the outcome of all possible mixing experiments conducted by changing the value of k_x in time. For example, equation (6.22) describes the behaviour of coupled systems that are mixed "adiabatically", so that the system moves along a path of steady-state points in the R_1, R_2 plane. When k_x reaches k_x^{MS} , the matrix \underline{M} is singular. Then unless $k_0 = k_0^*$, an infinitesimal increase in k_x leaves the system in the domain of attraction of a new steady state, which may be homogeneous or inhomogeneous.

In the limit as k_x approaches infinity, the results of instantaneous mixing experiments are obtained. Any difference in outcomes of mixing experiments with different functions $k_x(t)$ obviously result from the k_x dependence of the potential (see Figures 6.5 - 6.10). The cubic case is unusual, because

the outcome of instantaneous mixing experiments and gradual mixing experiments is necessarily the same.

6.3. COMPARISON WITH THE NOYES ANALYSIS

In this section, the above results for coupled-tank experiments are compared with the results of Noyes. These results are also contrasted with the proposed relative stability criterion. Noyes has proposed that dynamic equilibrium at constant R_0 can be determined experimentally by mixing experiments, beginning with one tank in the R_α state and the other (initially uncoupled) tank in the R_β state. Then the reactors will go to the (α', β') state.

Initially $k_0 + \frac{\partial v}{\partial R} > 0$ for both the α' and β' states. As k_x increases it decreases for α' and β' . If $k_0 + \frac{\partial v}{\partial R} \Big|_{\alpha'} = 0$ for a given k_x value while $k_0 + \frac{\partial v}{\partial R} \Big|_{\beta'} \neq 0$, then according to Noyes a further increase in k_x will drive the combined system to settle in the β state and therefore the β state is more stable than the α state. If $k_0 + \frac{\partial v}{\partial R} \Big|_{\beta'}$ reaches zero first then the α state is said to be more stable. As shown above and as noted by Noyes, the actual condition for marginal stability of the coupled tanks is given in equation (6.17). Therefore, if $k_0 + \frac{\partial v}{\partial R} \Big|_{\alpha'} = 0$, but $k_0 + \frac{\partial v}{\partial R} \Big|_{\beta'} > 0$, the coupled tank state is stable. This raises the possibility of finding counterexamples to Noyes prediction of the outcomes of mixing experiments. Two mathematical counterexamples are considered below. The first is provided by the quintic form Q_1 where

$k_0 + \left. \frac{\partial v}{\partial R} \right|_{\alpha} = 0$ when $k_x = 9.373 \times 10^{-10} \text{ s}^{-1}$ but an increase in k_x by a factor of ~ 40 is required to reach the marginal stability point and when k_x is increased slightly beyond k_x^{MS} , the system initially in the (α, β) state settles into the (R_α, R_α) state, contrary to Noyes prediction. In the second counterexample provided by Q_2 , a small increase in k_x beyond the point at which $k_0 + \left. \frac{\partial v}{\partial R} \right|_{\alpha} = 0$ does suffice to drive the inhomogeneous tank state to the marginal stability point; but it does not settle into a homogeneous steady state. Instead, it is driven to a new inhomogeneous state. When with further increase in k_x the new inhomogeneous state goes unstable, the system again settles into the (R_α, R_α) state.

It is important to recognize that coupling between the tanks alters the nature of the steady states in the single tanks to the extent that information about the relative stabilities of single-tank steady states is not available from mixing experiments, even if all mixing experiments have the same outcome. This point can be illustrated in several ways. For example, the equation for the change in R concentration in tank 1 when coupled to tank 2 can be written in the form

$$\frac{dR_1}{dt} = (k_0 + k_x) \left[\frac{k_0 R_0 + k_x R_2}{k_0 + k_x} - R_1 \right] - v(R_1, R_T). \quad (6.26)$$

This is identical to a single-tank equation with k_0 replaced by \bar{k}_0 (see equation (6.28)), R replaced by \bar{R}_0 , and R_T left unchanged. Similarly

$$\frac{dR_2}{dt} = \bar{k}_0(\bar{R}_0' - R_2) - v(R_2, R_T), \quad (6.27)$$

with

$$\bar{k}_0 = k_0 + k_x$$

$$\bar{R}_0 = (k_0 R_0 + k_x R_2) / (k_0 + k_x)$$

$$\text{and } \bar{R}_0' = (k_0 R_0 + k_x R_1) / (k_0 + k_x). \quad (6.28)$$

\bar{R}_0 and \bar{R}_0' satisfy the identities $\bar{R}_0 < R_0$ and $\bar{R}_0' < R_0$. At the steady state (\bar{R}_1, \bar{R}_2) of the coupled tank system, the concentration \bar{R}_1 in tank 1 satisfies the equation

$$\bar{k}_0(\bar{R}_0 - \bar{R}_1) - v(\bar{R}_1, R_0) = 0. \quad (6.29)$$

Hence a single-tank system with parameters \bar{k}_0 , \bar{R}_0 , and R_T has a steady state with the same R concentration \bar{R}_1 . In this sense, the coupled tank steady states may be mapped onto single-tank steady states. However, the single-tank parameter \bar{R}_0 differs for the two coupled tanks, and both \bar{k}_0 and \bar{R}_0 differ from the values for the original single-tank

experiments. Additionally, the stability properties for the coupled tank states differ from those for single-tank states, even when the adjustment for the change in effective flow rates and input-stream reactant concentrations is made. This is apparent from a plot of the coupled tank steady states on single-tank plots, as in Figure 6.11; the coupled-tank marginal stability points do not coincide with the single-tank marginal stability points.

Finally, it is significant to notice that the eigenvector of the matrix \underline{M} with eigenvalue zero has nonvanishing components in both R_1 and R_2 , except for the case when one tank is at marginal stability prior to coupling. Thus, in the general case, the stability of the coupled tanks cannot be localized in a single tank.

The analysis above has shown several new features for coupled multiple steady state systems. First, an effective potential and the shifts in location of the steady states have been derived for model coupled flow tank reactors. Second, it has been shown that the stability properties of the coupled tank systems differ in general from single tank stability properties; coupling stabilizes the tanks to small concentration fluctuations and makes it possible to operate coupled tanks in a region of the concentration space where stable operation of single tanks is impossible.

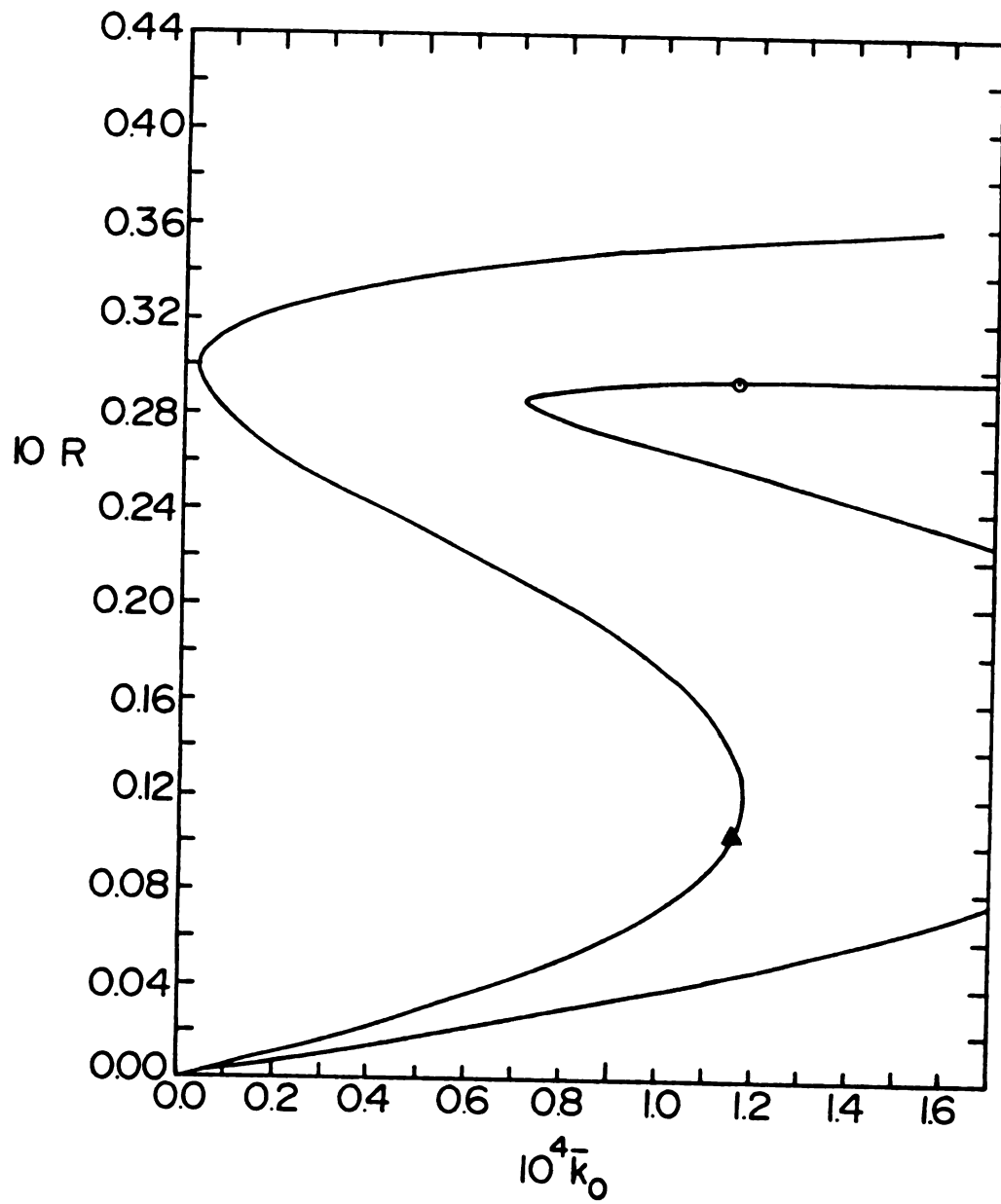


Figure 6.11 Comparison of steady state patterns of the single and coupled flow reactors.

CHAPTER VII

FUTURE WORK AND DEVELOPMENT

Transitions between multiple steady states and hysteresis were studied using the birth-and-death master equation. This does not include local fluctuations. A complete mesoscopic description is provided by the multivariate master equation. It is possible that the multivariate master equation leads to slightly different results for these problems from those presented here. Schlögl's coexistence condition⁴ is obtained by including the effect of diffusion but neglecting fluctuations in the particle number, whereas the Nicolis condition³⁰ is obtained by including number fluctuations and neglecting spatial inhomogeneities. Grassberger³⁸ has recently argued that there is no sharp coexistence point when both kinds of fluctuations are taken into account. If this is the case, a study using the multivariate master equation may indicate a static contribution to hysteresis. Hence such a study seems worthwhile.

Since the eigenvector method and the simulation method involve extensive computations, it is desirable to have a set of evolution equations for the first few moments from the birth-and-death master equation. By multiplying the master equation by x^n and summing, we get

$$\frac{d}{dt}\langle x^n \rangle = \sum_{r=1}^n \binom{n}{r} \langle x^{n-r} [a_+(x) + (-1)^r a_-(x)] \rangle .$$

Since $a_+(x)$ and $a_-(x)$ are cubic in x , the equation for $\langle x^n \rangle$ involves $\langle x^{n+2} \rangle$. A systematic approximation might be developed by a truncation scheme.

Finally, it would be interesting to study the stochastic and time-dependent behaviour of the coupled tank reactor system.

APPENDICES

APPENDIX A

Proof that the transitions generating hysteresis cannot occur before a marginal stability point is reached according to the deterministic rate equation:

Eliminating t from equation (5.7), we obtain

$$\frac{dX}{dB} = \pm F(X,B)/\beta, \quad (\text{A.1})$$

where

$$F(X,B) = \frac{c_1}{2} BX^2 - \frac{c_2}{6} X^3 + c_3B - c_4X.$$

The initial condition is specified by (X_s, B) where X_s is the X -value at a stable steady state corresponding to B . Since $F(X,B)$ has a bounded derivative in a finite interval (Lifshitz condition), the solution is unique. i.e., single-valued (and continuous). Since $\beta > 0$, (A.1) gives

$$\frac{dX}{dB} = 0 \quad \text{at any steady state.} \quad (\text{A.2})$$

The set of steady states are described by

$$F(X_s(B), B) = 0.$$

Considering the derivative of F along the steady state curve, we find

$$\left. \frac{\partial F}{\partial B} \right|_{X=X_s} + \left. \frac{\partial F}{\partial X} \right|_{X=X_s} \frac{dX_s}{dB} = 0.$$

Therefore,

$$\frac{dX_s}{dB} = - \left. \frac{\partial F}{\partial B} \right|_{X=X_s} / \left. \frac{\partial F}{\partial X} \right|_{X=X_s}. \quad (\text{A.4})$$

Also

$$\left. \frac{\partial F}{\partial B} \right|_{X=X_s} = k_1 X_s^2 + k_3 > 0.$$

To find the sign of $\left. \frac{\partial F}{\partial X} \right|_{X=X_s}$, we expand F at a steady state:

$$\frac{dX}{dt} = \left. \frac{\partial F}{\partial X} \right|_{X=X_s} (X - X_s) + \dots \quad (\text{A.5})$$

when B is time-independent. Thus

$$\left. \frac{\partial F}{\partial X} \right|_{X=X_s} < 0 \quad \text{if } X_s \text{ is stable,} \quad (\text{A.6})$$

and hence from (A.4)

$$\frac{dx_s}{dB} > 0 \quad (A.7)$$

at all stable steady states.

Suppose there exists a solution which crosses the middle (unstable) branch of the steady state curve. In order to satisfy the initial condition the solution has to pass through a stable steady state. This is possible only if its slope exceeds that of the steady state curve at the point of intersection. Since the slope of the stable branch is always positive according to equation (A.7), this contradicts equation (A.2). Thus the supposed solution does not exist.

APPENDIX B

Method and program to find the eigenvalues of the transition matrix

The infinite state-space of the stochastic process is made finite by setting $a_+(N) = 0$ for a large N . Then the characteristic polynomial of the tridiagonal matrix \underline{A} is given by $f_N(x)$ where

$$f_k(x) = - [a(k) + x]f_{k-1}(x) - a_+(k-1)a_-(k)f_{k-2}(x)$$

$$\text{for } k = 1, 2, \dots, N;$$

$$f_{-1}(x) = 1 \quad \text{and} \quad f_0(x) = - [a(0) + x].$$

Let $F_k(x) = f_k(x) / g(k)$ where $g(k)$ is chosen for numerical convenience (i.e., to avoid overflow) as

$$g(k) = 2^{-k} a(k)a(k-1)\dots a(1)a(0).$$

Then

$$F_k(x) = - 2 [1 + x/a(k)]F_{k-1}(x) - 4 \frac{a_+(k-1)}{a(k-1)} \frac{a_-(k)}{a(k)} F_{k-2}(x).$$

It is known that there are n roots of $f_k(x) = 0$ in the

interval $(-\infty, \alpha)$ if $f_k(\alpha) \neq 0$ and the sequence $f_{-1}(\alpha), f_0(\alpha), \dots, f_k(\alpha)$ changes sign n times.⁶² Since $g(k) > 0$ for all k , $f_k(\alpha)$ can be replaced by $F_k(\alpha)$ in the above statement. This lets one bracket the desired root suitably for solving the above equation using any root-finding routine.

PROGRAM EIGENVL

```

C
C Subroutine ZEROIN should be supplied for loading
C
  LOGICAL L(997:1001)
  DIMENSION P(997:1001), R(998:1001)
  EXTERNAL CHARPOL
  COMMON /CB/ C(4), B, K
  DATA C /0.3E-6, 0.1E-3, 0.15E-2, 1.7/
C
  OPEN (60, FILE = 'INPUT', STATUS = 'OLD')
  OPEN (61, FILE = 'OUTPUT', STATUS = 'UNKNOWN')
C
998 READ (60,*,END=999) C(4), BLOW, BHIGH, BSTEP
C Do this until input records are exhausted
C
  DO 40 B = BLOW, BHIGH, BSTEP
    L(997) = .FALSE.
    L(998) = .FALSE.
    L(999) = .FALSE.
    L(1000) = .FALSE.
    L(1001) = .FALSE.
C
C Hope that an eigenvalue will bite in the range between
C -500 and -10. This need not be one of the few we need.
C Since we will also know its position in the spectrum,
C it can be used as a bait to catch the ones we want.
C
    XA      = - 500.0
    X       = - 10.0
    XB      = 0.0
C
C First we find four ranges of X enclosed by P(i) and P(i-1)
C such that each interval contains exactly one eigenvalue.
C Note that K is common with CHARPOL and that Y is ignored
C since we are only interested in X and K.
C
10  CONTINUE
    Y = CHARPOL(X)
    IF (K .GT. 1001) THEN
      PRINT*, 'SIGN CHANGE OCCURRED ', K,
$      ' TIMES. B = ', B, ' X = ', X
      STOP 'BAD'
    ELSE IF (K .GE. 997) THEN
      L(K) = .TRUE.
      P(K) = X
    END IF
C
    IF ( .NOT. L(997) ) THEN
      IF (K .LT. 997) XA = X
      IF (K .GT. 997) XB = X
      X = (XA+XB) / 2.0
      GO TO 10

```

```

ELSE IF ( .NOT. L(998) ) THEN
  X = P(997) / 2.0
  IF ( L(1000) ) X = P(997) + (P(1000)-P(997))/3.0
  IF ( L( 999) ) X = P(997) + (P( 999)-P(997))/2.0
  GO TO 10
ELSE IF ( .NOT. L(999) ) THEN
  X = P(998) / 2.0
  IF ( L(1000) ) X = P(998) + (P(1000)-P(998))/2.0
  GO TO 10
ELSE IF ( .NOT. L(1000) ) THEN
  X = P(999) / 2.0
  GO TO 10
ELSE IF ( .NOT. L(1001) ) THEN
  X = 1.0
  GO TO 10
END IF

```

C
C Now the eigenvalues can be calculated to desired accuracy
C using any root finding routine.
C

```

DO 30 I = 998, 1001
  G1 = P(I-1)
  G2 = P(I)
  ABSERR = 1.0E-15
  RELERR = 1.0E-15
  CALL ZEROIN ( CHARPOL, G1, G2, ABSERR, RELERR,
$              IFLAG)
  IF (IFLAG .GT. 3) THEN
    PRINT*, 'ERROR FROM ZEROIN. IFLAG = ',
$          IFLAG, ' B = ', B, ' G1 = ', G1,
$          ' G2 = ', G2
    STOP 'BAD'
  END IF
  R(I) = G1
30 CONTINUE

```

C
C Write results
C

```

WRITE (61,4) C(4), B, R
4 FORMAT ( '0', 4X, F7.5, 4X, 1PE10.4, 3(4X,E20.13),
$        4X, E10.3)
40 CONTINUE
GO TO 998

```

C Go back to see if there is another input record
999 CONTINUE
END
FNCTION CHARPOL (X)

C
C This function routine evaluates the characteristic
C polynomial of the transition matrix and counts the
C number of sign changes during the evaluation
C

```
COMMON /CB/ C(4), B, KOUNT
```

C

```

C3B      = C(3) * B
C1BBY2  = C(1) * B / 2.0
C2BY6   = C(2) / 6.0

C
FKM1    = 1.0
KOUNT   = 0
AK      = C3B
FK      = - 1.0 - X/AK
IF ( FK .LT. 0.0 ) KOUNT = 1
APK     = C3B
DO 10 K = 1, 1000
    FKM2 = FKM1
    FKM1 = FK
    APKM1 = APK
    AKM1 = AK
    APK   = C1BBY2 * K * (K-1) + C3B
    AMK   = C2BY6 * K * (K-1) * (K-2) + C(4) * K
    IF ( K .EQ. 1000 ) APK = 0.0
    AK    = APK + AMK
    FK    = - 2.0 * ( 1.0 + X/AK ) * FKM1
    $      - 4.0 * APKM1/AKM1 * AMK/AK * FKM2
    IF ( SIGN(1.0,FK) .NE. SIGN(1.0,FKM1) ) KOUNT = KOUNT+1
10 CONTINUE
CHARPOL = FK
IF ( CHARPOL .EQ. 0.0 ) KOUNT = 995
RETURN
END

```

APPENDIX C

Programs to construct the eigenvectors of the transition matrix

The eigenvectors are constructed interactively because optimum values are to be selected for several parameters at intermediate stages.

An arbitrary value of $P_j(0)$ is selected, values of $P_j(x)$ are calculated recursively for $x > 0$, and finally \underline{P}_j is normalized. The value for $P_j(0)$ must be large enough not to cause underflow of $P_j(x)$ for some x and small enough not to cause overflow of the normalization constant. The normalization constant is obtained by summing $P_j(x)^2/P_s(x)$. This ratio as calculated is not at all accurate for large values of x for which both $P_j(x)$ and $P_s(x)$ are almost zero. Hence every individual case has a specific cut-off value of x .

Every step involved in the computation of an eigenvector is performed by invoking an appropriate command; after each step the results may be viewed, and if the results are not satisfactory the step can be repeated with different values for the parameters. The commands are:

INIT for initialization

DATA for changing the following values:

J - index of the current eigenvector
being computed. $J = 1, 2, \text{ or } 3$.

IMAX - index of component beyond which
terms need not appear in sum while

calculating the normalization constant.

IMIN - index of component before which terms
need not appear in sum (often IMIN = 0)

IMID - optional starting point for computing
 \underline{p}_s (For $x < \text{IMID}$, $\underline{p}_s(x)$ will be
calculated by backward iteration.)

P0 for calculating unnormalized \underline{p}_s

PJ for calculating unnormalized \underline{p}_j

TERM for calculating $P_j(x)^2/P_s(x)$ for all x (If the
result will cause overflow it is replaced by
- 1.0)

SHOW for a display of various vectors (EDIT with no
output) and the current values of the
parameters

SUM for calculating the normalization constant for \underline{p}_j

NORM for normalizing \underline{p}_j or \underline{p}_s

SAVE for saving an eigenvector for plotting

PLOT for plotting all four eigenvectors

TIME for plotting time-dependent asymptotic solutions

STOP

HELP

Since many components of the normalized \underline{p}_s are almost zero, it is recommended that \underline{p}_s be normalized after all other eigenvectors have been normalized. However the normalizing program performs correctly irrespective of whether the normalized or unnormalized \underline{p}_s is used for normalizing \underline{p}_j .

In a typical run the commands may be issued in the following order:

INIT (prompts for c_4 and B values)

P0 (prompts for $P_s(0)$)

For $j = 1, 2, 3$

DATA (set $J = j$)

PJ

TERM

SHOW

DATA (set IMAX)

DATA (set IMIN = 0)

SUM

NORM (J)

SAVE (J)

NORM (0)

SAVE (0)

PLOT

TIME

STOP

```

$ !
$ ! A procedure to compute the eigenvectors and time-
$ ! dependent asymptotic distributions interactively.
$ ! On-line instructions are expected to be self-explanatory.
$ !
$ ON ERROR THEN GOTO CMD
$ ON CONTROL Y THEN GOTO CMD
$ ASSIGN SYS$COMMAND SYS$INPUT
$ ASSIGN SYS$OUTPUT OUTPUT
$ INQ = "INQUIRE/NOPUNCTUATION"
$ WJ = "WRITE JOB"
$ WS = "WRITE SYS$OUTPUT"
$ !
$ !
$ !
$ CMD:
$ INQ COM "COMMAND ?"
$ IF COM.EQS."STOP" THEN EXIT
$ IF COM.EQS."HELP" THEN GOTO HEL
$ IF COM.EQS."TIME" THEN GOTO TIM
$ !
$ ! There is a file EIGx.EXE for every valid response x,
$ ! except when x = STOP, HELP, or TIME
$ !
$ RUN EIG'COM'
$ IF COM.EQS."SHOW" THEN EDIT/READONLY EIGOUT.DAT
$ IF COM.EQS."PLOT" THEN PRINT/NOFEED/DELETE VECPLOT.DAT
$ GOTO CMD
$ !
$ !
$ !
$ TIM:
$ !
$ ! A command procedure is prepared and submitted to a batch
$ ! queue.
$ !
$ DELETE EIGTIME.COM;*
$ OPEN/WRITE JOB EIGTIME.COM
$ WJ "$ASSIGN SYS$INPUT INPUT"
$ WJ "$ASSIGN SYS$OUTPUT OUTPUT"
$ WJ "$LINK/EXE=PGPLOT EIGFUN+[Z]PGPLOT+VPLOT+MACPLOT"
$ WJ "$RUN PGPLOT"
$ WJ "$DECK"
$ !
$ ! Conversation with user
$ !
$ WS " "
$ INQ NP "HOW MANY PLOTS ? ( 1 ) "
$ INQ Y "ALL IN ONE PAGE ?"
$ INQ T1 "TIME FOR FIRST PLOT = "
$ INQ T2 "TIME FOR LAST PLOT = "

```

```

$ INQ   XMAX   "MAXIMUM X = "
$ INQ   PMAX   "MAXIMUM P(x,t) EXPECTED = "
$ INQ   DELTA  "IS INITIAL DISTRIBUTION A DELTA FUNCTION ? "
$ IF DELTA THEN INQ INPOS "PEAKED AT ____ "
$ IF DELTA THEN GOTO SKIP
$       INPOS = - 1
$       WS " "
$       WS "Then other acceptable initial distributions are"
$       WS "restricted to the span of the first four eigenvectors"
$       WS " "
$       WS "Enter components of the initial distribution along"
$       WS "these eigenvectors"
$       WS " "
$       WS " A(1) = 1.0"
$       INQ   A2   "A(2) = "
$       INQ   A3   "A(3) = "
$       INQ   A4   "A(4) = "
$ SKIP:
$ !
$ ! Prepare a data deck compatible with program PGPLOT and
$ ! function PLFUN. The function reads data the first time
$ ! it is used in a job.
$ !
$ IF Y THEN WJ "1"
$ R = NP + 1
$ IF .NOT.Y THEN WJ R
$ !
$ IF Y THEN NN = NP + 1
$ IF .NOT.Y THEN NN = 1
$ !
$ IP = 0
$ X = "YES"
$ L1:
$   IF IP.EQ.NP THEN N = 100
$   IF IP.NE.NP THEN N = IP
$   IF X THEN WJ " ' ', 1, 'X', 1, 'P(X)', 4, "
$   IF X THEN WJ NN, ", 0.0, ", XMAX, ", 0.0", ", ", PMAX
$   WJ " .TRUE. ,", N, ", , , , , , , , , "
$   IF IP.NE.0 THEN GOTO L2
$   WJ "           ", T1, ", ", T2, ", ", INPOS, ", ", NP, ", "
$   IF .NOT.DELTA THEN WJ "           ", A2, ", ", A3, ", ", A4, ", "
$   L2:
$   IP = IP + 1
$   X = .NOT.Y
$ IF IP.LE.NP THEN GOTO L1
$ WJ "$ EOD"
$ WJ "$ PRINT/NOFEED/DELETE PLOT.DAT"
$ WJ "$ DELETE PGPLOT.*;*"
$ CLOSE JOB
$ WS " "
$ WS "A batch job is ready to be submitted. Say NO if you"
$ WS "have made a mistake."

```

```
$ WS " "  
$ INQ OK "SUBMIT? "  
$ IF OK THEN SUBMIT/QUEUE=FASTQ/NOPRINT EIGTIME.COM  
$ GOTO CMD  
$ HEL:  
$ WS " "  
$ WS "Valid responses are:"  
$ WS " "  
$ WS "   INIT   for initialization"  
$ WS "   DATA  for changing the following values"  
$ WS "       J    - index of the current eigenvector"  
$ WS "              being computed. J = 1,2,3."  
$ WS "       IMAX - index of component beyond which"  
$ WS "              terms need not appear in sum"  
$ WS "       IMIN - index of component before which"  
$ WS "              terms need not appear in sum"  
$ WS "       IMID - optional starting point when"  
$ WS "              computing P0"  
$ WS "   P0    for calculating unnormalized P0"  
$ WS "   PJ    for calculating unnormalized PJ"  
$ WS "   TERM  for calculating  $PJ^2/P0$  for each component"  
$ WS "   SHOW  for a display of various vectors"  
$ WS "   SUM   for calculating the normalization constant"  
$ WS "   NORM  for normalizing PJ"  
$ WS "   SAVE  for saving current vector for plotting"  
$ WS "   PLOT  for plotting the normalized eigenvectors"  
$ WS "   TIME  for plotting time dependent solutions"  
$ WS "   STOP"  
$ WS "   HELP"  
$ WS " "  
$ GOTO CMD
```

```

PROGRAM EIGINIT
PARAMETER (NX=1500, NE=3)
IMPLICIT REAL*8 (A-H,O-Z)
DIMENSION APLUS(0:NX), AMINUS(0:NX), EV(0:NE), C(4),
$          P0(0:NX), PJ(0:NX), TERM(0:NX)
REAL SAVE(0:NX,0:NE)
DATA SAVE /6004*-1.0/, C /3D-7,1D-4, 1.5D-3, 1.7/
$          P0 /1501*-1D0/, PJ /1501*-1D0/, TERM /1501*-1D0/
C
WRITE (*,*) '                               INIT'
WRITE (*,1) ' C4 = '
1 FORMAT (/ '$', A6)
READ (*,*) CIN
WRITE (*,1) ' B = '
READ (*,*) BIN
C
C Search through the eigenvalue listing
C
EV(0) = 0.0
OPEN (15, FILE='EIGVALS', FORM='FORMATTED',
$      STATUS = 'OLD')
WRITE (*,*) 'Searching for eigenvalues'
DO WHILE (C(4).NE.CIN .OR. B.NE.BIN)
  READ (15,2,END=20) C(4), B, EV(3), EV(2), EV(1)
2  FORMAT ( 5X, E7.0, 4X, E10.0, 3(4X,E20.0))
END DO
CLOSE (15)
C
J = 0
IMIN = -1
IMAX = -1
IMID = -1
C
C Compute aplus and aminus and store in a file.
C
C1BBY2 = C(1) * B * 0.5D0
C2BY6  = C(2) / 6D0
C3B    = C(3) * B
DO 10 I = 0, NX
  X = DBLE(I)
  APLUS(I) = C1BBY2 * X * (X-1D0) + C3B
  AMINUS(I) = C2BY6 * X * (X-1D0) * (X-2D0) + C(4)*X
10 CONTINUE
OPEN (10,FILE='EIGDATA', STATUS='UNKNOWN',
$     FORM='UNFORMATTED')
WRITE (10) C, B, EV, APLUS, AMINUS, J, IMIN, IMAX, IMID
C
C Erase numbers from previous work in the following files
C
OPEN (20, FILE='EIGP0', STATUS='UNKNOWN',
$     FORM='UNFORMATTED')
SUM0 = -1D0

```

```
WRITE (20) P0,SUM0
CLOSE (20)
OPEN (30, FILE='EIGPJ', STATUS='UNKNOWN',
$      FORM='UNFORMATTED')
SUMJ = -1D0
PNORMJ = -1D0
WRITE (30) PJ, SUMJ, PNORMJ
CLOSE(30)
OPEN (40, FILE='EIGTERM', STATUS='UNKNOWN',
$      FORM='UNFORMATTED')
WRITE (40) TERM
CLOSE (40)
OPEN (60, FILE='EIGSAVE', STATUS='UNKNOWN',
$      FORM='UNFORMATTED')
WRITE (60) C(4), B, EV, SAVE
CLOSE (60)
STOP ' '
```

C
C
C

Normal termination at this point

```
20 CLOSE (15)
STOP 'Eigenvalues not available'
END
```

```

PROGRAM EIGDATA
PARAMETER (NX=1500, NE=3)
IMPLICIT REAL*8 (A-H, O-Z)
DIMENSION C(4), EV(0:NE), APLUS(0:NX), AMINUS(0:NX),
$      PJ(0:NX), TERM(0:NX)
CHARACTER VAR*4
DATA PJ / 1501*-1D0 /, SUMJ / -1D0 /, PNORMJ / -1D0 /
$      TERM / 1501*-1D0 /

C      WRITE (*,*) '                                DATA'
      OPEN (10, FILE='EIGDATA', STATUS='OLD',
$      FORM='UNFORMATTED')
      READ (10) C, B, EV, APLUS, AMINUS, J, IMIN, IMAX, IMID
      CLOSE (10)

C      WRITE(*,1) ' VARIABLE ? '
1  FORMAT ('$ ', A11)
      READ (*,2) VAR
2  FORMAT (A10)
      WRITE (*,*) ' '
      WRITE (*,3) VAR, ' = '
3  FORMAT ('$ ', A4, A3)
      READ (*,*) IVAR

C      IF (VAR.EQ.'J' .OR. VAR.EQ.'j') THEN
          J = IVAR
          IMIN = -1
          IMAX = -1
          IMID = -1
          OPEN (30, FILE='EIGPJ' , STATUS='UNKNOWN',
$      FORM='UNFORMATTED')
          WRITE (30) PJ, SUMJ, PNORMJ
          CLOSE (30)
          OPEN (40, FILE='EIGTERM', STATUS='UNKNOWN',
$      FORM='UNFORMATTED')
          WRITE (40) TERM
          CLOSE (40)
      END IF
      IF (VAR.EQ.'IMIN' .OR. VAR.EQ.'imin') IMIN = IVAR
      IF (VAR.EQ.'IMAX' .OR. VAR.EQ.'imax') IMAX = IVAR
      IF (VAR.EQ.'IMID' .OR. VAR.EQ.'imid') IMID = IVAR

C      OPEN (10, FILE='EIGDATA', STATUS='UNKNOWN',
$      FORM='UNFORMATTED')
      WRITE (10) C, B, EV, APLUS, AMINUS, J, IMIN, IMAX, IMID
      CLOSE (10)
      END

```

```

PROGRAM EIGP0
PARAMETER (NX=1500, NE=3)
IMPLICIT REAL*8 (A-H, O-Z)
DIMENSION P0(0:NX), APLUS(0:NX), AMINUS(0:NX), EV(0:NE),
$          C(4)
CHARACTER RES

C
WRITE( *,*) '                                P0'
OPEN (10, FILE='EIGDATA', STATUS='OLD',
$     FORM='UNFORMATTED')
READ (10) C, B, EV, APLUS, AMINUS, J, IMIN, IMAX, IMID
CLOSE (10)
WRITE (*,1) ' STARTING FROM x = 0 ?'
1 FORMAT ('$ ', A21)
READ (*,2) RES
2 FORMAT (A1)
WRITE (*,1) 'STARTING CONSTANT = '
READ (*,*) CONST
IF ( RES.EQ.'Y' .OR. RES.EQ.'y' ) THEN
    P0(0) = CONST
    SUM0 = P0(0)
    DO 10 I = 1, NX
        P0(I) = APLUS(I-1) / AMINUS(I) * P0(I-1)
        SUM0 = SUM0 + P0(I)
10    CONTINUE
    ELSE
        IF (IMID.EQ.-1) STOP 'IMID not initialized'
        P0(IMID) = CONST
        SUM0 = P0(IMID)
        DO 20 I = IMID-1, 0, -1
            P0(I) = AMINUS(I+1) / APLUS(I) * P0(I+1)
            SUM0 = SUM0 + P0(I)
20    CONTINUE
        DO 30 I = IMID+1, NX
            P0(I) = APLUS(I-1) / AMINUS(I) * P0(I-1)
            SUM0 = SUM0 + P0(I)
30    CONTINUE
    END IF

C
OPEN (20, FILE='EIGP0', STATUS='UNKNOWN',
$     FORM='UNFORMATTED')
WRITE (20) P0, SUM0
CLOSE (20)

C
END

```

```

PROGRAM EIGPJ
PARAMETER (NX=1500, NE=3)
IMPLICIT REAL*8 (A-H, O-Z)
DIMENSION PJ(0:NX), APLUS(0:NX), AMINUS(0:NX), EV(0:NE),
$          C(4)
C
WRITE(*,*) '                                PJ'
OPEN (10, FILE='EIGDATA', STATUS='OLD',
$      FORM='UNFORMATTED')
READ (10)C, B, EV, APLUS, AMINUS, J, IMIN, IMAX, IMID
CLOSE (10)
OPEN (30, FILE='EIGPJ', STATUS='OLD',
$      FORM='UNFORMATTED')
READ (30) PJ, SUMJ, PNORMJ
CLOSE (30)
WRITE (*,1) 'PJ(0) = '
1 FORMAT ('$ ', A21)
READ (*,*) PJ(0)
PJ(1) = ( APLUS(0) + AMINUS(0) + EV(J) ) * PJ(0)/AMINUS(1)
DO 10 I = 2, NX
    PJ(I) = ( ( APLUS(I-1) + AMINUS(I-1)) * PJ(I-1)
$           - APLUS(I-2) * PJ(I-2) + EV(J) * PJ(I-1) )
$           / AMINUS(I)
10 CONTINUE
C
OPEN (30, FILE='EIGPJ', STATUS='UNKNOWN',
$      FORM='UNFORMATTED')
WRITE (30) PJ, SUMJ, PNORMJ
CLOSE (30)
C
END

```

```

PROGRAM EIGTERM
PARAMETER (NX=1500, NE=3)
IMPLICIT REAL*8 (A-H, O-Z)
DIMENSION P0(0:NX), PJ(0:NX), TERM(0:NX)
C
WRITE(*,*) '                                TERM'
OPEN (20, FILE='EIGP0', STATUS='OLD',
$      FORM='UNFORMATTED')
READ (20) P0, SUM0
CLOSE (20)
OPEN (30, FILE='EIGPJ', STATUS='OLD',
$      FORM='UNFORMATTED')
READ (30) PJ, SUMJ, PNORMJ
CLOSE (30)
C
DO 10 I = 0, NX
  IF ( DABS(PJ(I)) .GT. 1D19*DSQRT(P0(I)) ) THEN
    TERM(I) = -1D0
  ELSE
    TERM(I) = PJ(I) / P0(I) * PJ(I)
  END IF
10 CONTINUE
C
PNORMJ = DSQRT (SUM0)
OPEN (30, FILE='EIGPJ', STATUS='UNKNOWN',
$      FORM='UNFORMATTED')
WRITE (30) PJ, SUMJ, PNORMJ
CLOSE (30)
OPEN (40, FILE='EIGTERM', STATUS='UNKNOWN',
$      FORM='UNFORMATTED')
WRITE (40) TERM
CLOSE (40)
END

```

```

PROGRAM EIGSHOW
PARAMETER (NX=1500, NE=3)
IMPLICIT REAL*8 (A-H, O-Z)
DIMENSION C(4), EV(0:NE), APLUS(0:NX), AMINUS(0:NX),
$         P0(0:NX), PJ(0:NX), TERM(0:NX)
C
WRITE (*,*) '                               SHOW'
WRITE (*,*) ' 1 : Data'
WRITE (*,*) ' 2 : P0'
WRITE (*,*) ' 3 : P0, Pj'
WRITE (*,*) ' 4 : P0, Pj, Term'
WRITE (*,1) 'SELECT A NUMBER : '
1 FORMAT (/ '$', A18)
READ (*,*) MODE
C
OPEN (10, FILE='EIGDATA', STATUS='OLD',
$     FORM='UNFORMATTED')
OPEN (20, FILE='EIGP0', STATUS='OLD',
$     FORM='UNFORMATTED')
OPEN (30, FILE='EIGPJ', STATUS='OLD',
$     FORM='UNFORMATTED')
OPEN (40, FILE='EIGTERM', STATUS='OLD',
$     FORM='UNFORMATTED')
C
READ (10) C, B, EV, APLUS, AMINUS, J, IMIN, IMAX, IMID
READ (20) P0, SUM0
READ (30) PJ, SUMJ, PNORMJ
READ (40) TERM
C
CLOSE (10)
CLOSE (20)
CLOSE (30)
CLOSE (40)
C
OPEN (50, FILE='EIGOUT', STATUS='UNKNOWN',
$     FORM='UNFORMATTED')
IF (MODE.EQ.1) THEN
WRITE (*,2) C(4), B, EV, J, IMIN, IMAX, IMID
2 FORMAT (5X, 'C4 = ', F5.3 /
$        5X, 'B = ', 1PE11.4 /
$        5X, 'EV(0)= ', 0PF5.3 /
$        5X, 'EV(1)= ', 1PE11.4 /
$        5X, 'EV(2)= ', E11.4 /
$        5X, 'EV(3)= ', E11.4 /
$        5X, 'J = ', I1 /
$        5X, 'IMIN = ', I4 /
$        5X, 'IMAX = ', I4 /
$        5X, 'IMID = ', I4 /
$        15X, 'The next line is irrelevant. ',
$        'Please type QUIT'/)
ELSE
IF (MODE.EQ.2) THEN
WRITE ( 50,3) (I, P0(I), I=0,NX )

```

```

3      FORMAT ( 5X, I4, 5X, 1PE11.4 /)
      ELSE IF (MODE.EQ.3) THEN
          WRITE (50,4) ( I, P0(I), PJ(I), I=0,NX)
4      FORMAT ( 5X, I4, 5X, 1PE11.4, 5X, E11.4 / )
      ELSE IF (MODE.EQ.4) THEN
          WRITE (50,5) (I, P0(I), PJ(I), TERM(I), I=0,NX)
5      FORMAT ( 5X, I4, 5X, 1PE11.4, 5X, E11.4, 5X,
$          E11.4 / )
      END IF
      WRITE (*,*) ' '
      WRITE (*,*) ' Type C for viewing. '
      WRITE (*,*) ' Type Control-Y (or Control-Z follow',
$          'ed by QUIT) to terminate SHOW'
      WRITE (*,*) ' '
      END IF
      END

```

```

PROGRAM EIGSUM
PARAMETER (NX=1500, NE=3)
IMPLICIT REAL*8 (A-H, O-Z)
DIMENSION C(4), EV(0:NE), APLUS(0:NX), AMINUS(0:NX),
$      TERM(0:NX), PJ(0:NX)
C
WRITE (*,*) '                                SUM'
OPEN (10, FILE='EIGDATA', STATUS='OLD',
$      FORM='UNFORMATTED')
READ (10) C, B, EV, APLUS, AMINUS, J, IMIN, IMAX, IMID
CLOSE (10)
OPEN (40, FILE='EIGTERM', STATUS='OLD',
$      FORM='UNFORMATTED')
READ (40) TERM
CLOSE (40)
OPEN (30, FILE='EIGPJ', STATUS='OLD',
$      FORM='UNFORMATTED')
READ (30) PJ, SUMJ, PNORMJ
CLOSE (30)
C
IF (IMIN.EQ.-1) STOP 'IMIN is not initialized'
IF (IMAX.EQ.-1) STOP 'IMAX is not initialized'
C
SUMJ = 0D0
DO 10 I = IMIN, IMAX
    IF (TERM(I).EQ.-1) STOP 'term negative'
    SUMJ = SUMJ + TERM(I)
10 CONTINUE
C
WRITE (*,1) SUMJ
IF (IMIN.NE.0) WRITE (*,2) TERM(IMIN-1)
IF (IMAX.NE.NX) WRITE (*,3) TERM(IMAX+1)
1 FORMAT ( '0', 5X, 'sum                = ', 1PE11.4 )
2 FORMAT ( '0', 5X, 'previous term = ', 1PE11.4 )
3 FORMAT ( '0', 5X, 'next term        = ', 1PE11.4 )
C
OPEN (30, FILE='EIGPJ', STATUS='UNKNOWN',
$      FORM='UNFORMATTED' )
WRITE (30) PJ, SUMJ, PNORMJ
CLOSE (30)
END

```

```

PROGRAM EIGNORM
PARAMETER (NX=1500, NE=3)
IMPLICIT REAL*8 (A-H, O-Z)
CHARACTER JA
DIMENSION P0(0:NX), PJ(0:NX)

C
WRITE (*,*) '                                NORM'
10 CONTINUE
WRITE (*,1) ' 0 OR J ?'
1 FORMAT ('$ ', A10)
READ (5,2) JA
2 FORMAT (A1)
IF (JA.EQ.'0') THEN
    OPEN (20, FILE='EIGP0', STATUS='OLD',
$         FORM='FORMATTED')
    READ (20) P0, SUM0
    CLOSE (20)
    IF (SUM0.EQ.-1D0) STOP
$         'Normalization constant not available'
    DO 20 I = 0, NX
        P0(I) = P0(I) / SUM0
20 CONTINUE
    SUM0 = 1D0
    OPEN (20, FILE='EIGP0', STATUS='UNKNOWN',
$         FORM='UNFORMATTED')
    WRITE (20) P0, SUM0
    CLOSE (20)
ELSE IF (JA.EQ.'J' .OR. JA.EQ.'j') THEN
    OPEN (30, FILE='EIGPJ', STATUS='OLD',
$         FORM='UNFORMATTED')
    READ (30) PJ, SUMJ, PNORMJ
    CLOSE (30)
    IF (PNORMJ.EQ.-1D0) STOP
$         'Normalization constant not available'
    PNORMJ = PNORMJ * DSQRT (SUMJ)
    DO 30 I = 0, NX
        PJ(I) = PJ(I) / PNORMJ
30 CONTINUE
    PNORMJ = 1D0
    SUMJ = 1D0
    OPEN (30, FILE='EIGPJ', STATUS='UNKNOWN',
$         FORM='UNFORMATTED')
    WRITE (30) PJ, SUMJ, PNORMJ
    CLOSE (30)
ELSE
    GO TO 10
END IF
END

```

```

PROGRAM EIGSAVE
PARAMETER (NX=1500,NE=3)
REAL*8 P(0:NX), SUM, PNORM, C(4), C4, B, EV(0:NE),
$      APLUS(0:NX), AMINUS(0:NX)
REAL SAVE(0:NX,0:NE)
CHARACTER JA
C
WRITE (*,*) '                               SAVE'
OPEN (60, FILE='EIGSAVE', STATUS='OLD',
$     FORM='UNFORMATTED')
READ (60) C4, B, EV, SAVE
CLOSE (60)
WRITE (*,1) '0 OR J ?'
1 FORMAT ('$ ', A10)
READ (*,2) JA
2 FORMAT (A1)
IF (JA.EQ.'0') THEN
    OPEN (20, FILE='EIGP0', STATUS='OLD',
$        FORM='UNFORMATTED')
    READ (20) P, SUM
    IF (SUM.NE.1D0) STOP 'Not normalized'
    DO 10 I = 0, NX
        SAVE(I,0) = SNGL (P(I))
10 CONTINUE
ELSE IF (JA.EQ.'J' .OR. JA.EQ.'j') THEN
    OPEN (10, FILE='EIGDATA', STATUS='OLD',
$        FORM='UNFORMATTED')
    READ (10) C, B, EV, APLUS, AMINUS, J, IMIN, IMAX,
$        IMID
    CLOSE (10)
    OPEN (30, FILE='EIGPJ', STATUS='OLD',
$        FORM='UNFORMATTED')
    READ (30) P, SUM, PNORM
    CLOSE (30)
    IF (PNORM.NE.1D0) STOP 'Not normalized'
    DO 20 I = 0, NX
        SAVE(I,J) = SNGL (P(I))
20 CONTINUE
END IF
OPEN (60, FILE='EIGSAVE', STATUS='UNKNOWN',
$     FORM='UNFORMATTED')
WRITE (60) C4, B, EV, SAVE
CLOSE (60)
END

```

PROGRAM EIGPLOT

C
C Files [Z]VPLOT.OBJ and [Z]MACPLOT.OBJ should be provided
C for LINKing.
C

```

PARAMETER (NX=1500, NE=3)
REAL*8 C4, B, EV(0:NE)
REAL P(0:NX,0:NE)
LOGICAL DONE(0:NE)
CHARACTER PLBL*10, ANS*3

```

C
C
C

```

WRITE (*,*) '                                PLOT'
WRITE (*,1)
$ 'MAXIMUM VALUE OF X TO APPEAR ON PLOT AXIS = '
1 FORMAT ('$ ', A45)
READ (*,*) LIMIT
OPEN (60, FILE='EIGSAVE', STATUS='OLD,
$ FORM='UNFORMATTED')
READ (60) C4, B, EV, P
CLOSE (60)

```

C
C

```

DO 10 J = 0, NE
  DONE(J) = P(0,J).NE.-1.0
  IF (.NOT.DONE(J)) THEN
    WRITE (*,2) J
    2 FORMAT (/1X, 'P(', I1, ') is not available')
    WRITE (*,3) 'OK ?'
    3 FORMAT ('$ ', A4)
    READ (*,4) ANS
    4 FORMAT (A3)
    IF (ANS(:1).NE.'Y' .AND. ANS(:1).NE.'y') STOP
    $ 'Ignore the following message:'
    END IF
10 CONTINUE

```

C
C

```

OPEN (61, FILE='OUTPUT', STATUS='UNKNOWN',
$ FORM='FORMATTED')
OPEN (71, FILE='VEC PLOT', STATUS='UNKNOWN')

```

C
C Each eigenvector is drawn separately
C

```

DO 60 J = 0, NE
  IF (DONE(J)) THEN

```

C
C Y-axis limit is determined below
C

```

  PMAX = 0.0
  DO 20 I = 0, LIMIT
    AP = ABS(P(I,J))
    IF (AP.GT.PMAX) PMAX = AP
20 CONTINUE

```

```

WRITE (71,5) C4, B, EV(J)
5   FORMAT ('1', 30X, 'C4 = ', F4.2, 5X, 'B = ',
$       1PE11.4, 5X, 'EIGENVALUE = ', E11.4 )
C
CALL PLOTS (9.5, 12.0, 71)
C
C Scales for the two axes are calculated below
C
XSCALE = FLOAT (LIMIT) /11.0
IF ( J.EQ.0 ) THEN
    YL = 0.0
    YH = PMAX
ELSE
    YL = - PMAX
    YH = PMAX
END IF
YSCALE = (YH - YL) / 8.0
C
C The axes are drawn
C
CALL PLOT (0.5, 1.0, -3)
CALL PLOT (8.0, 0.0, 2)
CALL PLOT (8.0, 12.0, 2)
C
C The X-axis is marked
C
DEL = LIMIT / 10
AX = 0.0
DO 30 AN = 0.0, FLOAT(LIMIT), DEL
    CALL PLOT ( 8.0, AX, 3)
    CALL PLOT ( 8.1, AX, 2)
    CALL NUMBER (8.2, AX-0.1, 0.1, AN, 90.0, -1)
    AX = AX + DEL / XSCALE
30 CONTINUE
CALL SYMBOL ( 8.6, 5.45, 0.1, 'X', 90.0, 1)
C
C Y-axis is marked
C
IEXP = LOG10(YH)
DEL = FLOAT(INIT((YH-YL)/10.0**(IEXP-1)))*
$     10.0**(IEXP-2)
AY = 8.0
DO 40 AN = YL/10.0**IEXP, YH/10.0**IEXP,
$     DEL/10.0**IEXP
    CALL PLOT (AY, 0.0, 3)
    CALL PLOT (AY, -0.1, 2)
    CALL NUMBER (AY, -0.7, 0.1, AN, 90.0, 3)
    AY = AY - DEL/YSCALE
40 CONTINUE
IF (IEXP.LT.-9) THEN
    PLBL = 'P(X)*10^' // CHAR (-IEXP/10+48) //
$     CHAR ( MOD(-IEXP,10) + 48 )
    NLBL = 10

```

```

ELSE
    PLBL = 'P(X)*10^' // CHAR (-IEXP+48)

    NLBL = 9
END IF
CALL SYMBOL (4.45, -0.9, 0.1, PLBL, 180.0, NLBL)
C
C Let the user know what is happening at the moment
C
    WRITE (61,6) J
6    FORMAT ( // '0', 5X, 'INITIALIZATION FOR PLOT',
    $        I1, 'COMPLETED' )
C
C An eigenvector is now drawn
C
    XIN = 0.0
    YIN = 8.0 - (P(0,J)-YL) / YSCALE
    CALL PLOT ( YIN, XIN, 3)
    DO 50 I = 1, LIMIT
        XIN = FLOAT (I) / XSCALE
        YIN = 8.0 - (P(I,J)-YL) / YSCALE
        CALL PLOT ( YIN, XIN, 2 )
50    CONTINUE
C
    CALL PLOT (0.0, 0.0, 999)
C
C Inform the user
C
    WRITE (61,7) J
7    FORMAT ( '0', 5X, 'PLOT ', I1, ' COMPLETED')
    END IF
60 CONTINUE
END

```

```

FUNCTION PLFUN (IND, X)
PARAMETER (NX=1500, NE=3)
REAL*8 C4, B, EV
LOGICAL FIRST
DIMENSION A(0:NE), EV(0:NE), P(0:NX,0:NE)
SAVE P, FIRST T1, TSTEP
DATA FIRST /.TRUE./
C
IF (FIRST) THEN
FIRST = .FALSE.
READ (*,*) T1, T2, INPOS, N
TSTEP = (T2-T1) / (N-1)
C
OPEN (50, FILE='EIGSAVE', STATUS='OLD',
$      FORM='UNFORMATTED')
READ (50) C4, B, EV, P
CLOSE (50)
C
A(0) = 1.0
IF (INPOS.LT.0) THEN
READ (*,*) ( A(J), J=1,NE )
ELSE
DO 20 J = 1, NE
A(J) = P(INPOS,J) / P(INPOS,0)
20 CONTINUE
END IF
END IF
C
PLFUN = 0.0
T = T1 + IND * TSTEP
DO 30 J = 0, NE
I = INT (X)
PX = (I+1-X)*P(I,J) + (X-I)*P(I+1,J)
PLFUN = PLFUN + A(J)*PX * EXP (SNGL(EV(J)) * T )
30 CONTINUE
C
RETURN
END

```

APPENDIX D

Deterministic simulation of hysteresis

```

PROGRAM DETERM
C
C Files ZEROIN8.OBJ and [Z]ADAMSPC.OBJ should be provided
C for LINKing
C
PARAMETER (N=1)
IMPLICIT REAL*8 (A-H, O-Z)
EXTERNAL AUX, F1
DIMENSION B(0:1000), XF(0:1000), XB(0:1000), C(4),
$          X(N,8), SAVE(N,11), YMAX(N), ERROR(N)
LOGICAL FORW
COMMON /Z/ BZ
COMMON /BC/ BETA, C
DATA C /3.0D-7, 1.0D-4, 1.5D-3, 1.7D0 /
C
OPEN (60, FILE='INPUT', FORM='FORMATTED', STATUS='OLD')
OPEN (61, FILE='OUTPUT', FORM='FORMATTED',
$      STATUS='UNKNOWN')
C
READ (60,*) C(4), B1, B2, BETA
WRITE (61,*) C(4), B1, B2, BETA
1 FORMAT ('1', 10X, 'C(4) = ', F5.3 /
$        '0', 10X, 'B1 = ', 1PE11.4 /
$        '0', 10X, 'B2 = ', E11.4 /
$        '0', 10X, 'BETA = ', E11.4 )
C
C The B-interval is divided into 1000 subintervals and data
C are collected at the dividing points.
C
BSTEP = (B2 - B1) / 1000.0
B(0) = B1
DO 10 I = 1, 1000
    B(I) = B(I-1) + BSTEP
10 CONTINUE
C
C Two integrations are needed in the same interval. First in
C the forward direction, (i.e., with B increasing; the loop
C control variables are adjusted accordingly
C
FORW = .TRUE.
BZ = B(0)
ISTART = 1
IEND = 1000
IDIFF = 1
H = 1.0D-12
C
C Set initial condition (B = BZ, X = X(1,1) ) depending on

```

```

C  whether forward or backward variation of B.
C
20 CONTINUE
   G1 = 10.0
   G2 = 1500.0
   CALL ZEROIN8 (F1, G1, G2, 1.0E-8, 1.0E-8, IFLAG)
   IF (IFLAG.GT.2) THEN
       WRITE (61,2) IFLAG, BZ, G1, G2
2  FORMAT ( '0ERROR FROM ZEROIN' /
$          '0', ' ', IFLAG = ' ', I1 /
$          '0', ' ', B      = ' ', 1PE11.4 /
$          '0', ' ', G1    = ' ', E11.4 /
$          '0', ' ', G2    = ' ', E11.4 )
       STOP 'ERROR'
   END IF
C
   IF (FORW) THEN
       XF(0) = G1
   ELSE
       XB(1000) = G1
   END IF
   X(1,1) = G1
   HMIN = 1.0E-18
   EPS = 1.0E-8
   JSTART = 0
C
   DO 30 I = 1, N
       YMAX(I) = 1.0
30 CONTINUE
C
C  Integration loop
C
   DO 40 I = ISTART, IEND, IDIFF
       CALL ADAMS (AUX, N, BZ, X, SAVE, H, HMIN, B(I),
$               EPS, YMAX, ERROR, KFLAG, JSTART)
       IF (KFLAG.LT.0) THEN
           WRITE (61,3) KFLAG, FORW, BZ, B(I)
3  FORMAT ('0', 5X, 'ERROR FROM ADAMS' /
$         '0', 10X, 'KFLAG = ', I2 /
$         '0', 10X, 'FORW = ', L10 /
$         '0', 10X, 'BZ = ', E10.4 /
$         '0', 10X, 'B(I) = ', E10.4 )
           STOP 'ERROR'
       END IF
C
C  Collect data after each step
C
   IF (FORW) THEN
       XF(I) = X(1,1)
   ELSE
       XB(I) = X(1,1)
   END IF
40 CONTINUE

```

```
C
C Integration is complete
C
C   IF (FORW) THEN
C       prepare for the backward sweep
C       FORW = .FALSE.
C       BZ   = B(1000)
C       ISTART = 999
C       IEND = 0
C       IDIFF = -1
C       H = - H
C       BETA = - BETA
C       GO TO 20
C   END IF
C
C Write data for plotting
C
C   OPEN (71, FILE='DET PLOT', STATUS='UNKNOWN',
C   $     FORM='FORMATTED')
C   WRITE (71,4) (B(I), XF(I), XB(I), I=0,1000)
C   4 FORMAT (1001(3(5X,E10.4)/))
C
C Area inside the loop is computed by simplest (rectangular)
C method
C
C   AREA = 0.0
C   DO 50 I = 0, 1000
C       AREA = AREA + BSTEP*(XB(I) - XF(I))
50 CONTINUE
C   WRITE (61,6) AREA
C   6 FORMAT ( '0', 10X, 'AREA = ', 1PE11.4)
C   END
```

```

SUBROUTINE AUX (B, X, XD, N)
IMPLICIT REAL*8 (A-H, O-Z)
DIMENSION X(N), XD(N), C(4)
COMMON /BC/ BETA, C

```

```

C
C This routine computes dB/dX. It is used indirectly through
C the library subroutine ADAMS
C

```

```

XD(1) = F1 (X(1)) / BETA
RETURN
END

```

```

REAL*8 FUNCTION F1(X)
IMPLICIT REAL*8 (A-H, O-Z)
DIMENSION C(4)
COMMON /Z/ B
COMMON /BC/ BETA, C

```

```

C
C This function computes dX/dt. It is called by AUX and
C indirectly used by program DETERM through ZEROIN8.
C

```

```

F1 = ( 0.5*C(1)*X*(X-1.0)+C(3) ) * B
$      -C(2)/6.0 *X*(X-1.0)*(X-2.0) - C(4)*X
RETURN
END

```

APPENDIX E

Stochastic simulation of hysteresis

```

PROGRAM GILSIMT
C
C File ZEROIN8.OBJ should be supplied for LINKing.
C
      DOUBLE PRECISION X, B, APLUS, AMINUS, AMBYAP, QGAN,
$          FACTOR, BETA, C1, C2, C3, C4, C2BY6,
$          C1BY2
      EXTERNAL F1
      PARAMETER (IDIM=2001)
      DIMENSION XSUM(0:IDIM-1,2), BGRID(0:IDIM-1), A(4),
$          XNOW(0:IDIM-1), AR(2)
      LOGICAL FORW, GET, PUT, PLOT
      COMMON /AA/ BZ, C(4)
C
      OPEN (60, FILE='INPUT', STATUS='OLD')
      OPEN (61, FILE='OUTPUT', STATUS='UNKNOWN')
C
      READ (60,*) B1, B2, C, BETA, NTIMES, ISEED, FORW, GET,
$          PUT, PLOT
      C1 = C(1)
      C2 = C(2)
      C3 = C(3)
      C4 = C(4)
      WRITE (61,1) B1, B2, C, BETA, NTIMES, ISEED, GET, PUT,
$          PLOT
1 FORMAT ( '1', 1P, 10X, 'B1      = ', E11.4      /
$          '0',      10X, 'B2      = ', E11.4      /
$          '0',      10X, 'C        = ', 4(E11.4,3X) /
$          '0',      10X, 'BETA     = ', E11.4      ///
$          '0',      10X, 'NTIMES  = ', I10         /
$          '0',      10X, 'ISEED   = ', I10         /
$          '0',      10X, 'GET      = ', L10         /
$          '0',      10X, 'PUT      = ', L10         /
$          '0',      10X, 'PLOT    = ', L10         /// )
C
C The B-interval is divided into IDIM-1 subintervals and
C data will be collected at the dividing points.
C
      BGRID(0) = B1
      BSTEP = (B2-B1) / FLOAT(IDIM-1)
      DO 10 I = 1, IDIM-1
          BGRID(I) = BGRID(I-1) + BSTEP
10 CONTINUE
C
C This program can be run either to refine existing data
C statistically, or to acquire new data. In the former case

```

C data should be read and in the latter case initial
 C condition should be set.

C

```

    IF (GET) THEN
      OPEN (70, FILE='GRPREV', STATUS='OLD',
        $      FORM='UNFORMATTED')
      READ (70) NPREV, XSUM, ASUM, A2SUM
      CLOSE (70)
      DO 20 I = 1, IDIM-1
        XSUM(I,1) = XSUM(I,1) * NPREV
        XSUM(I-1,2) = XSUM(I-1,2) * NPREV
20     CONTINUE
      ELSE
        DO 30 J = 1, 2
        DO 30 I = 0, IDIM-1
          XSUM(I,J) = 0.0
30     CONTINUE
        ASUM = 0.0
        A2SUM = 0.0
        NPREV = 0
  
```

C

C Starting values of X are obtained by solving the cubic
 C steady state equation.

C

```

    G1      = 1.0
    G2      = 1500.0
    BZ      = BGRID(0)
    ABSERR  = 0.0
    RELERR  = 1.0E-5
  C Note that BZ appears in common block AA.
    CALL ZEROIN (F1, G1, G2, ABSERR, RELERR, IFLAG)
    IF (IFLAG.GT.2) THEN
      WRITE (61,2) G1, G2, IFLAG
2     FORMAT ('0ERROR FROM ZEROIN. G1 = ', F8.4,
      $       ' G2 = ', F8.4, ' IFLAG = ', I1)
      STOP 'ERROR'
    END IF
    XSUM(0,1) = G1
  
```

C

```

    G1      = 1.0
    G2      = 1500.0
    BZ      = BGRID(IDIM-1)
  C Note that BZ appears in common block AA
    CALL ZEROIN (F1, G1, G2, ABSERR, RELERR, IFLAG)
    IF (IFLAG.GT.2) THEN
      WRITE (61,2) G1, G2, IFLAG
      STOP 'ERROR'
    END IF
  
```

C

```

    C1BY2 = C1 / 2.0
    C2BY6 = C2 / 6.0
  
```

C

```

C The outermost loop begins *****
C
C DO 70 N = 1, NTIMES
C
C The same B-interval is covered twice. J = 1 means B is
C increasing. J = 2 means B is decreasing. Variables
C controlling the innermost DO are adjusted in accordance
C with J.
C
C DO 65 J = 1, 2
C   BETA = ABS (BETA)
C   IF (J.EQ.1) THEN
C     B = BGRID(0)
C     X = XSUM(0,1)
C     XNOW(0) = X
C     ISTART = 0
C     IEND = IDIM - 1
C     IDIFF = 1
C   ELSE
C     BETA = - BETA
C     B = BGRID(IDIM-1)
C     X = XSUM(IDIM-1,2)
C     XSUM(IDIM-1) = X
C     ISTART = IDIM-1
C     IEND = 0
C     IDIFF = -1
C   END IF
C
C   APLUS = ( C1BY2 * X * (X-1.0) + C(3) ) * B
C   AMINUS = ( C2BY6 * (X-1.0) * (X-2.0) + C(4) ) * X
C   These must have some values to begin with.
C
C   DO 60 I = ISTART+IDIFF, IEND, IDIFF
C
C ***** The simulation section begins
C
50 CONTINUE
   QRAN = 1D0 - 2D0 * BETA / APLUS / B *
   $      ALOG (1.0-RAN(ISEED) )
   AMBYAP = AMINUS / APLUS
   IF ( ( J.EQ.1 .OR. QRAN .GT. -2D0*AMBYAP )
   $    .AND. DABS(QRAN/AMBYAP+2D0) .GT.
   $    AMBYAP*1D-5 ) THEN
   $    FACTOR = - AMBYAP + DSQRT ( QRAN +
   $      (2D0+AMBYAP) * AMBYAP )
   ELSE
   $    FACTOR = 1D0 + 0.5D0 * QRAN / AMBYAP
   END IF
   B = B * FACTOR
   APLUS = APLUS * FACTOR
   IF (1.0/(1.0-RAN(ISEED)).GE.1.0+AMBYAP) THEN
   $    APLUS = APLUS + C1*B*X
   $    AMINUS = AMINUS + 3D0 * C2BY6 * X * (X-1D0) + C4

```

```

        X = X + 1D0
    ELSE
        X = X - 1D0
        APLUS = APLUS - C1*B*X
        AMINUS = AMINUS - 3D0*C2BY6*X*(X-1D0) - C4
    END IF
    IF (B.LT.BGRID(I) .EQV. J.EQ.1) GO TO 50
C
C ***** Simulation section ends.
C
C Collect data after each step
C
        XSUM(I,J) = XSUM(I,J) + X
        XNOW(I) = X
    60 CONTINUE
C
C A one-way trajectory has been completed. Find area under
C this trajectory and update sums involved in average and
C standard deviation.
C
        AR(J) = 0.0
        DO 62 K = 1, IDIM-1
            AR(J) = AR(J) + 0.5*(XNOW(K)+XNOW(K-1))*BSTEP
    62 CONTINUE
    65 CONTINUE
        AREA = AR(2) - AR(1)
        ASUM = ASUM + AREA
        A2SUM = A2SUM + AREA*AREA
    70 CONTINUE
C
C The outermost loop ends *****
C
C Sums are converted to averages.
C
        NTOTAL = NPREV + NTIMES
        DO 80 I = 1, IDIM-1
            XSUM(I,1) = XSUM(I,1) / NTOTAL
            XSUM(I-1,2) = XSUM(I-1,2) / NTOTAL
    80 CONTINUE
C
C Save results if desired.
C
        IF (PUT) THEN
            OPEN (71, FILE='GRNOW', STATUS='NEW',
$             FORM='UNFORMATTED')
            WRITE (71) NTOTAL, XSUM, ASUM, A2SUM
        END IF
C
C Write a few lines on the output.
C
        AVEG = ASUM / NTOTAL
        SDEV = SQRT (A2SUM/(NTOTAL-1) - ASUM/NTOTAL*ASUM/
$             (NTOTAL-1))

```

```

      WRITE (61,3) AVEG, SDEV, SDEV/AVEG
3  FORMAT ( '0', 'AREA = ', 1PE11.4 //
$          '0', 'SDEV = ', 1PE11.4 //
$          '0', 'RATIO= ', 1PE11.4 //
$          '0', '*****' )

```

C
C Write formatted output if desired. These can be later
C read by a plotting program
C

```

      IF (PLOT) THEN
          OPEN (72, FILE='PLOTFL', STATUS='NEW',
$              FORM='FORMATTED')
          WRITE (72,4) (BGRID(I), XSUM(I,1), XSUM(I,2),
$                      I = 0, IDIM-1 )
4  FORMAT ( 5X, 1PE11.5, 5X, E11.5, 5X, E11.5 )
          END IF

```

C
C
C END

FUNCTION F1(X)

C
C The cubic equation used for setting initial conditions.
C Note that program GILSIMT uses this indirectly through
C subroutine ZEROIN.
C

```

      COMMON /AA/ B, C(4)
      F1 = C(1) * B * X * (X-1.0) / 2.0 - C(2) * X * (X-1.0)
$          * (X-2.0) / 6.0 + C(3) * B - C(4) * X
      RETURN
      END

```

APPENDIX F

Special features of the cubic mechanism in a coupled flow tank reactor

Let $v(R_1, R_0)$ be a cubic rate law, supporting three steady states in a flow tank. Let k_0 be chosen so that $R_\beta - R_\gamma = R_\gamma - R_\alpha$. Let R_+ and R_- define the points satisfying

$$k_0 + \left. \frac{\partial v}{\partial R} \right|_{R_\pm} = 0. \quad (\text{F.1})$$

Then

- i) $\phi(R_1, R_2; k_0, k_x)$ is symmetric with respect to the line $R_1 + R_2 = 2 R_\gamma$,
 - ii) $R_+ + R_- = 2 R_\gamma$,
 - iii) (R_+, R_-) is a solution of the coupled tank equations (6.7),
- and iv) the state (R_+, R_-) is marginally stable.

Proof:

The potential for the coupled tank satisfies

$$- \frac{\partial \phi}{\partial R_1} = \frac{dR_1}{dt} = k_0 (R_0 - R_1) - v(R_1, R_0) + k_x (R_2 - R_1)$$

and
$$- \frac{\partial \phi}{\partial R_2} = \frac{dR_2}{dt} = k_0 (R_0 - R_2) - v(R_2, R_0) + k_x (R_1 - R_2). \quad (\text{F.2})$$

Since R_α , R_β , and R_γ are the single-tank steady states,

$$\begin{aligned}
k_0(R_0-R) - v(R, R_0) &= c (R-R_\alpha)(R-R_\beta)(R-R_\gamma) \\
&= c [R^3 - (R_\alpha+R_\beta+R_\gamma)R^2 + (R_\alpha R_\beta + R_\alpha R_\gamma + R_\beta R_\gamma)R \\
&\quad - R_\alpha R_\beta R_\gamma]. \tag{F.3}
\end{aligned}$$

The point obtained by reflecting (R_1, R_2) on the line $R_1 + R_2 = 2R_\gamma$ is $(2R_\gamma - R_2, 2R_\gamma - R_1)$. Let us compare $\phi(R_1, R_2)$ and $\phi(2R_\gamma - R_2, 2R_\gamma - R_1)$.

$$\phi(R_1, R_2) - \phi(2R_\gamma - R_2, 2R_\gamma - R_1) = f(R_1) + f(R_2), \tag{F.4}$$

where

$$\begin{aligned}
f(R) &= c \left\{ -\frac{1}{4} [R^4 - (2R_\gamma - R)^4] + \frac{1}{3} (R_\alpha + R_\beta + R_\gamma) [R^3 - \right. \\
&\quad \left. (2R_\gamma - R)^3] - \frac{1}{2} (R_\alpha R_\beta + R_\alpha R_\gamma + R_\beta R_\gamma) [R^2 - (2R_\gamma - R)^2] \right. \\
&\quad \left. + R_\alpha R_\beta R_\gamma [R - (2R_\gamma - R)] \right\} \tag{F.5}
\end{aligned}$$

Expanding $f(R)$, it is found that the coefficients of all powers of R vanish when $R_\beta - R_\gamma = R_\gamma - R_\alpha$. Therefore,

$$\phi(R_1, R_2) = \phi(2R_\gamma - R_2, 2R_\gamma - R_1). \tag{F.6}$$

This proves (i).

From (F.1) and (F.2) it follows that R_\pm satisfy

$$3R_\pm^2 - 2(R_\alpha + R_\beta + R_\gamma)R_\pm + (R_\alpha R_\beta + R_\alpha R_\gamma + R_\beta R_\gamma) = 0. \tag{F.7}$$

Therefore,

$$R_+ + R_- = \frac{2}{3}(R_\alpha + R_\beta + R_\gamma) = 2R_\gamma \quad (\text{F.8})$$

since $R_\alpha + R_\beta = 2R_\gamma$.

ii) is Proved.

Solving (F.7), we obtain

$$R_\pm = R_\gamma \pm \frac{1}{\sqrt{3}}(R_\gamma^2 - R_\alpha R_\beta)^{\frac{1}{2}}. \quad (\text{F.9})$$

$$\text{Let } R_\beta - R_\gamma = R_\gamma - R_\alpha = \Delta. \quad (\text{F.10})$$

$$\text{Then } R_\pm = R_\gamma \pm \frac{1}{\sqrt{3}} \Delta. \quad (\text{F.11})$$

(R_+, R_-) is a coupled steady state if

$$k_0(R_0 - R_+) - v(R_+, R_0) + k_x(R_- - R_+) = 0 \quad (\text{F.12})$$

and

$$k_0(R_0 - R_-) - v(R_-, R_0) + k_x(R_+ - R_-) = 0. \quad (\text{F.13})$$

(F.12) can also be written as

$$c(R_+ - R_\alpha)(R_+ - R_\beta)(R_+ - R_\gamma) + k_x(R_- - R_+) = 0.$$

$$\text{i.e., } -\frac{2}{3\sqrt{3}} c\Delta^3 - k_x \frac{2}{\sqrt{3}} \Delta = 0. \quad (\text{F.14})$$

Therefore, (R_+, R_-) is a steady state when

$$k_x = -\frac{c}{3} \Delta^3. \quad (c < 0) \quad (\text{F.15})$$

Thus (iii) is proven.

The condition for marginal stability is

$$\begin{aligned} & \left(k_0 + \frac{\partial v}{\partial R} \Big|_{R_\alpha} \right) \left(k_0 + \frac{\partial v}{\partial R} \Big|_{R_\beta} \right) \\ & + k_x \left(2k_0 + \frac{\partial v}{\partial R} \Big|_{R_\alpha} + \frac{\partial v}{\partial R} \Big|_{R_\beta} \right) = 0. \quad (\text{F.16}) \end{aligned}$$

(R_+, R_-) satisfies this condition by construction (F.1).

REFERENCES

REFERENCES

1. G. Nicolis and I. Prigogine, "Self-organization in Nonequilibrium Systems" (John-Wiley, New York, 1977).
2. A. A. Andronov, A. A. Vitt, and S. E. Khaikin, "Theory of Oscillations" (Pergamon, Oxford, 1966).
3. F. Schlögl, Z. Phys. 248, 446 (1971).
4. F. Schlögl, Z. Phys. 253, 147 (1972).
5. I. Matheson, D. F. Walls, and C. W. Gardiner, J. Stat. Phys. 12, 21 (1975).
6. D. A. Sanchez, "Ordinary Differential Equation and Stability Theory: An Introduction" (Dover, New York, 1968).
7. J. L. Doob, "Stochastic Processes" (John-Wiley, New York, 1953).
8. I. Oppenheim, K. E. Shuler, and G. H. Weiss, Adv. Mol. Relax. Proc. 1, 13 (1968).
9. D. T. Gillespie, Physica 95A, 69 (1979).
10. D. T. Gillespie, J. Comp. Phys. 22, 403 (1976).
11. H. A. Kramers, Physica, 7, 284 (1940); J. E. Moyal, J. Roy. Stat. Soc. B2, 150 (1949).
12. A. D. Fokker, Ann. Phys. 43, 810 (1914); M. Planck, Sitzber. Preuss. Acad. Wissensch. 1917, p.324.
13. N. G. van Kampen, Adv. Chem. Phys. 34, 245 (1976).
14. R. Kubo, K. Matsuo, and K. Kitahara, J. Stat. Phys. 9, 51 (1973).
15. D. T. Gillespie, J. Chem. Phys. 72, 5363 (1980).

16. K. Matsuo, K. Lindenberg, and K. E. Shuler, J. Stat. Phys. 19, 65 (1978).
17. L. Arnold, "Stochastic Differential Equations: Theory and Applications", (John-Wiley, New York, 1974).
18. S. Chandrasekhar, Rev. Mod. Phys. 15, 1 (1943).
19. P. G. Hoel, S. C. Port and C. J. Stone, "Introduction to Stochastic Processes" (Houghton-Mifflin, Boston, 1972).
20. D. T. Gillespie, J. Comp. Phys. 28, 395 (1978).
21. L. Onsager and S. Machlup, Phys. Rev. 91, 1505 (1953);
S. Machlup and L. Onsager, Phys. Rev. 91, 1512 (1953).
22. K. L. C. Hunt and J. Ross, J. Chem. Phys. 75, 976 (1981) and references therein.
23. For example, U. Weiss, Z. Phys. B 30, 429 (1978);
J. D. Bekenstein and L. Parker, Phys. Rev. D23, 2850 (1981); H. Hara, Z. Phys. B 45, 159 (1981).
24. A. Nitzan, Phys. Rev. A 17, 1513 (1978).
25. C. Escher and J. Ross, J. Chem. Phys. 79, 3773 (1983).
26. F. Schlögl, C. Escher, and R. S. Berry, Phys. Rev. A 27, 2698 (1983).
27. D. Förster, "Hydrodynamic fluctuations, Broken Symmetry and Correlation Functions" (W. A. Benjamin Inc. Reading, Mass., 1975) Ch.7.
28. K. Matsuo, J. Stat. Phys. 16, 169 (1977).
29. R. M. Noyes, J. Chem. Phys. 71, 5144 (1979).
30. G. Nicolis and J. W. Turner, Ann. N. Y. Acad. Sci. 316, 251 (1979).

31. I. Oppenheim, K. E. Shuler, and G. H. Weiss, *Physica* 88A, 191 (1977).
32. I. Procaccia and S. Mukamel, *J. Stat. Phys.* 18, 633 (1978).
33. I. Procaccia and J. Ross, *J. Chem. Phys.* 67, 5558 (1978).
34. R. D. Levine *J. Chem. Phys.* 65, 3302 (1976).
35. I. Procaccia and R. D. Levine, *J. Chem. Phys.*, 65, 3357 (1976).
36. D. T. Gillespie, *Physica* 95A, 69 (1979).
37. V. Seshadri, B. J. West, and K. Lindenberg, *J. Chem. Phys.* 72, 1146 (1980).
38. P. Grassberger, *Z. Phys. B* 47, 365 (1982).
39. M. Malek-Mansour and G. Nicolis, *J. Stat. Phys.* 13, 197 (1975).
40. D. T. Gillespie, *J. Stat. Phys.* 16, 311 (1977).
41. D. T. Gillespie, *J. Phys. Chem.* 81, 2340 (1977).
42. W. Horsthemke, M. Malek-Mansour, and B. Hayez. *J. Stat. Phys.* 16, 201 (1977).
43. G. Nicolis and M. Malek-Mansour, *J. Stat. Phys.* 22, 495 (1980).
44. H. E. Stanley, "Introduction to Phase Transition and Critical Phenomena" (Oxford University Press, New York, 1971).
45. G. Dewel, D. Walgraef, and P. Borckmans, *Z. Phys. B.* 28, 235 (1977).
46. D. Walgraef, G. Dewel, and P. Borckmans, *Adv. Chem. Phys.* 49, 311 (1982).

47. S. K. Ma, "Modern Theory of Critical Phenomena"
(W. A. Benjamin, Inc., Reading, Mass., 1976).
48. F. Schlögl, Z. Phys. B 22, 301 (1975).
49. H. K. Janssen, Z. Phys. 270, 67 (1974).
50. C. W. Gardiner, K. J. McNeil, D. F. Walls, and
I. S. Matheson, J. Stat. Phys. 14, 309 (1976).
51. S. Grossmann and R. Schraner, Z. Phys. B 30, 325
(1978).
52. M. Mangel, J. Chem. Phys. 69, 3697 (1978).
53. C. L. Creel and J. Ross, J. Chem. Phys. 65, 3779 (1976).
54. H. A. Kramers, Physica 7, 284 (1940).
55. C. W. Gardiner, J. Stat. Phys. 30, 157 (1983).
56. A. Lotka, Proc. Nat. Acad. Sci. USA. 6, 420 (1920).
57. I. Prigogine and R. Lefever, J. Chem. Phys. 48, 1695
(1968).
58. J. Tyson, J. Chem. Phys. 58, 3919 (1973).
59. R. J. Field and R. M. Noyes, J. Chem. Phys. 60, 1877
(1974).
60. R. Field, J. Chem. Phys. 63, 2289 (1975).
61. J. S. Turner, Bull. Math. Biology, 36, 205 (1974);
Adv. Chem. Phys. 29, 63 (1975).
62. S. J. Hammarling, "Latent Roots and Latent Vectors"
(University of Toronto Press, Toronto, 1970). Ch. 5.